# Sizing Storage and Wind Generation Capacities in Remote Power Systems

by

Andy Gassner
B.Sc., University of Wisconsin – Madison, 2003

A Thesis Submitted in Partial Fulfillment of the Requirements for the Degree of
MASTERS OF APPLIED SCIENCE
in the Department of Mechanical Engineering


University of Victoria

# Sizing Storage and Wind Generation Capacities in Remote Power Systems

by

Andy Gassner
B.Sc., University of Wisconsin – Madison, 2003

## Supervisory Committee

---

Dr. Andrew Rowe, (Department of Mechanical Engineering)
**Supervisor**

---

Dr. Peter Wild, (Department of Mechanical Engineering)
**Co-Supervisor**

---

Dr. G. Cornelis van Kooten, (Department of Economics)
**Co-Supervisor**

# Abstract

## Supervisory Committee

Dr. Andrew Rowe, (Department of Mechanical Engineering)
**Supervisor**

Dr. Peter Wild, (Department of Mechanical Engineering)
**Co-Supervisor**

Dr. G. Cornelis van Kooten, (Department of Economics)
**Co-Supervisor**

Global adoption of renewable energy is increasing due to growing concern over climate change, increasing costs associated with conventional generation, and decreasing capital investment costs of renewable energy technologies. Specifically, wind power represents the most technologically mature renewable alternative and is recognized as a cost effective generation source in both large and small power systems. However, the variability due to the stochastic nature of the wind resource introduces technological limitations to the amount of wind power which can be integrated in a power system. Energy storage is seen as a solution to mitigate the variability in wind power output.

Wind power and energy storage devices have the potential to contribute a substantial amount of renewable generation to meet the electricity demand in remote power systems. Remote power systems are characterized by their self reliance on electrical generation. The basic function of a remote power system is to provide the necessary power to satisfy the community's electricity demand requirements as economically as possible with an adequate level of continuity and reliability.

In this thesis a probabilistic method for analyzing the integration of wind power and energy storage in a remote power system is developed, extending previous work done by Barton and Infield. The main objective of the method is to use a probabilistic model of a wind-storage system to estimate the required storage capacity and analyze the adequacy of power system components for a specified firm power commitment. A validation study and sensitivity analysis is provided comparing the probabilistic estimates of performance metrics to calculations from a time sequential simulation. The results of the study show the probabilistic method is limited in its general application due to the sensitivity of predicted metrics to system parameters such as installed wind capacity, firm power commitment, and confidence level. A method to reduce the residuals of the probabilistic estimates compared to calculations from a time sequence simulation method is provided. A case study for a remote power system located on Haida Gwaii is included to illustrate how the method can be used in a cost-benefit analysis of wind power and energy storage integration.

# Table of Contents

**ABSTRACT** ..... **III**
**TABLE OF CONTENTS** ..... **V**
**LIST OF TABLES** ..... **VII**
**LIST OF FIGURES** ..... **VIII**
**NOMENCLATURE** ..... **X**
**ACKNOWLEDGMENTS** ..... **XIV**
**1 INTRODUCTION** ..... **1**
1.1 BACKGROUND ..... 1
1.2 WIND INTEGRATION ..... 2
1.3 ENERGY STORAGE INTEGRATION ..... 2
1.4 ENERGY STORAGE DEVICES ..... 4
*1.4.1 Flywheels* ..... *5*
*1.4.2 NAS batteries* ..... *6*
*1.4.3 VRB* ..... *6*
*1.4.4 Pumped hydro* ..... *7*
*1.4.5 Conclusion* ..... *7*
1.5 METHODS FOR CALCULATING REQUIRED STORAGE CAPACITY ..... 8
1.6 THESIS OBJECTIVE ..... 10
**2 POWER SYSTEM ANALYSIS USING A PROBABILISTIC METHOD** ..... **12**
2.1 INTRODUCTION ..... 12
2.2 MODEL OF WIND-STORAGE SYSTEM ..... 13
2.3 WIND SPEED MODEL ..... 17
2.4 MODEL OF WIND ENERGY CONVERTER SYSTEM ..... 23
2.5 MODEL OF ENERGY STORAGE DEVICE ..... 25
2.6 SYSTEM PERFORMANCE METRICS ..... 27
2.7 CALCULATION OF REQUIRED STORAGE CAPACITY ..... 30
*2.7.1 Required storage capacity calculation with ESD constraints* ..... *31*
2.8 BACKUP GENERATOR ..... 34
2.9 CONCLUSION ..... 35
**3 VALIDATION STUDY AND SENSITIVITY ANALYSIS** ..... **37**
3.1 INTRODUCTION ..... 37
3.2 TIME SEQUENTIAL SIMULATION METHODOLOGY ..... 37
3.3 IMPLEMENTATION ..... 38
3.4 VALIDATION STUDY ..... 41

*3.4.1 Wind speed data* ... *41*
*3.4.2 Power system parameters* ... *41*
*3.4.3 Confidence level calculation* ... *42*
3.5 SENSITIVITY ANALYSIS ... 47
*3.5.1 Case A: Installed wind capacity* ... *47*
*3.5.2 Case B: Firm power commitment* ... *50*
*3.5.3 Case C: ESD charging and discharging rates* ... *51*
*3.5.4 Case D: ESD efficiency* ... *52*
*3.5.5 Case F: Backup generation* ... *54*
3.6 CONCLUSIONS AND DISCUSSION ... 56
**4 HAIDA GWAII: A CASE STUDY ... 58**
4.1 INTRODUCTION ... 58
4.2 MASSET DGS ... 60
4.3 LPC FOR MASSET DGS ... 62
4.4 COST-BENEFIT ANALYSIS ... 65
*4.4.1 Integration of wind power* ... *65*
*4.4.2 Integration of wind power and an ESD* ... *66*
4.5 RESULTS AND DISCUSSION ... 68
**5 CONCLUSIONS AND RECOMMENDATIONS ... 72**
**REFERENCES ... 74**
**APPENDIX ... 78**
A FILTER FOR THE VARIANCE IN WIND SPEEDS ... 78
B FILTER FOR THE VARIANCE IN MEAN WIND SPEED ... 80
C FILTER FOR THE VARIANCE IN THE CHANGE OF SOC ... 81
*C.1 Power conversion factor calculation* ... *84*
D SPECTRAL REPRESENTATION OF WIND SPEED ... 86
E VARIANCE CALCULATION FROM FILTERED WIND SPECTRUM ... 91
F ESD UTILIZATION METRICS ... 94
*F.1 Surplus net system power* ... *94*
*F.2 Deficit net system power* ... *97*
G ESTIMATING WEIBULL SHAPE FACTOR BY METHOD OF MOMENTS ... 99
H TIME SEQUENTIAL SIMULATION ESD CONTROL ALGORITHM ... 100

# List of Tables

Table 1.1 - General representation of ESD applications in power systems [4]. ..... 3
Table 1.2 – Summary of ESD characteristics. ..... 7
Table 2.1 – Power system performance metrics used in the probabilistic method. ..... 29
Table 3.1 – Power system configurations used in the sensitivity analysis ..... 47
Table 4.1 – Masset DGS generation units [28]. ..... 60
Table 4.2 – Economic model assumptions for the DGS LPC calculation. ..... 64
Table 4.3 – Economic model assumptions for wind power and ESD. ..... 69
Table 4.4 – Cost-benefit results for wind power and ESD integration in Masset DGS. .. 70

# List of Figures

Figure 1.1 – ESD characteristics for various technologies [5]. ..... 5
Figure 2.1 – Schematic of the modeled wind-storage system. ..... 13
Figure 2.2 – Sampled wind speed time series for storage period $\tau$. ..... 14
Figure 2.3 – Sampled wind power time series for storage period $\tau$..... 14
Figure 2.4 – Sampled net system power time series for storage period $\tau$..... 15
Figure 2.5 – Filter functions for a 24 hour storage period..... 17
Figure 2.6 – PDF of mean wind speed constructed for a 10 hour storage period at Sandspit, BC. ..... 20
Figure 2.7 – PDF of wind speeds within a 10 hour storage period at Sandspit, BC..... 21
Figure 2.8 – PDFs $p(\bar{u}_\tau)$ and $p(u(t))$ for three sampled values of $\bar{u}_\tau$ for a 10 hour store period. ..... 23
Figure 2.9 – Wind turbine power curve normalized to $P_{R,w}$..... 24
Figure 2.10 – Power balance for an ESD including efficiency and power ratings. constraints. ..... 25
Figure 2.11 – Generic net system power PDF. ..... 32
Figure 2.12 – Schematic of the modeled power system with backup generation..... 34
Figure 3.1 – Flowchart of the probabilistic methodology..... 39
Figure 3.2 – Flowchart of the time sequential method. ..... 40
Figure 3.3 – Performance metrics for 1000 kW installed wind capacity, 400 kW firm power, and γ = 2..... 43
Figure 3.4 – ESD utilization metrics for 1000 kW installed wind capacity, 400 kW firm power, and γ = 2..... 43
Figure 3.5 – RMSE of system performance metrics for various confidence levels. ..... 45
Figure 3.6 – Performance metrics for 1000 kW installed wind capacity, 400 kW firm power, and γ = 4..... 46
Figure 3.7 – ESD utilization metrics for 1000 kW installed wind capacity, 400 kW firm power, and γ = 4..... 46
Figure 3.8 – Performance metrics for 700kW installed wind capacity, 400 kW firm power, and γ = 4..... 48
Figure 3.9 – Performance metrics for 1300 kW installed wind capacity, 400 kW firm power, and γ = 4..... 49
Figure 3.10 – RMSE analysis for Case A. ..... 49

Figure 3.11 – RMSE analysis for Case B. ..... 50
Figure 3.12 – Performance metrics for a maximum ESD power rating of 200 kW. ..... 51
Figure 3.13 – RMSE analysis for Case C. ..... 52
Figure 3.14 – Performance metrics for an ESD round-trip efficiency of 60%. ..... 53
Figure 3.15 – ESD utilization metrics for round-trip efficiency of 60%. ..... 53
Figure 3.16 – RMSE analysis for Case D. ..... 54
Figure 3.17 – Performance metrics for a backup generation capacity of 350 kW..... 55
Figure 3.18 – ESD utilization metrics for a backup generation capacity of 400 kW. ..... 55
Figure 3.19 – RMSE analysis for Case E. ..... 56
Figure 4.1 – Haida Gwaii generation asset map. ..... 59
Figure 4.2 – Forecasted annual energy demand for the Masset DGS to 2030..... 61
Figure 4.3 – NPV of system costs for each integration alternative in the Masset DGS. .. 70

# Nomenclature

## Acronyms

| | |
|---|---|
| AEP | Annual energy production |
| BOP | Balance of plant |
| CRF | Capital recovery factor |
| DGS | Diesel generation system |
| ESD | Energy storage device |
| FS | Flywheel storage |
| GHG | Green house gas |
| HOMER | Hybrid Optimization Model for Electric Renewables |
| LPC | Levelized production cost |
| NAS | Sodium-sulfur |
| NPV | Net present value |
| PCS | Power conversion system |
| PDF | Probability density function |
| PH | Pumped hydro |
| PV | Present Value |
| RFP | Request for proposal |
| RMSE | Root mean squared error |
| SOC | State of charge |
| VRB | Vanadium redox battery |

## Symbols

| | |
|---|---|
| $c_E$ | ESD energy capital cost [$/kW-installed] |
| $C_{env,i}$ | Annual variable costs associated with GHG emissions [$/kWh] |
| $C_{f,i}$ | Annual variable costs associated with fuel consumption [$/kWh] |
| $c_f$ | Consumption rate of fuel [L/kWh] |
| $C_{inv}$ | Capital investment [$] |
| $c_{OM,D}$ | DGS fixed operational and maintenance cost [$/kW] |
| $c_{OM,ESD}$ | Fixed ESD operational and maintenance cost [$/kW-installed |
| $c_{OM,w}$ | Wind power operational and maintenance cost [$/kW] |
| $c_{P,ESD}$ | ESD power capital cost [$/kW-installed] |
| $c_{P,w}$ | Wind power capital cost [$/kW-installed] |
| $C_r$ | Reinvestment cost [$] |
| $E[\cdot]$ | Expected value operator |
| $e_{CO_2}$ | Emission rate of $CO_2$ [tonne/kWh] |
| $E_{ESD}$ | Annual energy contribution from wind-storage system [kWh] |
| $E_{DGS}$ | Annual energy contribution from diesel generation system [kWh] |
| $E_i$ | Annual energy delivered to grid from backup generation [kWh] |
| $E_{L,i}$ | Annual energy demand [kWh] |
| $E_t$ | Energy charge state of ESD [kWh] |
| $\Delta E_t$ | Excursion in SOC [kWh] |
| $E_w$ | Annual wind energy generated [kWh] |
| $E_{w/ESD}$ | Annual energy generated from the wind storage system [kWh] |

| | |
|---|---|
| $IC_D$ | Installed power capacity of DGS [kW] |
| $IC_w$ | Installed capacity of wind power [kW] |
| $OM$ | Fixed operational and maintenance cost [$/kW] |
| $P_b$ | Power supplied by backup generation [kW] |
| $P_{ch}$ | Power delivered to ESD [kW] |
| $P_{ch/dch}$ | Power flows to and from ESD [kW] |
| $p_{CO_2}$ | Price of $CO_2$ emissions [$/tonne] |
| $P_d$ | Power sent to dump load [kW] |
| $P_{dch}$ | Power dispatched from ESD [kW] |
| $P_{ESD}$ | Available ESD power [kW] |
| $p_f$ | Price of fuel [$/L] |
| $P_{fp}$ | Firm power commitment [kW] |
| $P_{net}$ | Net system power [kW] |
| $P_u$ | Unmet system power [kW] |
| $p(u(t))$ | PDF of wind speeds within the storage period |
| $p(\bar{u}_\tau)$ | PDF of mean wind speeds for storage period |
| $P_R$ | Rated power capacity [kW] |
| $P_w$ | Wind power [kW] |
| $r_{CO_2}$ | Escalation rate of $CO_2$ emissions [%/yr] |
| $r_d$ | Discount rate [%/yr] |
| $r_f$ | Escalation rate of fuel [%/yr] |
| $r_i$ | General inflation rate [%/yr] |

| | |
|---|---|
| $t_{ch}$ | Percent of time ESD spends in charging state [%] |
| $t_{dch}$ | Percent of time ESD spends in discharging state [%] |
| $t_{emty}$ | Percent of time ESD spends in an empty state [%] |
| $t_{full}$ | Percent of time ESD spends in an s full capacity [%] |
| $u(t)$ | Wind speeds within the storage period [m/s] |
| $\bar{u}_{\tau}$ | Mean wind speed for storage period [m/s] |
| $V_s$ | Salvage value [$] |

## Greek

| | |
|---|---|
| $\alpha$ | ESD scaling ratio to account for store constraints |
| $\gamma$ | Confidence level |
| $\zeta_{\tau}$ | Required storage energy capacity for store period [kWh] |
| $\eta$ | ESD efficiency |
| $\mu_X$ | Expected value of a random variable X |
| $\tau$ | Storage period [h] |
| $\sigma_{u(t)}$ | Standard deviation of wind speeds within the storage period [m/s] |
| $\sigma_{\bar{u}_{\tau}}$ | Standard deviation of mean wind speed of the storage period [m/s] |
| $\sigma_{\Delta E_t}$ | Standard deviation of excursions of SOC [kWh] |

## Subscripts

| | |
|---|---|
| *ch/dch* | Charging and discharging |
| *s* | Sampled mean wind speed |
| *b* | Balanced ESD power flow |
| *LT* | Long term mean wind speed |
| *rt* | Round-trip |

# Acknowledgments

This project has been an extremely valuable experience. The challenges I have encountered along the journey have taught me a great deal about myself. At times the task of completing such an assignment seemed insurmountable. It was with the help of my friends and family that I found the patience and motivation to complete the project.

I would specifically like to thank my family. Your endless support and encouragement have undoubtedly pushed me to achieve everything I have thus far. For this I am truly grateful.

The friends I have made along the way have helped me through the ceaseless frustrations throughout the last two years. Between sharing waves on the west coast, experiences with thesis completion, and MATLAB secrets, I have appreciated your support.

Last but not least I would like to thank my supervisors Drs. Andrew Rowe, Peter Wild, and Kees van Kooten. I sincerely appreciate the opportunity you gave me, your support over the last two years, and your friendship.

# 1 INTRODUCTION

## 1.1 Background

There are over 300 remote communities in Canada that do not have an electrical connection to a central electrical network [1]. These communities are referred to as remote power systems and are self reliant on electricity generation. There are many remote power systems installed worldwide, each geographical location having its own environmental, social, and cultural conditions that present unique system requirements. For example, remote power systems are located at scientific research centers in the Antarctic, island communities in the Caribbean, and isolated communities in the Pacific North West. Each location will not only have specific power requirements but will also have different available resources for power generation.

The basic function of a remote power system is to provide the necessary power to satisfy the community's electricity demand requirements as economically as possible with an adequate level of continuity and reliability. Remote rural electrification has traditionally been achieved using diesel engine generators. A diesel generation system (DGS) provides reliable power generation at a relatively low capital investment cost. The majority of remote power systems rely on a diesel engine driving a generator to fulfill some, or all, of its electrical demand. However, due the difficulties in transporting fuel to remote geographical locations and growing concern over climate change, there has recently been a movement towards renewable energy integration in remote power systems.

Wind power represents the most technologically mature renewable alternative, reflected in its continued growth in the global energy market and declining capital investment costs. However, a series of technical challenges need to be considered when examining the potential benefit of replacing diesel generation with wind power in remote power systems.

## 1.2 Wind integration

Wind power integration in isolated electrical networks can have negative system effects due to the variability in power output associated with fluctuating wind speeds. The variability in wind power causes increased action of the diesel governors to control system balance between generation and demand, which can result in decreased efficiency and increased mechanical degradation of the DGS. The intensity of these adverse effects is directly related to the penetration level, which can be defined in terms of both power and energy. The power penetration level is defined as the instantaneous power output of the wind turbine divided by the peak system load, whereas the energy penetration level is calculated from the ratio of the annual energy contribution from wind generation to the annual energy demand.

Remote power systems that contain both wind and diesel generation, referred to as wind-diesel systems, have different operating characteristics depending on the power and energy penetration levels [2,3]. All power systems containing wind generation require a certain level of control due to reliability issues caused by the renewable power fluctuations. In low penetration systems, wind power is treated as a negative system load; therefore, the amount of supervisory control required is minimal. In high wind penetration systems, the DGS is allowed to go offline if there is sufficient wind power to cover the electrical demand. The sophistication in the supervisory control is increased to maintain power quality, regulate reserves, and to dispatch generators as needed. Additional system components are required to regulate voltage levels and provide reactive power support. The additional controls, components, and the increased curtailed wind power associated with integrating large amounts of wind generation in a remote power system increases overall system costs and complexity.

Energy storage can be integrated with wind power in remote power systems to attenuate the negative effects of stochastic power production.

## 1.3 Energy storage integration

Energy storage can add value in a power system for various applications. The current applications of energy storage devices (ESDs) can be grouped into general categories

corresponding to their intended use: bulk energy storage, distributed generation, and power quality. A general representation of the applications of energy storage in power systems is provided in Table 1.1. The storage period, $\tau$, is defined as the characteristic time it takes the device to complete one full discharge to charge cycle at rated power capacity.

Table 1.1 - General representation of ESD applications in power systems [4].

| CATEGORY | $\tau$ (hr) | APPLICATION |
|---|---|---|
| Bulk storage | 2 - 24 | Load shifting and spinning reserve |
| Distributed generation | 1 – 8 | Peak shaving and transmission deferral |
| Power quality | < 1 | Power quality and reliability |

Energy storage can be used with wind power generation in each application listed in Table 1.1 to provide value to the power system. If wind power generation exceeds local demand, energy can be stored and used during times when wind power is not available or the electrical load increases. In systems with high wind penetration levels, the potential for large scale system faults is increased due to a significant amount of wind power suddenly going off-line caused by a turbine operational issue, e.g. wind speed exceeds the operational limit. During these events, an ESD can act as the system spinning reserve to replace the wind turbine. Furthermore, the required grid capacity to accommodate wind power is inherently larger than it would be to integrate generation from a traditional thermal unit. Transmission lines are sized to the installed capacity of wind power; although, on average only 30 to 40% of the rated capacity is produced. Due to the costs associated with upgrading the transmission capacity, wind power can be prohibitively expensive to integrate in a power system with transmission constraints. Energy storage can absorb large power swings seen in wind generation and provide an alternative to transmission upgrades. Energy storage devices are also used in wind-diesel systems to provide stability and reliability services such as frequency, voltage, and reactive power support.

In addition to the possible energy storage benefits associated with transmission and operational issues caused by the intermittent nature of wind power generation, an ESD is

also able to provide value to the local grid by delivering firm power from an otherwise stochastic source. In deregulated markets, pricing signals and market rules determine the value of firm power generation from a wind-storage system. Not only can penalties be avoided with firm power output from an ESD, but load shifting, or energy arbitrage, can provide economic gains if market conditions are favourable.

In wind-diesel systems without an energy market to provide economic incentive to integrate energy storage, the firm power from the ESD can be used to reduce regulation services provided from the DGS. This allows the power system to operate at a more efficient design point, reducing fossil fuel consumption and associated green house gas (GHG) emissions.

## 1.4 Energy storage devices

The main technical characteristics that distinguish an ESD for a particular application are its power rating, energy capacity, and storage period. A graphical illustration showing the most prevalent energy storage technologies currently available and their associated operating characteristics is provided in Figure 1.1.

In this thesis four storage technologies are studied that are representative of the range of storage periods and different applications: flywheel storage (FS), sodium-sulfur (NAS) batteries, vanadium redox batteries (VRBs), and pumped hydro (PH).

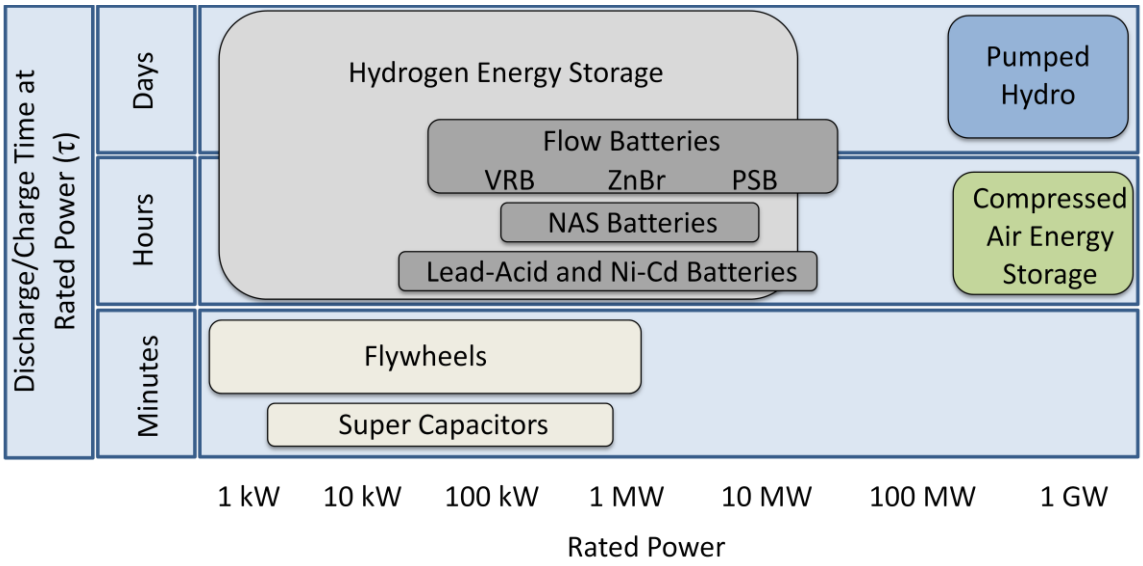


Figure 1.1 – ESD characteristics for various technologies [5].

### 1.4.1 Flywheels

Flywheels are mechanical devices that store the kinetic energy of a rotating mass. The available energy that can be stored is directly proportional to the moment of inertia of the rotating body and its angular velocity. Flywheels are comprised of a mass attached to a rotating shaft, the rotor, which is connected to a motor-generator. Modern flywheels are housed inside a vacuum sealed assembly and magnetic bearings are used to support the mass on the rotor. During charging mode electricity is sent to the stator, causing the rotor to spin and creating kinetic energy in the form of a rotating mass. During discharging mode the process is reversed, whereby the mechanical energy from the rotating inertia is transferred to the rotor, causing electrical production in the generator. Rotor design is of significant importance due to the high rotational and thermal stresses that can be experienced during operation.

Flywheel ESDs are generally characterized by fast power delivery response, high power and energy density, relatively high round-trip efficiency, short recharge time, and low environmental impact. Characteristic storage periods range from 30 seconds to minutes and flywheel round-trip efficiencies can be as high as 95% [6].

### 1.4.2 NAS batteries

Battery technology is currently the most common type of energy storage system used for wind-diesel applications [2]. Battery storage devices consist of an assembly of electrochemical cells, capable of converting chemical energy into electricity, and a power conversion system, including a rectifier, inverter, and power controls. Operational constraints that effect the lifetime of battery technologies include: depth of discharge, operating temperature, and cycling frequency.

Sodium-sulfur batteries are a relatively new battery technology characterized by high energy and power density, increased round-trip efficiency, and decreased operational and maintenance costs compared to traditional battery types such as Lead-acid [6]. Some differentiating characteristics of NAS batteries are the high operational temperatures, approximately 300º C, and the use of a solid electrolyte membrane. Currently a Japanese company, NGK Insulators Ltd. (NGK), is the leading manufacturer of NAS energy storage systems with utility scale application. Various installations are currently in operation including a 34 MW/204 MWh NAS energy storage system to firm the variable output of a 51 MW wind farm in Japan [7].

### 1.4.3 VRB

Vanadium-redox batteries are a relatively new energy storage technology that is broadly classified as a flow battery. Flow batteries consist of three main system components: electrolyte holding tanks, cell stacks, and a power conversion system (PCS). Chemical energy is stored in liquid electrolyte solutions held in large external tanks. During discharge mode the aqueous electrolyte is pumped through the cell stack where chemical energy is converted to electrical energy. The process is reversed during charging mode. The main advantages of the flow battery technology are: low maintenance cost, low stand-by losses, fast response time, and independence of energy and power ratings. The main attraction of VRB storage systems is the modular design in which energy capacity is related to the volume of the electrolyte tanks, and power is dependent on the area of the cell stack and PCS capabilities. This allows the design of an energy storage system to remain flexible, including the ability to add energy capacity by

purchasing more electrolyte and larger tanks or adding power capacity by upgrading the cell stack. The main drawback of VRB technology is the low energy density and the negative environmental impact of the liquid electrolyte.

### 1.4.4 Pumped hydro

Pumped hydro systems are the oldest energy storage technology used for utility scale applications. The energy storage medium in a PH system is in the form of potential energy, from displacing water from a lower elevation reservoir to a higher elevation. The charging cycle consists of using electricity to pump water to an elevated storage reservoir. During discharge operation, water in the elevated reservoir is released through a turbine that drives a generator to produce electricity. Pumped hydro systems represent the most technologically mature storage option with fast reaction times and relatively good round-trip efficiency. However, pumped hydro systems can have large capital costs in comparison with other technologies and are extremely site and resource dependent.

### 1.4.5 Conclusion

The energy storage technologies described throughout this section represent technologically mature storage options that are currently being integrated in power systems. The optimal design for a given system will depend on the intended application of the ESD. A summary of the ESD technologies and their associated characteristics used in this thesis are provided in Table 1.2, where $\tau$ refers to the storage period and $\eta_{rt}$ is the round-trip efficiency of the ESD.

Table 1.2 – Summary of ESD characteristics.

| ESD TECHNOLOGY | $\tau$ (hr) | $\eta_{rt}$ |
|---|---|---|
| Flywheel | sec - min | 0.89 |
| NAS | 6 - 12 | 0.87 |
| VRB | 12 - 24 | 0.75 |
| PH | > 24 | 0.78 |

When analyzing the possible benefit of integrating wind power and energy storage in a remote power system, a techno-economic evaluation of the life cycle project costs are required to determine the most cost-effective integration option. The costs associated with a specific storage technology are dependent on the installed energy and power capacities. Recently, there has been much work done on the topic of estimating the required storage capacity based on the variability in wind power. In the following section a general survey of the modeling techniques currently used to calculate the required storage capacity is provided.

## 1.5 Methods for calculating required storage capacity

There are many different ways to approach the problem of estimating the required storage capacity for a power system with intermittent wind generation. Traditionally, the approach is carried out in the time domain, where time series of system load and available wind power are analyzed. Energy storage devices are added to the simulation, absorbing surplus generation and discharging energy during periods of deficit power. The system is investigated for various configurations of installed wind capacity, ESD power ratings, and ESD energy capacities. A combination of economic metrics, based on the realized savings, and performance metrics, based on increased system reliability, are used to evaluate the possible benefit due to integrating the ESD. In this approach, the ESD capacity value is required as a simulation input and the optimal size is calculated by iteratively solving for the various configurations and ranking the results based on the evaluation metric.

Kaldellis has studied the possible benefits of integrating wind and solar power in many of the isolated networks located on islands in the Aegean sea [8,9]. Specifically, in [8] the authors study the effect of increasing wind penetration levels on the island of Lesbos. A detailed simulation methodology is presented where the excess wind energy produced is utilized by a PH storage system. The energy stored by the PH system is used to supply the island with firm power during the hours of peak demand. The analysis uses an iterative procedure to size the PH components based on the economic benefits of various energy capacities.

In [10] large simulations are used to investigate power systems with stochastic generation sources and energy storage to determine the capability of an ESD to convert variable generation into a firm source of power. The sensitivity of ESD control schemes, power and energy limits, as well as the ability to forecast wind speed to provide a load levelling service to the local electrical grid is investigated. The algorithm developed iteratively solves the simulation, giving the optimal storage size as a function of reliability in firm power delivered.

One of the most popular software packages to evaluate remote power systems is the Hybrid Optimization Model for Electric Renewables (HOMER), which was originally developed by the National Renewable Energy Laboratory. HOMER provides a user-friendly platform for analyzing integration options in remote power systems. The results from the model include reliability performance metrics, an economic optimization, and a sensitivity analysis for various system parameters. Energy storage devices are sized by iteratively solving the simulation for a range of capacities and rating them on the basis of minimum life cycle costs [11].

Recently there has been a growing interest in estimating the required storage capacity in a probabilistic framework to accurately model the stochastic nature of wind power generation [12]. This proves to be a formidable task since the time history of the state of charge (SOC) of the ESD cannot be tracked in a probabilistic domain. Some methods include probabilistic characteristics in a time simulation framework, allowing for a more robust simulation strategy due to a stochastic element. In [13] the authors include system reliability metrics, such as the loss of load probability, into an overall description of the "system well-being". A Monte Carlo simulation method is used to assess the performance of different system configurations of installed solar and wind power with an ESD based on these reliability metrics. In [14] the authors compare simulation results that compute reliability metrics for an off-grid residence with wind power generation and an ESD from a Monte Carlo simulation method, and a Monte Carlo method using a first order Markov Chain. Furthermore, the authors in [15] use a stochastic optimization programming approach to solve for the optimal energy storage capacity in a wind-diesel system. The

problem is formulated to minimize the capital investment and operational costs subject to a set of technical constraints.

Purely probabilistic methods to estimate the required storage capacity of a power system operating with intermittent power sources have not been available until recently. In [16] the author provides a probabilistic method to determine the expected level of firm power available from the ESD for a specified wind power capacity, maximum ESD power capacity, ESD efficiency, and a probability density function (PDF) of wind speeds. The required storage capacity is sized from the maximum expected power flow into the ESD. As pointed out in the analysis, this method of estimating the required storage capacity can easily over-size the ESD since it is based on the maximum charging power.

In [17] a probabilistic method is presented that employs spectral analysis to estimate the statistical characteristics of the wind regime, which is used to size the required storage capacity and evaluate the adequacy of power system components. This approach is a novel method to size the required energy storage capacity based on the variability of the wind regime. Surprisingly, further work has not been done to validate the application of the proposed probabilistic method to individual case studies.

## 1.6 Thesis objective

The objective of this thesis is to investigate the probabilistic method developed in [17,18] by conducting a validation study, sensitivity analysis, and applying the approach to a specific case study. The main findings are that the method is well suited for estimating the necessary energy capacity for various storage device technologies. In addition, the model is useful for studying the effects of increasing or decreasing the value of installed wind capacity, firm power commitment, and the ESD power ratings on the overall power system performance. However, the application of the probabilistic method is limited due to sensitivity of the estimated metrics on power system configuration parameters. A case study for a remote power system located on Haida Gwaii is included to illustrate how the method can be used in a cost-benefit analysis of multiple integration options.

The probabilistic theory of the method is provided in Chapter 2. The spectral analysis techniques are included in Appendix A through C. A validation study is presented in Section 3.4 comparing the estimated power system metrics from the probabilistic method with calculations from a time sequential simulation method. In Section 0 a sensitivity analysis of the accuracy of the probabilistic estimates for various system configurations is provided. Finally, in Chapter 4 a case study is presented for a remote power system on Haida Gwaii. The results from a cost-benefit analysis for various storage integration options and 1 MW wind capacity to displace current diesel generation are included. In Chapter 5 recommendations for further work to improve the probabilistic method are discussed.

# 2 POWER SYSTEM ANALYSIS USING A PROBABILISTIC METHOD

## 2.1 Introduction

In this chapter a probabilistic method for analyzing the performance of a remote power system is developed. The main objective of the method is to use a probabilistic model of a wind-storage system to estimate the required storage size and analyze the adequacy of power system components for a specified firm power commitment. The method is based on previous work done by Barton and Infield in [17,18]. The required storage capacity is estimated for the combined wind-storage system based on the variability of the wind resource, a wind power curve and a general representation of the storage device. The main objective of the ESD is to smooth power fluctuations caused by the variable output of wind power generation while operating in a charge sustaining mode. Performance metrics are used to help evaluate the sizing adequacy of system components for the specified firm power commitment. The method is well suited for investigating the necessary energy capacity for various storage device technologies. In addition, the model is useful for studying the effects of increasing or decreasing the value of installed wind capacity, firm power commitment, and the ESD power ratings on the reliability of the power system.

It should be noted that the model does not provide information on the temporal behaviour of the power system and therefore does not give any insight into system dynamics at any specific point in time. This is in contrast to a time domain method where chronological simulations are able to keep track of the time history of the SOC of the storage device.

The main advantage of the probabilistic method is the considerable reduction in computational effort compared to a time domain method. This allows for increased efficiency when investigating various permutations of system components.

## 2.2 Model of wind-storage system

The model of the wind-storage system includes wind power, a firm power commitment, and an ESD. The available wind power, $P_w$, is calculated from PDFs of wind speed and a wind turbine power curve. The firm power commitment, $P_{fp}$, is modeled as a constant load that is met by a combination of wind power and discharged power from the ESD. A schematic of the modeled power system is illustrated in Figure 2.12.

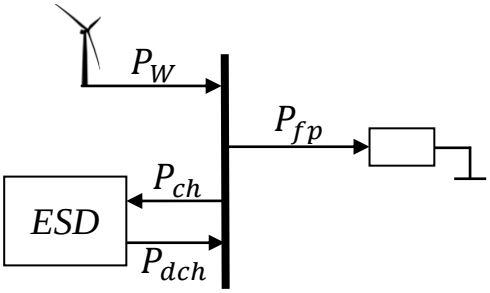


Figure 2.1 – Schematic of the modeled wind-storage system.

The net power is defined as the available wind power minus the electrical demand.

$$P_{net} = P_w - P_{fp} \tag{2.1}$$

When wind power exceeds the firm power commitment, $P_{net}$ is positive. The surplus power is sent to the ESD and is denoted by $P_{ch}$. When the available wind power is less than the firm power commitment, $P_{net}$ is negative. The deficit power is satisfied by power discharged from the ESD, and is represented as $P_{dch}$.

The foundation of the probabilistic method is a statistical description of the wind regime over the storage period of an ESD. The storage period of an ESD is defined as the characteristic time it takes to complete one full discharge to charge cycle at rated power and is denoted by the symbol $\tau$. Examples of storage periods for various technologies are provided in Figure 1.1.

A time domain example is provided to illustrate the concept of a storage period sample used in the probabilistic method. In Figure 2.2 a sample of the wind speed time series corresponding to the storage period $\tau$ is shown.

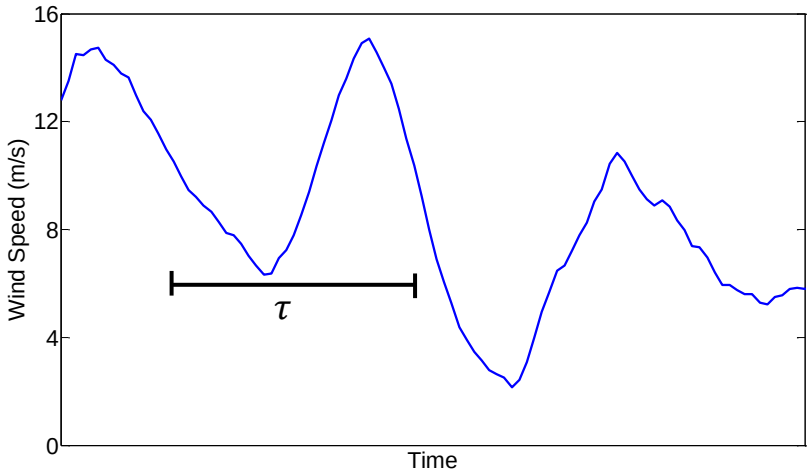


Figure 2.2 – Sampled wind speed time series for storage period $\tau$.

Wind speeds are converted into wind power values from a wind turbine power curve. Figure 2.3 shows the wind power time series for the same sampled storage period.

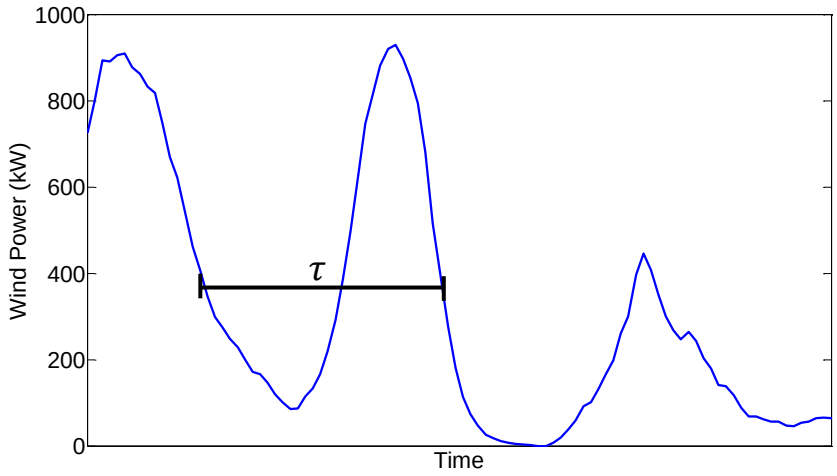


Figure 2.3 – Sampled wind power time series for storage period $\tau$.

Finally, the net power values are calculated according to (2.1) for each point in time. The net power time series for an installed wind capacity of 1000 kW and $P_{fp}$ equal to 400 kW is shown in Figure 2.4.

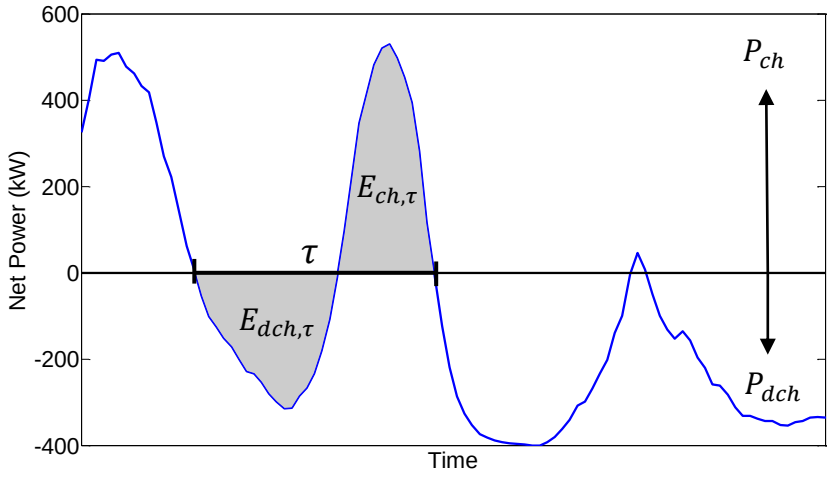


Figure 2.4 – Sampled net system power time series for storage period $\tau$.

The total energy sent to and taken from the ESD during the storage period, $E_{ch,\tau}$ and $E_{dch,\tau}$ respectively, is calculated from the time integral of the power flows to and from the ESD. The total charging and discharging energies for the example in Figure 2.4 are shown by the shaded portion of the plot.

$$E_{ch,\tau} = \int_{t_0}^{t_0+\tau} P_{ch}\,dt \tag{2.2}$$

$$E_{dch,\tau} = \int_{t_0}^{t_0+\tau} P_{dch}\,dt \tag{2.3}$$

Assuming a lossless storage device, the total change in SOC over the storage period is given by:

$$\Delta E_\tau = E_{ch,\tau} - E_{dch,\tau} \tag{2.4}$$

The ESD is assumed to operate in a steady state over the storage period. This implies that over each storage period of length $\tau$ the ESD returns to its initial SOC, ensuring the store will not move towards a sustained energy surplus or deficit. Therefore, the change

in energy over the storage period is zero and the discharging energy of the ESD is balanced by the charging energy over the storage period.

$$\Delta E_\tau = E_{ch,\tau} - E_{dch,\tau} = 0 \tag{2.5}$$

$$E_{ch,\tau} = E_{dch,\tau} \tag{2.6}$$

$$\int_{t_0}^{t_0+\tau} P_{ch} dt = \int_{t_0}^{t_0+\tau} P_{dch} dt \tag{2.7}$$

The statistical characteristics of the wind regime over the storage period are used to evaluate the performance of the power system and the energy capacity requirements of the ESD. Wind speed is modeled as a stationary stochastic process and spectral analysis is employed to estimate the variance in mean wind speeds, ${\sigma_{\overline{u}_\tau}}^2$, the variance in wind speeds within the storage period, ${\sigma_{u(t)}}^2$, and the variance in the excursions of SOC within the storage period, ${\sigma_{\Delta E_t}}^2$. The derivation of the filters and how they are used to calculate the variance values can be found in Appendix A through C and are referenced from [17].

An example of the filters constructed for a storage period of 24 hours is plotted on a logarithmic scale in Figure 2.5. The filter derived for the variance in mean wind speed for store period τ is a low pass filter and the filter designed for the variance of wind speeds within the store period is a high pass filter. Variance contributions from frequency components less than the store period frequency are attributable to the variance in mean wind speeds, whereas contributions from frequencies higher than the storage period are due to the variance within the store period. The maximum variance contribution to the excursion of SOC is from frequencies close to the storage period frequency. In Figure 2.5 the filter for the variance $\Delta E_t$ is scaled by an arbitrary value so that it could be shown on the same figure.

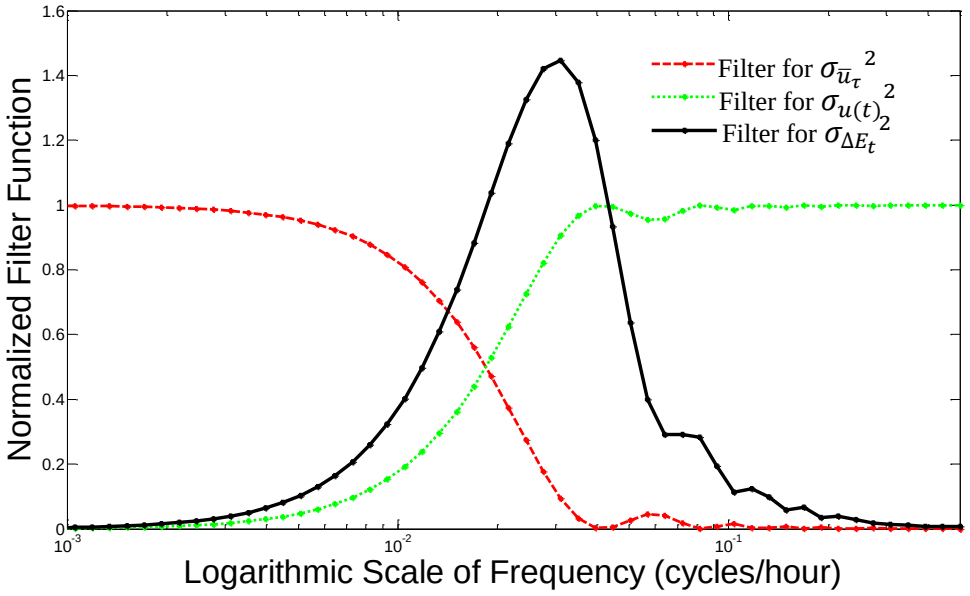


Figure 2.5 – Filter functions for a 24 hour storage period

The filter for the variance of $\Delta E_t$ is used to size the required ESD capacity for the storage period and the filters for the variance in $\bar{u}_\tau$ and $u(t)$ are used to construct PDFs of wind speed. The wind speed PDFs are combined with a wind turbine power curve to estimate the available wind power and evaluate the reliability of the power system.

## 2.3 Wind speed model

The wind regime at a given location can be characterized by a mean wind speed measured at a specified height and the standard deviation of wind speeds at that height [19]. The mean wind speed represents the intensity of the wind regime and the standard deviation is a measure of the variability of the wind speed about the mean.

Inter-temporal fluctuations of wind speed are typically modeled from a Gaussian process [19,20,21]. Therefore, the wind speeds within a storage period are assumed to follow a normal distribution centered on the mean wind speed of the storage period. A normal distribution describing wind speeds within the storage period is given by:

$$p(u(t)) = \frac{1}{\sqrt{2\pi\sigma_{u(t)}{}^2}} e^{-\frac{(u(t)-\bar{u}_\tau)^2}{2\sigma_{u(t)}{}^2}} . \tag{2.8}$$

In Eq. (2.8), $u(t)$ represents the wind speeds within the storage period, $\bar{u}_\tau$ is defined as the mean wind speed of the storage period, $\sigma_{u(t)}$ is the standard deviation of wind speeds within the storage period, and $t_0 \leq t \leq t_0 + \tau$.

Weibull distributions are typically used to model mean wind speed data [19,20,21]. Therefore, a Weibull distribution is used to model the mean wind speeds of the storage period. A Weibull PDF for mean wind speeds is given by:

$$p(\bar{u}_\tau) = \begin{cases} \frac{k}{c}\left(\frac{\bar{u}_\tau}{c}\right)^{k-1} e^{-\left(\frac{\bar{u}_\tau}{c}\right)^k} & \bar{u}_\tau \geq 0 \\ 0 & \bar{u}_\tau < 0 \end{cases} \tag{2.9}$$

where $c$ and $k$ are defined as the scale and shape parameters respectively. The scale and shape parameters of a Weibull distribution can be estimated from the expected value of the mean wind speed, $\mu_{\bar{u}_\tau}$, and the standard deviation in mean wind speed, $\sigma_{\bar{u}_\tau}$, by the method of moments [22]. The shape factor of the Weibull PDF is approximated by (see Appendix G for details):

$$k = \left(\frac{\sigma_{\bar{u}_\tau}}{\mu_{\bar{u}_\tau}}\right)^{-1.086} . \tag{2.10}$$

The scale parameter can be calculated by:

$$c = \frac{\mu_{\bar{u}_\tau}}{\Gamma\left(1 + \frac{1}{k}\right)}, \tag{2.11}$$

where Γ is the gamma function.

In Eqs. (2.10) and (2.11), the expected value of mean wind speed of the storage period is calculated by the expected value operator. The expected value of a random variable $X$ with a PDF of $p(x)$ is given by:

$$\mu_X = E[X] = \int_{-\infty}^{\infty} xp(x)dx\,. \tag{2.12}$$

Wind speeds are assumed to be a stationary stochastic process, implying $\mu_{\overline{u}_\tau}$ is equal to the long term mean wind speed of the original time series, denoted as $\mu_{LT}$.

$$\mu_{\overline{u}_\tau} = E[\bar{u}_\tau] = \int_{-\infty}^{\infty} \bar{u}_\tau p(\bar{u}_\tau)d\bar{u}_\tau = \mu_{LT} \tag{2.13}$$

Spectral analysis is employed to estimate the variance in mean wind speeds and the variance in wind speeds within the storage period using a wind speed spectrum and a set of filters. Probability density functions are constructed for $\bar{u}_\tau$ and $u(t)$ with the calculated variance values centered on the long term mean wind speed.

An example is provided to illustrate how the method constructs the PDFs for mean wind speeds for a storage period and for fluctuations about the mean wind speed within the store period. The wind speed time series data used in the analysis are from 1980 to 2001 inclusive for Sandspit, British Columbia (for details concerning the data set refer to Section 3.4.1). The long term mean wind speed is calculated to be 5.5 m/s from the original time series. Secondly, an ESD with a store period of 10 hours is selected for this example. A wind spectrum is computed for the site as described in Appendix C.1. Two filter functions are designed for the specified storage period of 10 hours, according to the methods presented in Appendix A and B. Finally, the variance of the wind speed components for a storage period of 10 hours are calculated from the filtered wind spectrum according to the methods described in Appendix E.

The variance in mean wind speeds for the specified storage period is found to be 13.96 $(\text{m/s})^2$ from Eq. (A.55). This gives a value for $\sigma_{\overline{u}_\tau}$ of 3.74 m/s. Using Eqs. (2.9), (2.10), and (2.11) a Weibull distribution is constructed for $\overline{u}_\tau$. A plot of the density function for mean wind speeds for a 10 hour storage period is shown in Figure 2.6.

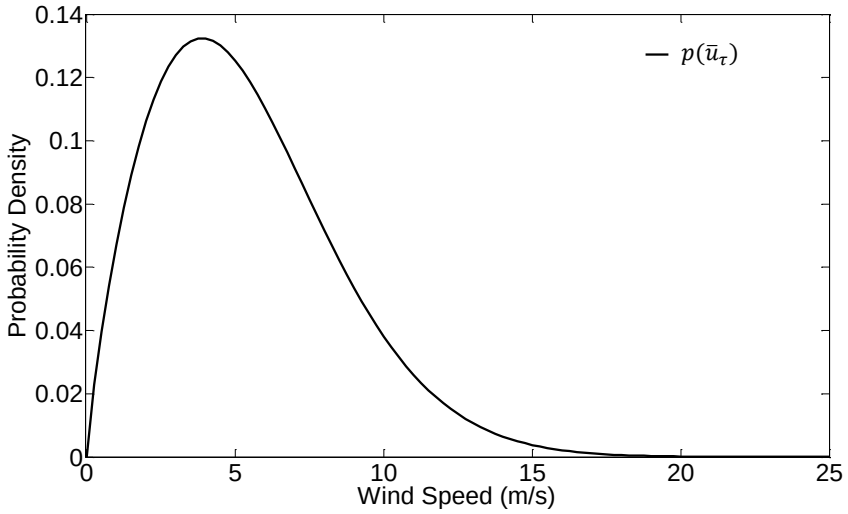


Figure 2.6 – PDF of mean wind speed constructed for a 10 hour storage period at Sandspit, BC.

The variance of wind speeds within the 10 hour store period is found to be 4.06 $(m/s)^2$ from Eq. (A.56). This gives a value for $\sigma_{u(t)}$ of 2.02 m/s. The distribution of wind speeds within the storage period is modeled as a Gaussian process with the calculated value of $\sigma_{u(t)}$ centered on the long term mean wind speed. A plot of the PDF constructed for $u(t)$ for a 10 hour store period for Sandspit, BC is shown in Figure 2.7.

Thus far the probabilistic method has been used to describe the distribution of mean wind speeds for a storage period. Additionally, it is possible to characterize wind speed fluctuations about the long term mean wind speed within a storage period using this approach. However, there are many possible realizations of mean wind speeds for the storage period, modeled by the distribution $p(\bar{u}_\tau)$. Therefore, to fully describe wind speeds within the storage period, distributions for the fluctuations around these possible mean wind speeds are required. The distributions of wind speed within the storage period for different mean wind speeds are constructed using the coefficient of variation.

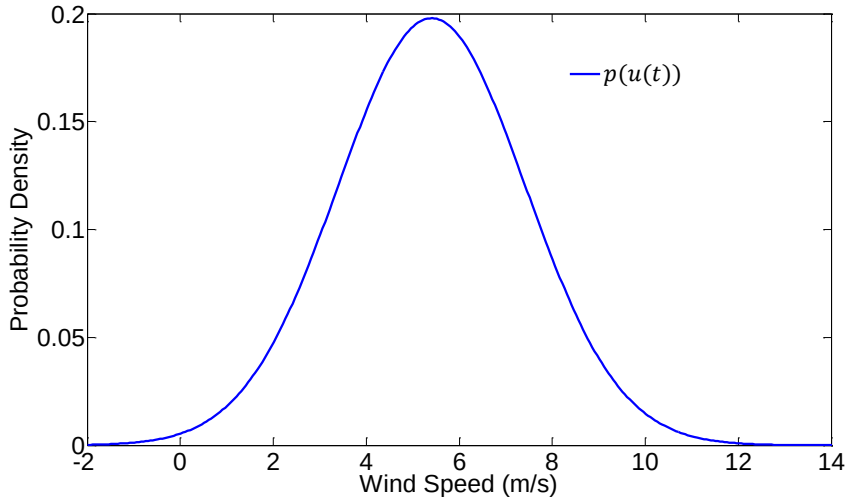


Figure 2.7 – PDF of wind speeds within a 10 hour storage period at Sandspit, BC.

The coefficient of variation, also referred to as the turbulence intensity in much of the literature concerning statistical analysis of wind speeds, is defined as the ratio of the standard deviation of the wind speed to the mean.

$$CV = \frac{\sigma}{\mu} \tag{2.14}$$

Traditionally, the standard deviation and mean used in the calculation of *CV* for wind speeds are computed over an averaging time period of 10 minutes but can be extended up to 1 hour [19]. This definition of *CV* gives a basic measurement of the variability of the sustained wind speed and is considered constant for the entire time series [19,23]. Using this relationship it is possible to estimate the expected variability of wind speed for a subset of the time series, e.g. the standard deviation of wind speeds for a month can be calculated from the long term *CV* and the mean wind speed for that month.

In the methods proposed in [17], the averaging time scale used in the definition of *CV* is extended to include periods beyond the conventional limit of 1 hour. This assumption allows the standard deviation in wind speeds within the storage period to be calculated for different mean wind speeds [18].

The coefficient of variation is calculated in the probabilistic method from the long term mean and the standard deviation about that mean.

$$CV_{LT} = \frac{\sigma_{u(t)_{LT}}}{\mu_{LT}} \tag{2.15}$$

*CV* represents a normalized measurement of the statistical variability of wind speeds within the storage period, which is assumed to be constant for all possible realizations of mean wind speeds.

A subscript, *s*, is used to denote a sampled mean wind speed from the population of $p(\bar{u}_\tau)$ and the corresponding standard deviation of wind speeds within the storage period.

$$CV_s = \frac{\sigma_{u(t)_s}}{\bar{u}_{\tau,s}} \tag{2.16}$$

From the assumption that the long term *CV* value is a constant, it is possible to determine $\sigma_{u(t)_s}$ for a sampled mean wind speed.

$$CV_s = CV_{LT} \tag{2.17}$$

$$\frac{\sigma_{u(t)_s}}{\bar{u}_{\tau,s}} = \frac{\sigma_{u(t)_{LT}}}{\mu_{LT}} \tag{2.18}$$

$$\sigma_{u(t)_s} = \bar{u}_{\tau,s}\left(\frac{\sigma_{u(t)_{LT}}}{\mu_{LT}}\right) \tag{2.19}$$

In this way it is possible to construct distributions for wind speeds within the storage period corresponding to each realization of mean wind speed in $p(\bar{u}_\tau)$. A graphical example of sampled distributions of $p(u(t)_s)$ is shown in Figure 2.8 for three values of $\bar{u}_{\tau,s}$: 3 m/s, 5.5 m/s, and 8 m/s. The storage period used in the example is 10 hours and the wind speed data are from Sandspit, BC. Each sampled mean wind speed is used to calculate the standard deviation of wind speed according to Eq. (2.19). These values are used to construct the PDFs of wind speed within the store period for the three different sampled means.

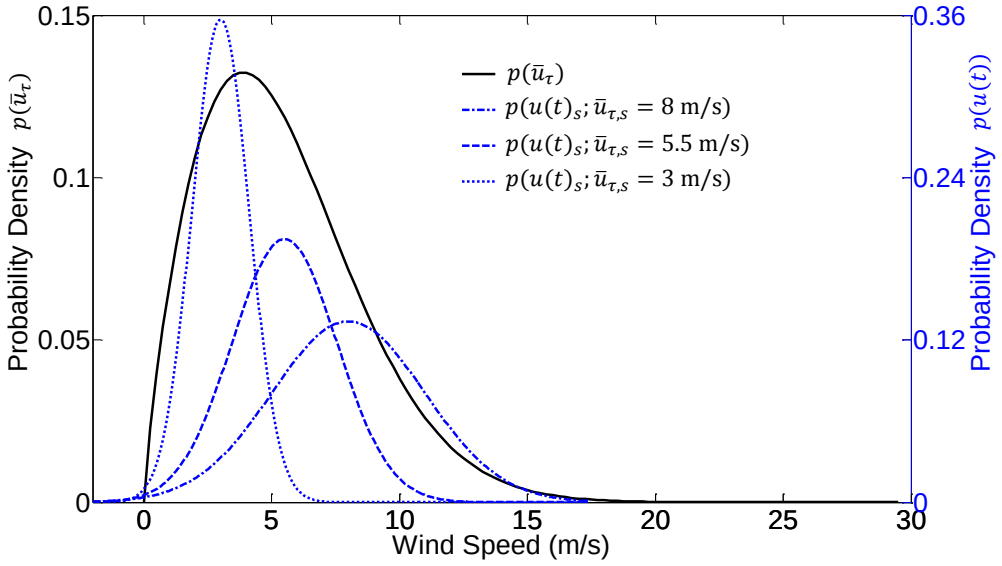


Figure 2.8 – PDFs $p(\bar{u}_\tau)$ and $p(u(t))$ for three sampled values of $\bar{u}_\tau$ for a 10 hour store period.

The distributions of $u(t)$ and $\bar{u}_\tau$ are combined with a simplified model of a wind energy converter system to determine the available power that can be generated from the wind resource over the storage period.

## 2.4 Model of wind energy converter system

The available power generated for different wind speeds is calculated from a wind turbine power curve and the distributions of wind speed. The power curve is equal to zero for wind speeds below the cut-in, $u_{ci}$, and above the cut-out, $u_{co}$, wind speeds. Typically the power curve follows a cubic function between the cut-in and rated, $u_R$, wind speeds, with maximum power generation at the nominal power output of the wind turbine, $P_{R,w}$.

$$P_w(u) = \begin{cases} 0 & for \;\; u < u_{ci}, \;\; u > u_{co} \\ \psi(u) & for \;\; u_{ci} \leq u \leq u_R \\ P_{R,w} & for \;\; u_R \leq u \leq u_{co} \end{cases} \tag{2.20}$$

The wind turbine power curve used in this study is modeled from an Enercon E48 800 kW wind turbine [24]. A cubic spline interpolation method is used to fit the power curve, which is then scaled to unity, and used to convert wind speeds to wind power values for a

specified installed capacity, $IC_w$. A graphical representation of the turbine power curve used to convert wind speeds to wind power is shown in Figure 2.9.

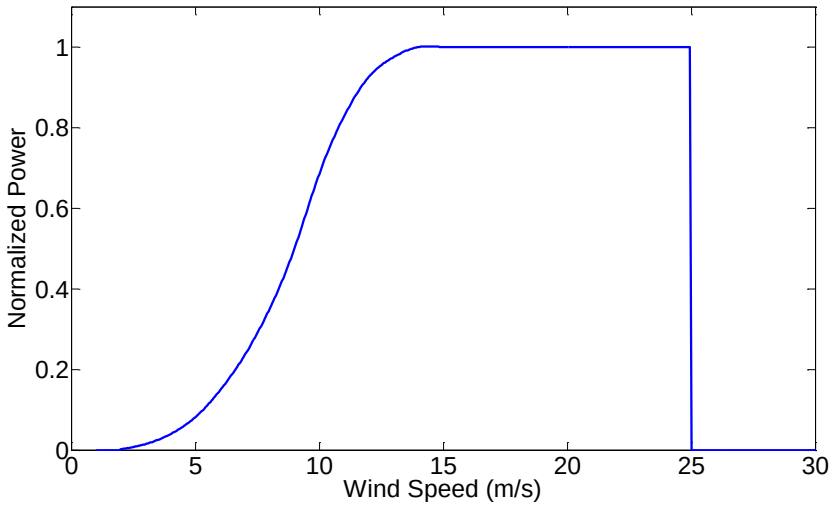


Figure 2.9 – Wind turbine power curve normalized to $P_{R,w}$.

The amount of available wind power for a sampled mean wind speed and storage period of length $\tau$ is calculated from the expected value of the converted wind power. The expected value for a function of a random variable is given by:

$$E[g(X)] = \int_{-\infty}^{\infty} g(X)p(X)dX\,, \tag{2.21}$$

where $p(X)$ is defined as the PDF of the random variable $X$. Therefore, the wind power available for a sampled mean wind speed, $P_w(\bar{u}_{\tau,s})$, is given by:

$$P_w(\bar{u}_{\tau,s}) \equiv E[P_w(u(t)_s)] = \int_{0}^{\infty} P_w(u(t)_s)p(u(t)_s)du(t)\,. \tag{2.22}$$

The expected value of wind power generated for all possible realizations of mean wind speeds for the storage period is denoted by $P_w(u_\tau)$ and is calculated from PDF of mean wind speeds.

$$P_w(u_\tau) \equiv E[P_w(\bar{u}_\tau)] = \int_0^\infty P_w(\bar{u}_\tau)p(\bar{u}_\tau)d\bar{u}_\tau \quad (2.23)$$

Equation (2.23) represents the average wind power that can be expected in a storage period of length $\tau$ weighted by the probability distribution of mean wind speeds.

## 2.5 Model of energy storage device

The ESD is modeled from four main characteristics: energy capacity constraints, maximum power rating constraints, charging and discharging efficiencies, and a typical time scale of discharge to charge at rated power.

The charging and discharging efficiencies, $\eta_{ch}$ and $\eta_{dch}$, and charging and discharging power ratings, $P_{R,ch}$ and $P_{R,dch}$, are included in the power balance for the ESD and shown in Figure 2.10.

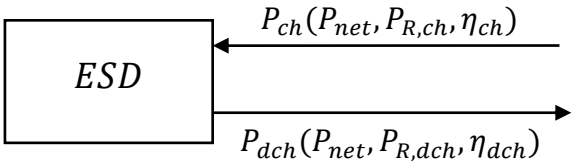


Figure 2.10 – Power balance for an ESD including efficiency and power ratings.

The ESD charging and discharging power values are defined when there is a surplus or deficit net system power. The net system power for wind speeds within the storage period is defined as the difference between the generated wind power minus the firm power commitment.

$$P_{net}(u(t)_s) = P_w(u(t)_s) - P_{fp} \quad (2.24)$$

The specified storage period is associated with a storage technology and its efficiency characteristics as described in Table 1.2. Efficiencies are simplified by defining a round-trip efficiency for each storage technology and assuming the charging and discharging efficiencies are equal.

$$\eta_{rt} = \eta_{ch}\,\eta_{dch} \tag{2.25}$$

$$\eta_{ch} = \eta_{dch} = \sqrt{\eta_{rt}} \tag{2.26}$$

Maximum power ratings of an ESD limit the amount of power that the device can absorb during charging operation and the amount of power that the store can deliver during discharging. If the surplus power is greater than the maximum charging rate, the power sent into the ESD is limited to the charging rate multiplied by the charging efficiency. If the surplus power is less than the maximum charging rate then all the available power is sent into the store minus the efficiency loss.

$$P_{ch}(u(t)_s) = \begin{cases} \eta_{ch}P_{R,ch} & for\ P_{net}(u(t)_s) \geq P_{R,ch} \\ \eta_{ch}P_{net}(u(t)_s) & for\ 0 < P_{net}(u(t)_s) < P_{R,ch} \\ 0 & for\ P_{net}(u(t)_s) \leq 0 \end{cases} \tag{2.27}$$

If there is a power deficit, the required power from the store is equal to the deficit power value divided by the discharging efficiency. However, if the demand exceeds the maximum discharging rate, the power dispatched from the ESD to meet the firm power commitment will be limited by $P_{R,dch}$.

$$P_{dch}(u(t)_s) = \begin{cases} {\eta_{dch}}^{-1}P_{R,dch} & for\ {\eta_{dch}}^{-1}|P_{net}(u(t)_s)| \geq P_{R,dch} \\ {\eta_{dch}}^{-1}P_{net}(u(t)_s) & for\ {\eta_{dch}}^{-1}|P_{net}(u(t)_s)| < P_{R,dch} \\ 0 & for\ P_{net}(u(t)_s) \geq 0 \end{cases} \tag{2.28}$$

The expected values of charging and discharging powers for a storage period $\tau$ and sampled mean wind speed are calculated by:

$$P_{ch}(\bar{u}_{\tau,s}) \equiv E[P_{ch}(u(t)_s)] = \int_0^\infty P_{ch}(u(t)_s)p(u(t)_s)du(t) \tag{2.29}$$

$$P_{dch}(\bar{u}_{\tau,s}) \equiv E[P_{dch}(u(t)_s)] = \int_0^\infty P_{dch}(u(t)_s)p(u(t)_s)du(t) \tag{2.30}$$

Equations (2.29) and (2.30) represent the expected power sent to and taken from the ESD over the storage period. To ensure the ESD is operating in a steady state the change in SOC over the storage period is required to be zero. The expected charging and discharging energy over the period is given by:

$$E_{ch,\tau} = P_{ch}(\bar{u}_{\tau,s}) \cdot \tau \,, \tag{2.31}$$

$$E_{dch,\tau} = P_{dch}(\bar{u}_{\tau,s}) \cdot \tau \,. \tag{2.32}$$

To maintain a steady state operation over the storage period the energy discharged from the ESD must be balanced by the energy sent to the ESD. Mathematically, this relationship can be expressed by constraining the value of the available power which the ESD can contribute to the power system over the storage period, $P_{ESD}$, to be equal to the minimum of the expected charging power and the discharging power:

$$P_{ESD}(\bar{u}_{\tau,s}) = min(P_{ch}(\bar{u}_{\tau,s}), |P_{dch}(\bar{u}_{\tau,s})|) \tag{2.33}$$

By constraining the charging and discharging energy values over the storage period to be equal there is a possibility that there will be excess power sent to the ESD which cannot be absorbed. This additional power would either have to be curtailed or sent to a dump load. Furthermore, there is also a possibility that there will be some unmet demand due to the steady state constraint. In the next section the metrics used by the probabilistic method to report on the reliability and performance of the power system are discussed.

## 2.6 System performance metrics

In the probabilistic method, the adequacy of power system components is determined from a set of performance metrics. Each metric is calculated from the power flows associated with net system power. Descriptions of the metrics used in the probabilistic approach are presented in this section.

The reliability of the power system is reflected by the expected value of unmet demand. The value of unmet demand, $P_u$, for a sampled mean wind speed is given by the

deficit power minus the power delivered from the ESD, including losses from the discharging efficiency. Therefore, the unmet demand is defined when $P_{net} < 0$ as:

$$P_u(\bar{u}_{\tau,s}) = \begin{cases} \left|P_{net}(\bar{u}_{\tau,s})\right| - \eta_{dch} P_{ESD}(\bar{u}_{\tau,s}) \; for \; \left|P_{net}(\bar{u}_{\tau,s})\right| > \eta_{dch} P_{ESD}(\bar{u}_{\tau,s}) \\ 0 \qquad\qquad\qquad\qquad\qquad\qquad for \; \left|P_{net}(\bar{u}_{\tau,s})\right| \leq \eta_{dch} P_{ESD}(\bar{u}_{\tau,s}) \end{cases} \tag{2.34}$$

The power sent to the dump load, $P_d$, gives an indication of how much wind power is curtailed due to either inadequate power ratings of the ESD or an oversized wind capacity. The power sent to the dump load is given by the amount of surplus power for a sampled mean minus the power sent to the ESD before charging efficiency loss. Therefore, the power sent to the dump load is defined when $P_{net} > 0$ as:

$$P_d(\bar{u}_{\tau,s}) = \begin{cases} P_{net}(\bar{u}_{\tau,s}) - \dfrac{P_{ESD}(\bar{u}_{\tau,s})}{\eta_{ch}} & for \; P_{net}(\bar{u}_{\tau,s}) > \dfrac{P_{ESD}(\bar{u}_{\tau,s})}{\eta_{ch}} \\ 0 & for \; P_{net}(\bar{u}_{\tau,s}) \leq \dfrac{P_{ESD}(\bar{u}_{\tau,s})}{\eta_{ch}} \end{cases} \tag{2.35}$$

The scenario in which the expected power sent into the ESD over the storage period is equal to the power removed from the store is defined as balanced and denoted with the subscript *b*. At this sampled mean wind speed, $\bar{u}_{\tau,b}$, the store utilization is maximised since the charging and discharging energy values are equal over the storage period, i.e. both the curtailed and unmet power values are minimized.

Lastly, a final value for the available ESD power contribution, unmet demand, and power sent to the dump load are calculated for all possible realizations of mean wind speeds of the storage period.

$$P_{ESD}(u_\tau) \equiv E[P_{ESD}(\bar{u}_\tau)] = \int_0^\infty P_{ESD}(\bar{u}_\tau) p(\bar{u}_\tau) d\bar{u}_\tau \tag{2.36}$$

$$P_u(u_\tau) \equiv E[P_u(\bar{u}_\tau)] = \int_0^\infty P_u(\bar{u}_\tau) p(\bar{u}_\tau) d\bar{u}_\tau, \tag{2.37}$$

$$P_d(u_\tau) \equiv E[P_d(\bar{u}_\tau)] = \int_0^\infty P_d(\bar{u}_\tau)p(\bar{u}_\tau)d\bar{u}_\tau. \quad (2.38)$$

In addition to the metrics presented in this section there are four other metrics recorded for the wind-storage system: percent of time the store spends charging, discharging, empty and full. These metrics reflect the ESD utilization, representing the fraction of time the store spends idle in an empty or full charge state compared to operating in an active charging or discharging state. The methods used to calculate the ESD utilization metrics are taken from [18] and are summarized in Appendix F.

A summary of the system performance metrics used in the base model are listed in Table 2.1. The unmet demand metric is used to evaluate the reliability of the power system for the specified firm power commitment and installed wind capacity. The power sent to the dump load gives an indication of the relative sizing adequacy of installed wind and ESD power ratings for the specified firm power commitment. The expected power utilized by the ESD and the fraction of time it spends in an active charging or discharging rate give a relative measure on the utilization of the ESD.

Table 2.1 – Power system performance metrics used in the probabilistic method.

| Symbol | Description |
|---|---|
| $P_d(u_\tau)$ | Expected value of power sent to the dump load for a store period τ |
| $P_u(u_\tau)$ | Expected value of unmet load for a store period τ. |
| $P_{ESD}(u_\tau)$ | Expected value of power utilized by the ESD for a store period τ. |
| $t_{ch}$ | Fraction of time store spends in charging state. |
| $t_{dch}$ | Fraction of time store spends in discharging state. |
| $t_{full}$ | Fraction of time store spends in full state. |
| $t_{empty}$ | Fraction of time store spends in empty state. |

## 2.7Calculation of required storage capacity

The calculation of the required storage capacity used in the probabilistic method is based on the variability in the SOC of the storage device. The energy charge state at any point in time within the storage period is given by the initial SOC plus an accumulation term that tracks the power flows across the ESD boundary through time. The filter derived for the variance in $\Delta E_t$ does not account for the ESD efficiency or power rating; therefore, the power flows used to size the storage capacity are equal to $P_{net}$.

$$E_t = E_0 + \int_0^t P_{net}\, dt \tag{2.39}$$

The deviation in the energy state at any time are defined as:

$$\Delta E_t \equiv \int_0^t P_{net}\, dt \tag{2.40}$$

To size the required storage capacity of the ESD, the probabilistic method employs spectral analysis to characterize the statistical properties of $\Delta E_t$ over the storage period. A filter for the expected variance in $\Delta E_t$ within the storage period is derived in Appendix C according to [17]. The methods used to calculate the variance in $\Delta E_t$ from a filtered wind speed spectrum are provided in Appendix C.

During the planning and design phase of integrating wind power and energy storage into a power system, sizing the required storage capacity is of primary concern. In theory, the larger the storage capacity, the more wind power can be integrated into the power system. However, over-sizing an ESD becomes prohibitively expensive and can limit the feasibility of project development. According to the findings by Barton in [18], an adequate storage capacity size is given by $\pm\sigma_{\Delta E_t}$. However, in [25,26] the authors use a similar approach to calculate the increase in operational reserves due to integrating wind power in an existing power system. They use the standard deviation associated with the increase in variability of net system load due to the integration of wind power as a metric to size the required reserve capacity. The authors show that the increase in reserves for a

particular operational area are dependent on the flexibility of the particular system, wind power penetration levels, and how fast the ancillary service is required to react to fluctuations in load. The size of the reserves required to compensate for the variability in wind power is calculated from multiplying the standard deviation in net load by a constant factor, which is referred to as the confidence level. The confidence level is defined as the range of standard deviations and is shown to be on the order of 2 to 6 depending on the characteristics of the power system [25,26]. For example, a confidence level of 2 corresponds to a range of $\pm\sigma_{\Delta E_t}$.

Therefore, the required energy capacity for a storage period, $\zeta_\tau$, of an ideal ESD without including power rating constraints is given by:

$$\zeta_\tau = \gamma\sigma_{\Delta E_t}\,, \tag{2.41}$$

where $\gamma$ denotes the confidence level and $\sigma_{\Delta E_t}$ is calculated by Eq. (A.57). A proposed method to calculate the confidence level used to size the required storage capacity is provided in Section 3.4.3.

### 2.7.1 Required storage capacity calculation with ESD constraints

The filter derived to estimate the required storage capacity does not include ESD efficiencies or power rating constraints. In this section the calculation for the required storage capacity in the wind-storage system, including power ratings and efficiency loss, is described. An additional term is included representing the change in the variability of the expected power flows to and from the ESD due to efficiency loss and power rating limits during the storage period [18].

The power flows to and from the ESD are constrained by the efficiency and maximum power ratings of the store. Therefore, the variability in $\Delta E_t$ is decreased and the required storage capacity is reduced. The change in the required storage capacity from the unconstrained base model is related to the change in the power flows to and from the store due to the power rate limitations. A simplified net power PDF is shown in Figure 2.11 for an ESD with a maximum charging and discharging storage rating of 200 kW.

Net system power PDFs are more complex than the simplified example shown; it is provided to illustrate the basic concepts covered in this section.

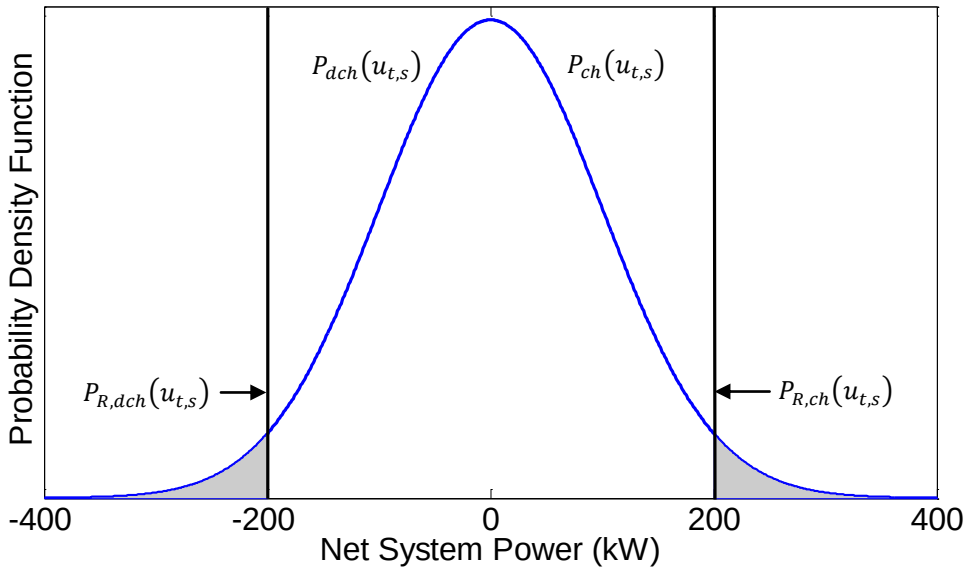


Figure 2.11 – Generic net system power PDF.

If the ESD is ideal and the power and energy capacities are large enough so that the power flows are unobstructed, the PDF of power flows to and from the store will be equal to the net system PDF. However, if the efficiency and rated capacity limits are included, the charging and discharging power values are constrained. Therefore, the variability in $P_{ch}$ and $P_{dch}$ is reduced. Figure 2.11 gives a graphical example of how the tails of the distribution of $P_{net}$ are affected when including the storage ratings. The shaded regions of the PDF represent the reduced variability in power flows to the ESD due to $P_{R,dch}$ and $P_{R,ch}$.

The notation used to refer to the power flows of the ESD is $P_{ch/dch}$, and is a function of the net system power, the store power ratings, and efficiency.

$$P_{ch/dch} = f(P_{net}(u(t)_s), P_{R,ch}, P_{R,dch}, \eta_{rt}) \tag{2.42}$$

The change in the variability of power flows of the ESD due to the power rating limits and efficiency losses can be expressed as a ratio of the variance in $P_{ch/dch}$ to the variance in $P_{net}$.

$$\alpha^2 \equiv \frac{\sigma^2{}_{P_{ch/dch}}}{\sigma^2{}_{P_{net}}} \tag{2.43}$$

Since $P_{ch/dch}$ includes the ESD rate limits and efficiencies while $P_{net}$ represents the unconstrained charging and discharging powers used in the base model, $\alpha^2$ in (2.43) represents a ratio of variability in the constrained and unconstrained charging and discharging powers for the storage period. This is used to weight the calculation of the required storage capacity of Eq. (2.41) to give the constrained ESD capacity size.

The variance values of $P_{ch/dch}$ and $P_{net}$ in Eq. (2.43) are evaluated for the sampled mean wind speed giving balanced conditions. The expected value operator is used to calculate the variance in $P_{net}$ and $P_{ch/dch}$:

$$Var(X) = E[X^2] - (E[X])^2. \tag{2.44}$$

Therefore, the variance in net power is given by:

$$\sigma^2{}_{P_{net}} = E\left[{P_{net}}^2\right] - (E[P_{net}])^2. \tag{2.45}$$

The variance in $P_{ch/dch}$ is calculated from:

$$\sigma^2{}_{P_{ch/dch}} = E\left[{P_{ch/dch}}^2\right] - \left(E\left[P_{ch/dch}\right]\right)^2. \tag{2.46}$$

The value of $\alpha^2$ in Eq. (2.43) gives a relative measure of the variability in the ESD expected power flows due to rate limits and efficiency losses compared to an unrestricted case. For an ideal ESD, the value of $\alpha$ is equal to 1, and between 0 and 1 for an ESD including $P_{R,ch}$, $P_{R,dch}$, and $\eta_{rt}$.

The probabilistic method estimates the required storage capacity, including the ESD constraints, by:

$$\zeta_\tau = \gamma\alpha\sigma_{\Delta E_t} \tag{2.47}$$

## 2.8 Backup generator

This section provides details of the backup generator model used in the probabilistic method. A backup generator is included to provide a more realistic model of remote power system operation. The backup generator is assumed to be a load following device with a maximum rated capacity denoted by $P_{R,b}$. There are no ramping or minimum operating constraints included in the backup generator model. A schematic of the power system including the backup generator is provided in Figure 2.12.

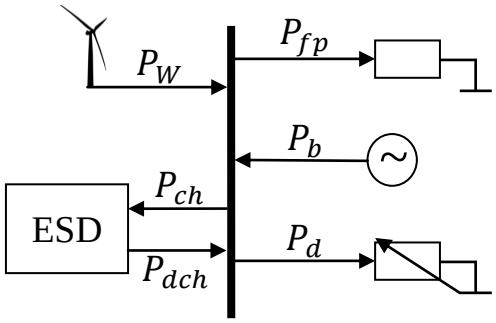


Figure 2.12 – Schematic of the modeled power system with backup generation.

The power balance equation for the system is given by:

$$P_{ch} + P_d - P_b - P_{dch} - P_u = P_w - P_{fp}\,. \tag{2.48}$$

Often in remote power systems the backup generator is powered by a DGS. The backup generator provides an easily controllable and predictable power source to help meet system demand. However, when multiple generation sources are operated in a power system, a control strategy is required to dispatch generators to meet the local electrical demand. The operational strategy used in this study is to minimize fossil fuel consumption and GHG emissions by dispatching the ESD first. The backup generator is only used if there is additional deficit power that cannot be met with the power available from the ESD, or if the deficit exceeds the maximum discharge rating of the store.

$$P_b(\bar{u}_{\tau,s}) = \begin{cases} P_{R,b} & for\ \left|P_{net}(\bar{u}_{\tau,s})\right| \geq \eta_{dch} P_{ESD}(\bar{u}_{\tau,s}) + P_{R,b} \\ P_b & for\ \eta_{dch} P_{ESD}(\bar{u}_{\tau}) < \left|P_{net}(\bar{u}_{\tau,s})\right| < \eta_{dch} P_{ESD}(\bar{u}_{\tau,s}) + P_{R,b} \\ 0 & for\ \left|P_{net}(\bar{u}_{\tau,s})\right| \leq \eta_{dch} P_{ESD}(\bar{u}_{\tau,s}) \end{cases} \tag{2.49}$$

In Eq. (2.49), $P_b$ is defined as the difference in deficit power and available storage power including efficiency loss, $P_b = \left|P_{net}(\bar{u}_{\tau,s})\right| - \eta_{dch}P_{ESD}(\bar{u}_{\tau,s})$.

If the deficit power is greater than the maximum combined power available from both the backup generator and the ESD there is some demand that is unmet. Therefore, a new definition of the unmet power is required to take into account the contribution of the backup generation. The following expression represents the unmet demand including the operation of the backup generator:

$$P_u(\bar{u}_{\tau,s}) = \begin{cases} P_u & for\ \left|P_{net}(\bar{u}_{\tau,s})\right| > \eta_{dch}P_{ESD}(\bar{u}_{\tau,s}) + P_{R,b} \\ 0 & for\ \left|P_{net}(\bar{u}_{\tau,s})\right| \leq \eta_{dch}P_{ESD}(\bar{u}_{\tau,s}) \end{cases} . \quad (2.50)$$

In Eq. (2.50) $P_u$ is defined as the difference between the deficit power and the maximum available power given by $\left|P_{net}(\bar{u}_{\tau,s})\right| - (\eta_{dch}P_{ESD}(\bar{u}_{\tau,s}) + P_{R,b})$.

The expected value of the backup power supplied and the unmet demand for the storage period are calculated with the distribution of mean wind speeds. These are included in the performance metrics of the wind-storage system.

$$P_b(u_\tau) \equiv E[P_b(\bar{u}_\tau)] = \int_0^\infty P_b(\bar{u}_{\tau,s})p(\bar{u}_\tau)d\bar{u}_\tau, \quad (2.51)$$

$$P_u(u_\tau) \equiv E[P_u(\bar{u}_\tau)] = \int_0^\infty P_u(\bar{u}_{\tau,s})p(\bar{u}_\tau)d\bar{u}_\tau. \quad (2.52)$$

## 2.9 Conclusion

In this chapter a probabilistic methodology is developed based on previous work done in [17]. A probabilistic model of a wind-storage system operating in an isolated electrical network is presented. Spectral analysis is employed to investigate the statistical characteristics of wind speed and the excursions of SOC over the specified storage period. These statistical characteristics are used to estimate the required storage size and analyze the adequacy of power system components for a specified firm power commitment. The operational strategy of the ESD is to supply a constant firm power

output to the electrical load. A simple model of a backup generator is included in the method to represent remote power systems that operate a DGS to meet some of the electrical demand.

The main assumptions used in the probabilistic method are listed below.

- The ESD operates in a steady state over the storage period.
- Mean wind speeds of the storage period can be modeled by a Weibull distribution.
- Wind speeds within the storage period can be modeled by a normal distribution.
- The coefficient of variation is constant and independent of the averaging time scale.
- The storage capacity can be calculated by scaling the standard deviation of the excursions in SOC by a factor referred to as the confidence level.

In the next chapter a validation study and sensitivity analysis are conducted to investigate the accuracy of the probabilistic method compared to a time sequential method.

# 3 VALIDATION STUDY AND SENSITIVITY ANALYSIS

## 3.1 Introduction

In this chapter a validation study and sensitivity analysis of the estimates calculated in the probabilistic approach for the power system performance metrics are provided. The purpose of the validation study is to investigate the accuracy of the probabilistic approach by a direct comparison between the probabilistic estimates and the predicted metrics from a time sequential simulation method. The sensitivity of the accuracy of the probabilistic estimates for various system properties such as installed wind capacity and firm power commitment levels are provided in Section 0. The accuracy of the probabilistic estimates of system metrics is shown to be dependent on the confidence level and a method to minimize the residuals of the predicted metrics is developed to determine the correct value for $\gamma$ in the calculation of the required storage size.

## 3.2 Time sequential simulation methodology

In this section a deterministic method used to evaluate a remote power system with wind generation and energy storage is described. The method is based on a time sequential simulation of an isolated electrical network consisting of wind generation, a diesel backup generator, and an energy storage device. These three power system components are operated to deliver a constant firm power commitment to the local grid. When sizing the storage capacity with a time domain approach the storage capacity is required as an external input. Traditionally, the power system metrics are solved iteratively for a range of storage capacities until an adequate size for the particular system configuration is found.

The time sequential simulation method calculates the states of the system variables at each incremental time step. The power system used in the time domain method is the same as the probabilistic approach and is shown mathematically in Eq. (2.48) and

schematically in Figure 2.12. The ESD is operated to deliver firm power to the local grid and the backup generator is operated according to the same control strategy described in Section 2.8.

To evaluate the power system in the time domain the initial SOC, $E(t_0)$, of the ESD is required as well as the maximum power ratings of the ESD, backup generation capacity, the ESD efficiency, installed wind capacity and the firm power commitment. At each incremental time step the available wind power is calculated from the historical wind speed data and the wind turbine power curve described in Section 2.4. The net system power is calculated by subtracting the firm power commitment from the wind power. During times of net surplus and deficit power the same ESD operational characteristics applied in the probabilistic method are used in the time domain approach. However, an additional control algorithm is used in the simulation to determine the current SOC and to dispatch power so the ESD is not overcharged or discharged past the lowest allowed limit. Details of the algorithms used in the time domain method for the ESD operation and the calculation of system performance metrics are provided in Appendix H. The main results from the time domain method are the average values of: $P_d$, $P_u$, $P_{ch}$, $P_{dch}$, $P_b$, $t_{ch}$, $t_{dch}$, $t_{full}$, and $t_{empty}$.

## 3.3 Implementation

Both the probabilistic and time sequential methods are implemented in a MATLAB environment using an object oriented programming approach. Flowcharts for the probabilistic and time sequential simulation methodology are provided in Figure 3.1 and Figure 3.2, respectively.

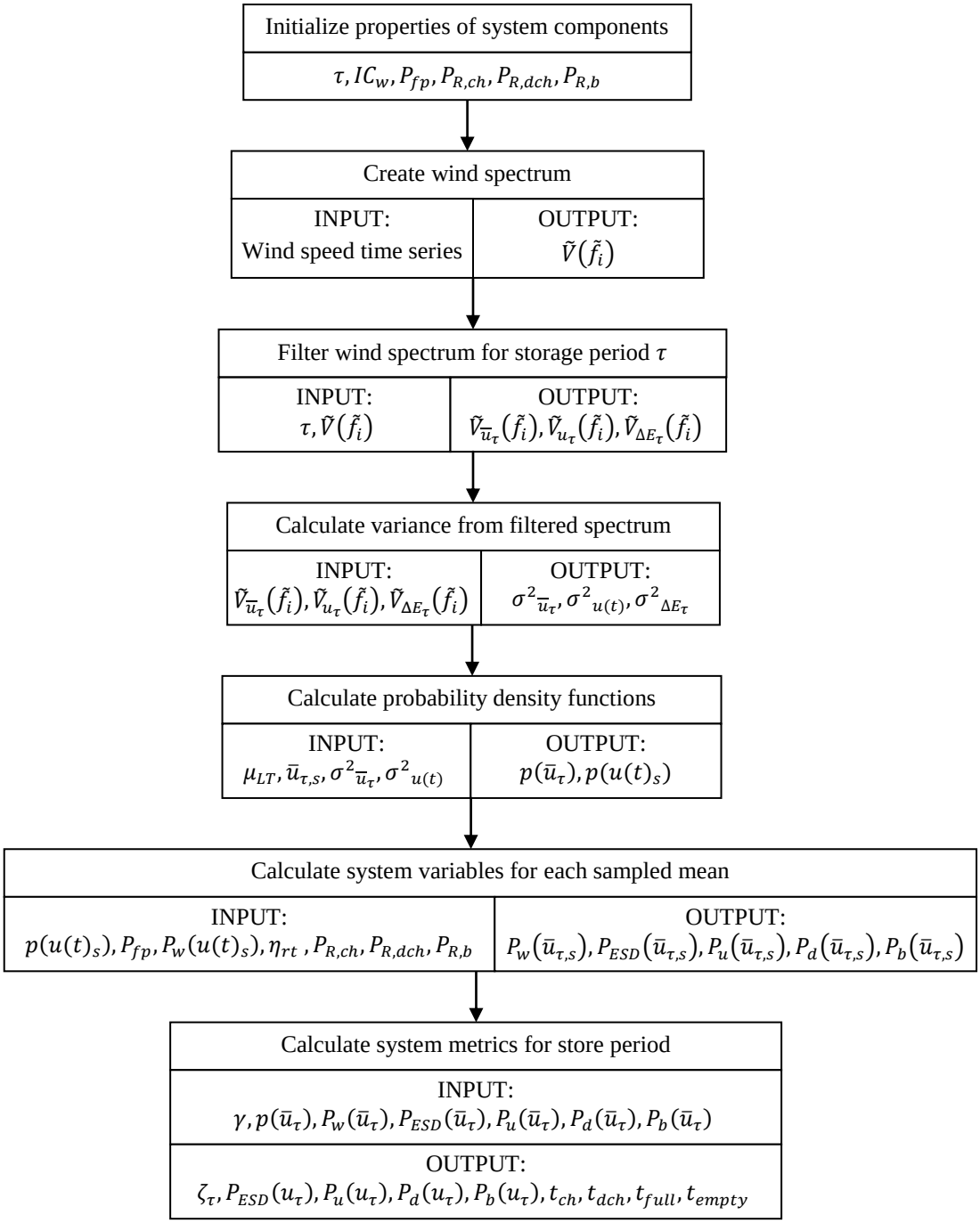


Figure 3.1 – Flowchart of the probabilistic methodology.

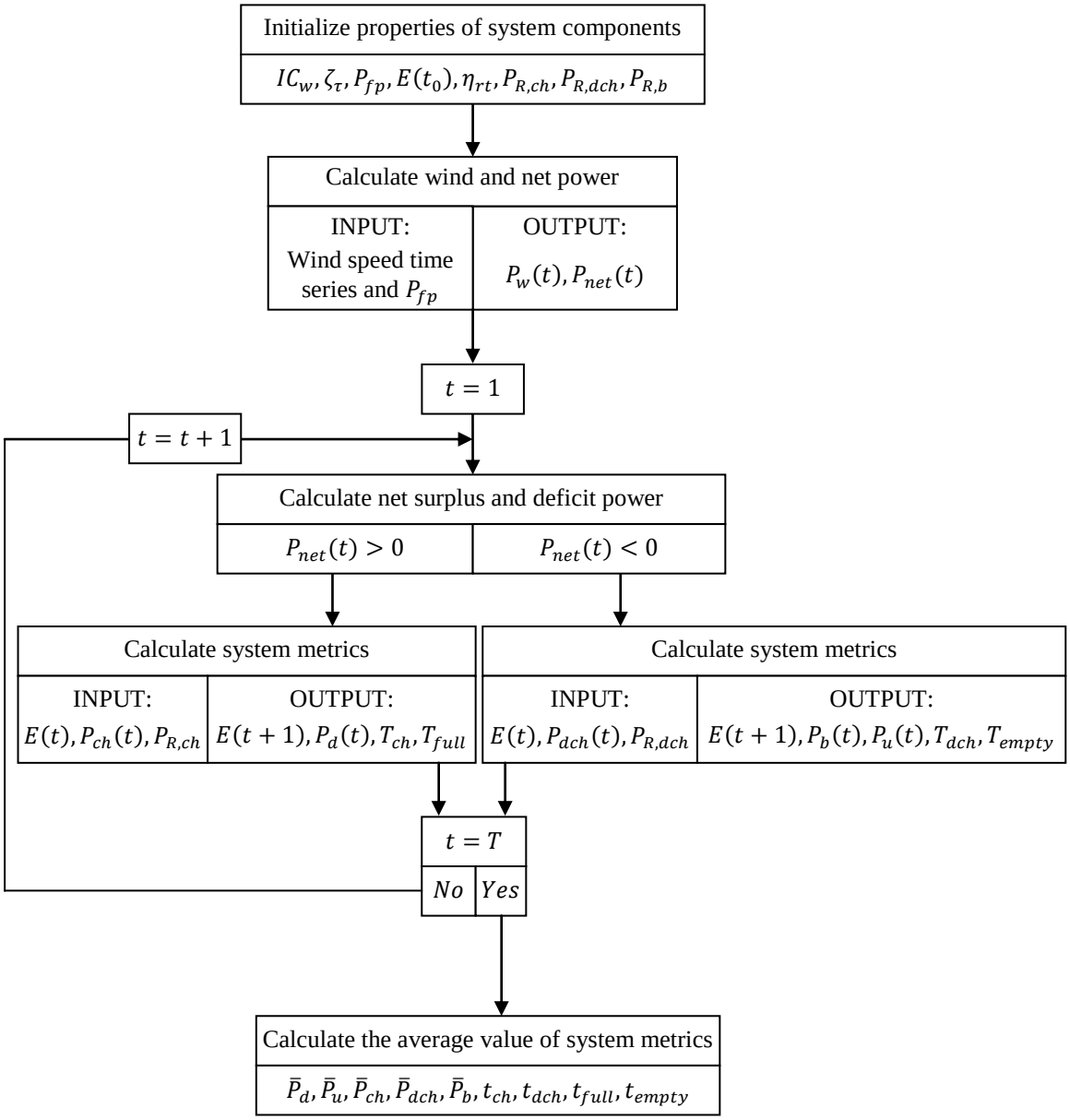


Figure 3.2 – Flowchart of the time sequential method.

## 3.4 Validation study

In this section a validation study is presented to compare the probabilistic and time sequential simulation methods in evaluating power system performance. The probabilistic method first estimates the required storage capacity, which is then used as an input in the time sequential model. The system metrics from both methods are recorded and compared.

### 3.4.1 Wind speed data

The wind speed data used in the study were obtained from Environment Canada's National Climate Archive for Sandspit, British Columbia. Wind speeds were recorded at a height of 10 meters at hourly intervals from 1980 to 2001, inclusive. The data set was visually inspected and gaps due to missing data were replaced by interpolating between hours.

A logarithmic profile was used to estimate wind speeds from the reference height at which the data was recorded to the wind turbine hub height. The equation used to adjust wind speeds to a height $z$ from a reference height of $z_r$ is given by:

$$u(z) = u(z_r)\frac{\ln\left(\frac{z}{z_0}\right)}{\ln\left(\frac{z_r}{z_0}\right)}. \tag{3.1}$$

In Eq. (3.1) $z_r$ is equal to 10 m, $z$ is the wind turbine hub height of 80 m, and $z_0$ is a terrain roughness parameter, which is chosen to be 0.01 corresponding to wind conditions in coastal areas [19,23].

### 3.4.2 Power system parameters

An isolated power system is modeled with 1 MW of installed wind capacity, a firm power commitment of 400 kW, no available backup generation, and no ESD charging or efficiency constraints. The probabilistic method is first used to compute a required storage capacity for a specified storage period and confidence level. The confidence level, $\gamma$, is set to the value suggested in [18] to a factor of 2, representing an interval of

$\pm\sigma_{\Delta E_t}$, to size the storage capacity in the probabilistic method. Since there are no ESD efficiency or power rating constraints included in this example, the value of $\alpha$ is equal to 1.

### 3.4.3 Confidence level calculation

In this section the results for the validation study, including a proposed method to calculate the confidence level, is presented. The first plot in Figure 3.3 shows the estimated storage capacity from the probabilistic method for different storage periods. The other plots in Figure 3.3 and Figure 3.4 show the accuracy of the probabilistic estimates compared to the time sequential results for the power system performance metrics. The curtailed power metric refers to the power sent to the dump load, $P_d$, and the ESD power is the average power that is sent to or taken from the ESD, as predicted by both the time and probabilistic methods. The time domain method tracks the charging and discharging powers over the simulation period and calculates the time average, which are approximately equal in magnitude. Therefore, the figures show only the discharge power calculated from the time sequential method plotted against probabilistic estimate of $P_{ESD}(u_\tau)$.

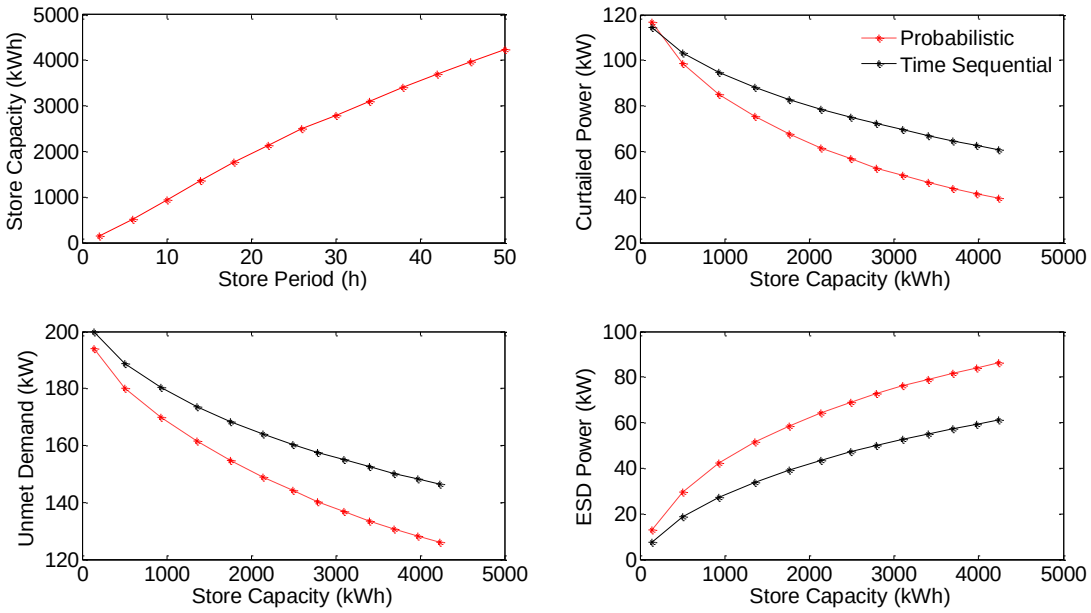


Figure 3.3 – Performance metrics for 1000 kW installed wind capacity, 400 kW firm power, and $\gamma = 2$.

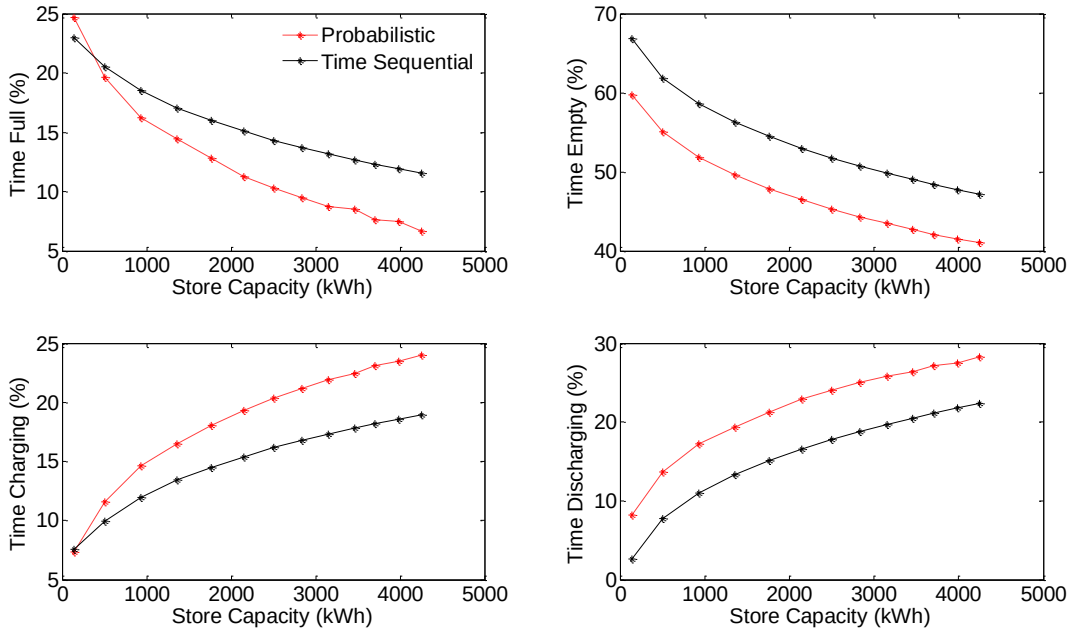


Figure 3.4 – ESD utilization metrics for 1000 kW installed wind capacity, 400 kW firm power, and $\gamma = 2$.

Although the probabilistic approach predicts the overall trend of the system metrics, it overestimates the utilization of the ESD compared to the results attained from the time domain method. This suggests that the confidence level used to size the storage capacity was not adequate. Increasing the confidence interval will increase the estimated storage capacity from the probabilistic method. The revised ESD capacity will allow more power to be utilized by the ESD in the time sequential method, resulting in a decrease in the unmet and curtailed power metrics. Therefore, the confidence level serves as a calibrating parameter that should be set to a level that reduces the error in the probabilistic estimates of the performance metrics to a minimal value.

A method based on minimizing the root mean squared error (RMSE) is developed to find a confidence level that gives the most accurate probabilistic estimates. The RMSE is calculated by:

$$RMSE = \sqrt{\frac{1}{n}\sum_{1}^{n}\left(x_{t,i} - x_{p,i}\right)^2}, \tag{3.2}$$

where $n$ is the total number of storage periods investigated, and $x_{t,i}$ and $x_{p,i}$ represent the time simulation and probabilistic metrics for each storage period. The RMSE gives an aggregated value for the residuals of the probabilistic estimates and is used to give a general metric of the predictive power of the probabilistic method.

The confidence level is varied from 2 to 8 while keeping all other power system components constant. The confidence level that produces the minimum RMSE value for all system metrics gives the most consistent estimates of the performance metrics. The results of the RMSE analysis for the system described in Section 3.4.2 are shown Figure 3.5.

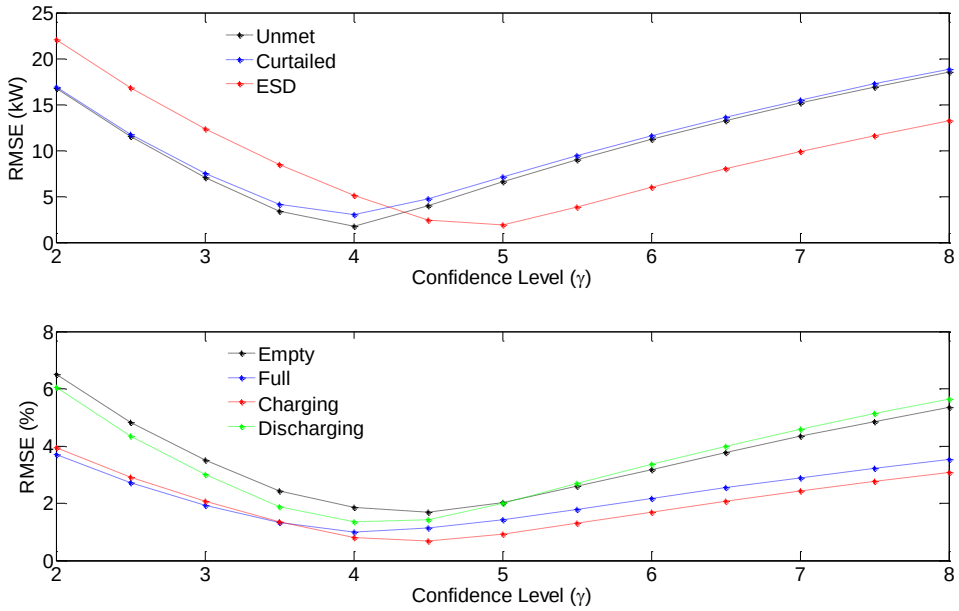


Figure 3.5 – RMSE of system performance metrics for various confidence levels.

The results of the RMSE analysis show that an appropriate confidence level for estimating the required storage capacity with the probabilistic method is in the range of 4 to 5. Analyzing the power system again with a confidence level equal to 4 produces accurate probabilistic estimates of performance metrics compared to the time domain calculations, which can be seen in Figure 3.6 and Figure 3.7. The first plot in Figure 3.6 shows the required storage capacity corresponding to the new confidence level value.

The results from the validation analysis show that the accuracy of the probabilistic estimates is dependent on the value of the confidence level. The range of $\gamma$ that gives the most accurate probabilistic estimates agrees with previous work in [25,26], where the authors have calculated the required reserve capacity due to the integration of wind generation in a power system.

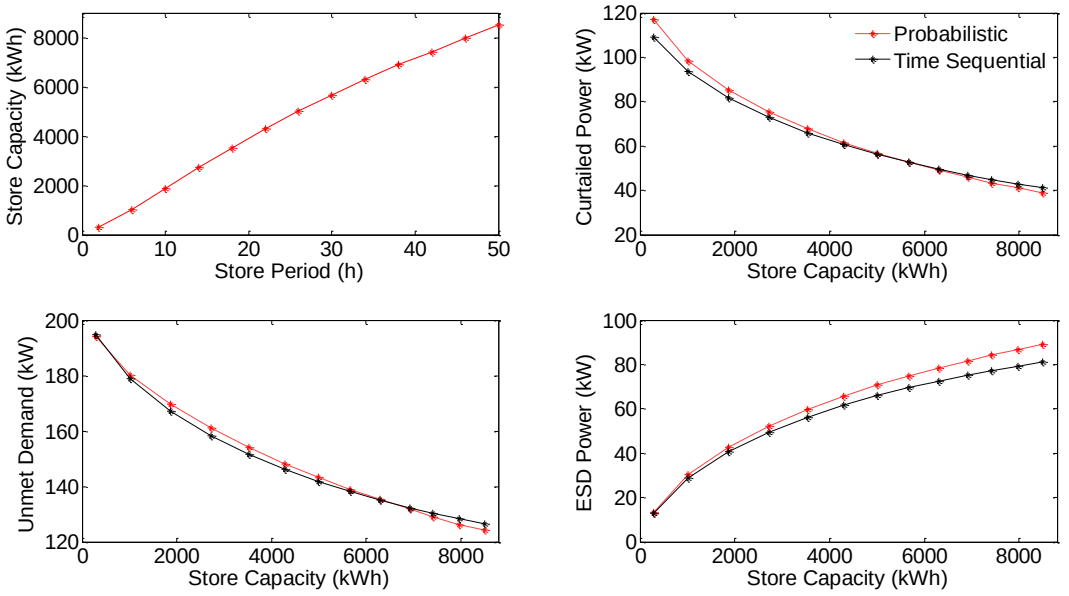


Figure 3.6 – Performance metrics for 1000 kW installed wind capacity, 400 kW firm power, and $\gamma = 4$.

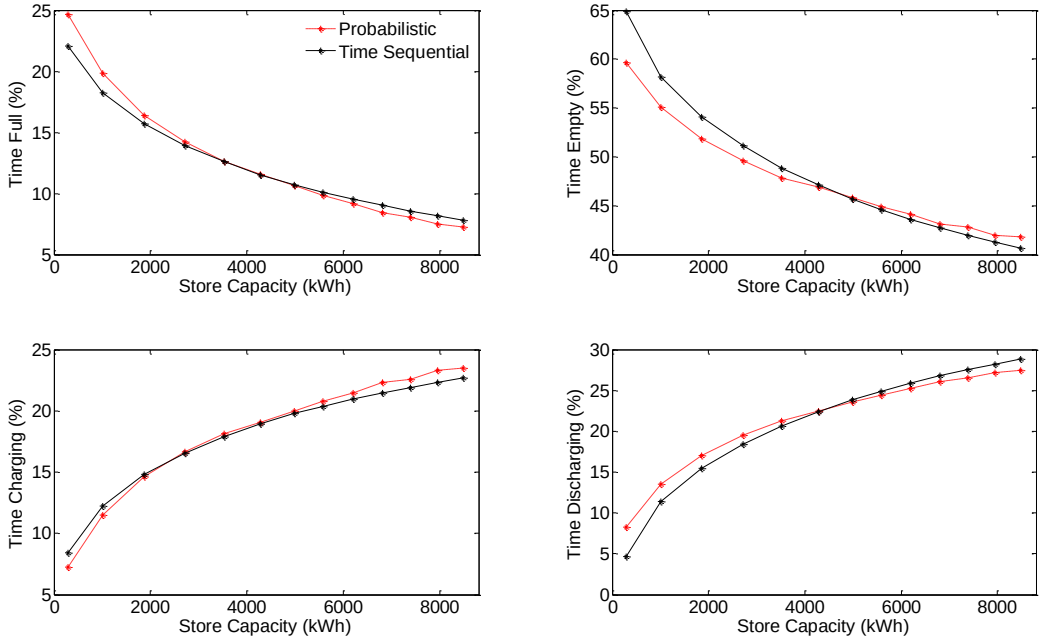


Figure 3.7 – ESD utilization metrics for 1000 kW installed wind capacity, 400 kW firm power, and $\gamma = 4$.

## 3.5 Sensitivity analysis

In this section a sensitivity analysis of the accuracy of the probabilistic performance estimates for various system configurations is presented. The accuracy of the performance metrics calculated from the probabilistic method are investigated for different levels of installed wind capacity, firm power commitment, ESD maximum charging and discharging rates, ESD efficiency, and backup capacity. The various system configurations used in the sensitivity analysis are shown in Table 3.1. The confidence level used for Cases A thru E is the value calculated in Section 3.4.3 that minimized the deviation of the probabilistic estimates from those calculated from the time simulation method. The main results for each case are presented in the following sections with a discussion and conclusion of the sensitivity analysis provided at the end of the chapter.

Table 3.1 – Power system configurations used in the sensitivity analysis

| CASE | γ | $P_{R,w}$ | $P_{fp}$ | $P_{R,ESD}$ | $\eta_{rt}$ | $P_{R,b}$ |
|---|---|---|---|---|---|---|
| A | 4 | 700:1500 | 400 | ∞ | 1 | 0 |
| B | 4 | 1000 | 200:600 | ∞ | 1 | 0 |
| C | 4 | 1000 | 400 | 100:1000 | 1 | 0 |
| D | 4 | 1000 | 400 | ∞ | 0.5:1 | 0 |
| E | 4 | 1000 | 400 | ∞ | 1 | 300:500 |

.

### 3.5.1 Case A: Installed wind capacity

In the first case of the sensitivity analysis, the installed wind capacity of the power system is varied from 700 kW to 1500 kW in 100 kW increments while all other power system components are kept constant. For each value of installed wind capacity the probabilistic method estimates the performance metrics and the required storage capacity. The ESD capacity is used as an input in the time domain method and the performance metrics of both methods are compared.

For low levels of installed wind capacity, the probabilistic estimate of the power utilized by the wind-storage system is greater than the time domain calculation, resulting in curtailed and unmet power values below those that would be expected from the time domain calculations. A graphical comparison of system metrics calculated from both methods for an installed wind capacity of 700 kW is shown in Figure 3.8.

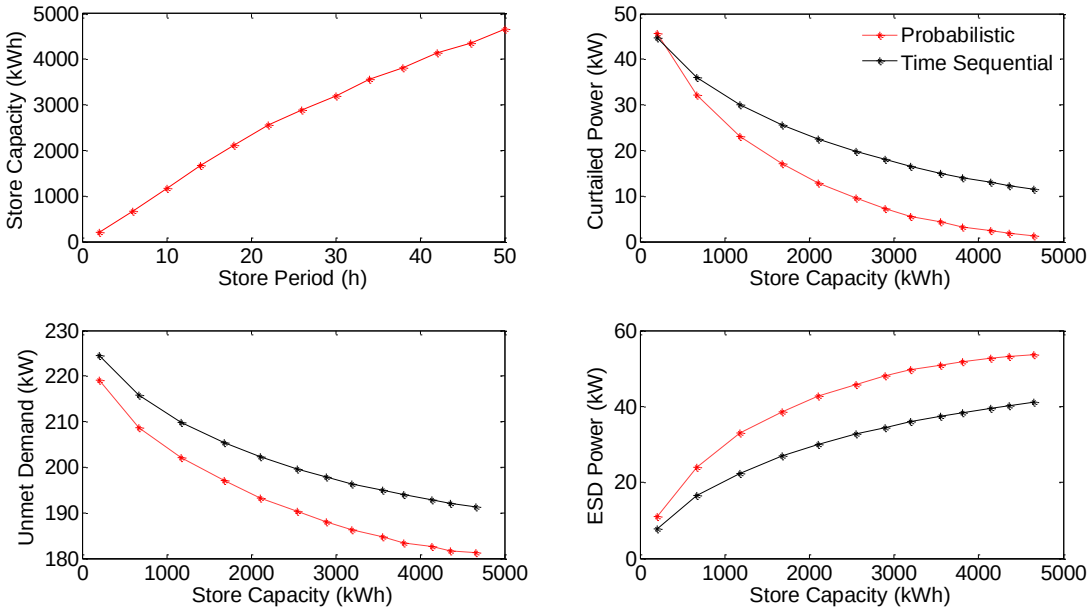


Figure 3.8 – Performance metrics for 700kW installed wind capacity, 400 kW firm power, and $\gamma = 4$.

In contrast, for levels of wind capacity exceeding 1 MW, the probabilistic method underestimates the power utilized by the ESD, resulting in probabilistic estimates of the curtailed and the unmet demand values that exceed the time domain calculations. An example of the system metrics calculated by both methods for an installed wind capacity of 1300 kW is shown in Figure 3.9.

It should be noted that the probabilistic method follows the same trend as the time sequential method for all installed wind capacity values used in the sensitivity analysis. Furthermore, the expected relationships between installed wind capacity and performance metrics are observed. For example, as wind capacity is increased the curtailed power increases and the unmet demand levels decrease. The RMSE of the probabilistic estimates for various installed wind capacities are shown in Figure 3.10.

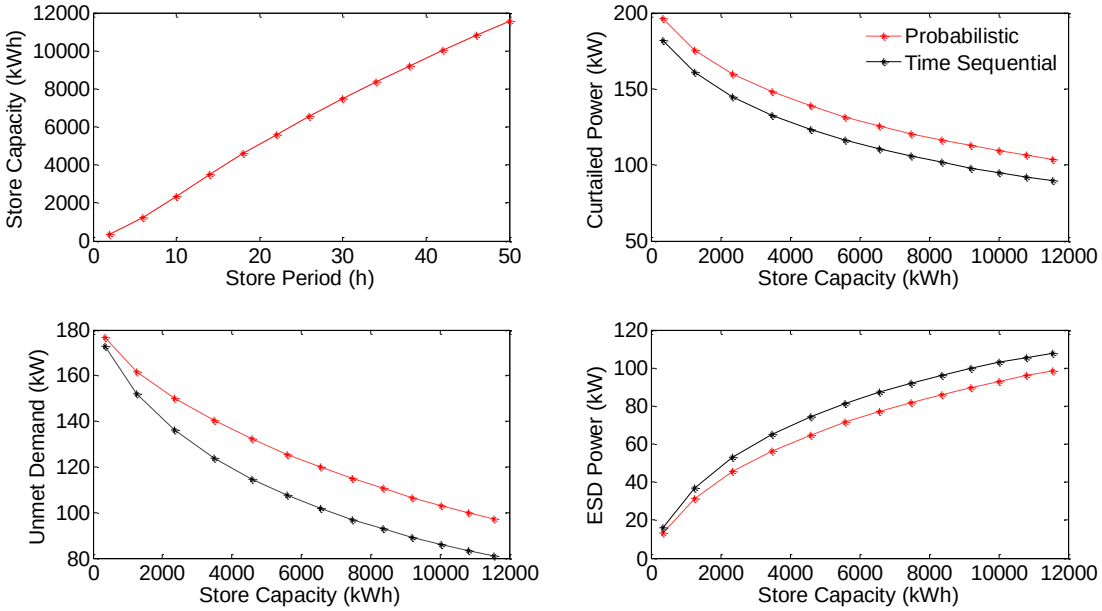


Figure 3.9 – Performance metrics for 1300 kW installed wind capacity, 400 kW firm power, and $\gamma = 4$.

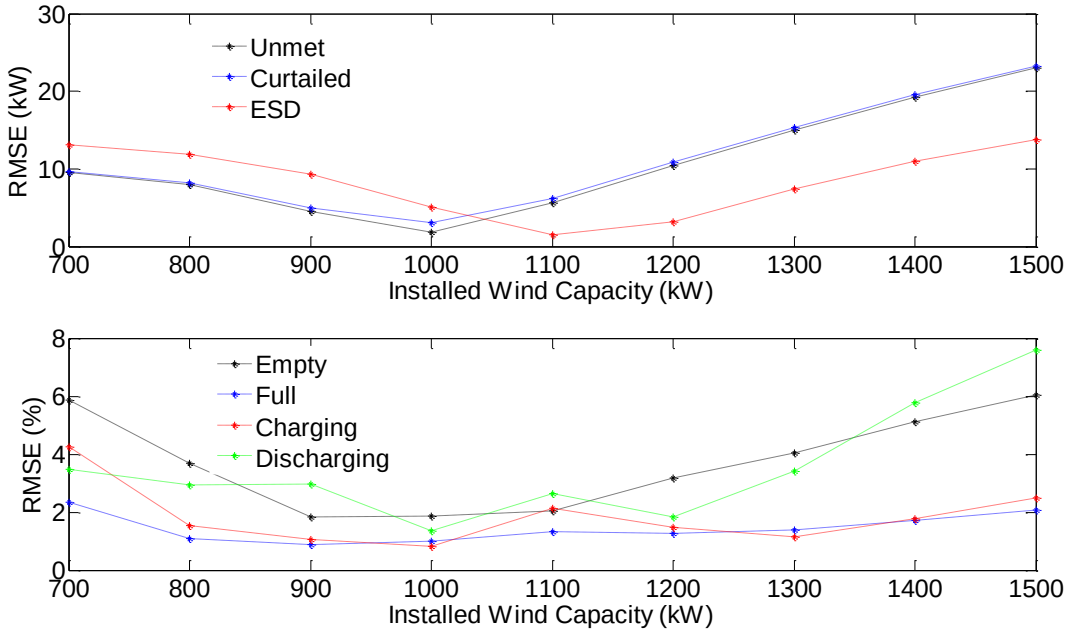


Figure 3.10 – RMSE analysis for Case A.

### 3.5.2 Case B: Firm power commitment

In the second case studied in the sensitivity analysis, the firm power commitment is varied from 200 kW to 600 kW in 100 kW increments while keeping all other system components constant. Varying the firm power commitment has the reverse effect as varying the installed wind capacity. For levels of firm power commitment below 400 kW the probabilistic method consistently estimates the value of $P_{ESD}$ to be much lower than that calculated by the time domain method, resulting in an over-estimation of $P_d$ and $P_u$. For levels of firm power above 400 kW the value of $P_{ESD}$ calculated from the probabilistic method exceeds the time domain prediction, resulting in estimates of $P_d$ and $P_u$ that are low in comparison. The RMSE analysis for various levels of $P_{fp}$ is plotted in Figure 3.11, showing a relative measurement of the deviations of the probabilistic estimates as a function of firm power.

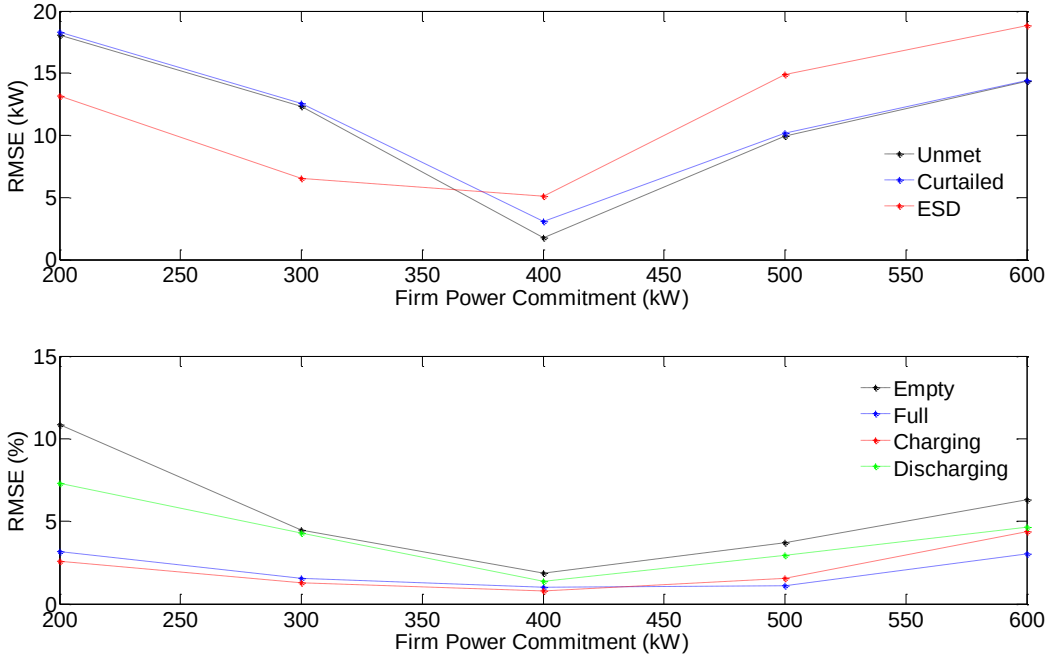


Figure 3.11 – RMSE analysis for Case B.

### 3.5.3 Case C: ESD charging and discharging rates

In the third case investigated in the sensitivity analysis, the maximum charging and discharging rates are varied from 100 kW to 1000 kW in increments of 100 kW while keeping all other system components constant.

As the charging and discharging rates are decreased the surplus power that can be utilized by the storage device is limited. This reduces the required storage size calculated in the probabilistic method by the factor denoted as $\alpha$ and given by Eq. (2.43). Due to the decreased ESD capacity and the increased charging and discharging power constraints, the curtailed power and unmet demand values are increased. The required storage capacity and system performance metrics are shown in Figure 3.12 for $P_{R,ch}$ and $P_{R,dch}$ equal to 200 kW.

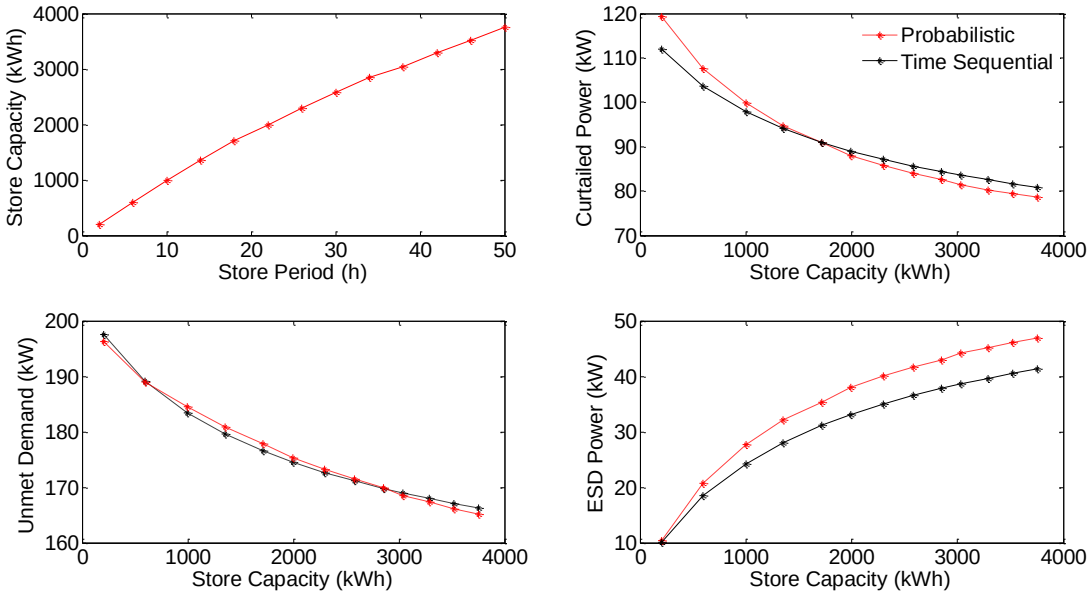


Figure 3.12 – Performance metrics for a maximum ESD power rating of 200 kW.

The accuracy of the probabilistic estimates for the range of $P_{R,ch}$ and $P_{R,dch}$ is consistent with the calculations from the time domain calculations. The results from the RMSE analysis are shown in Figure 3.13.

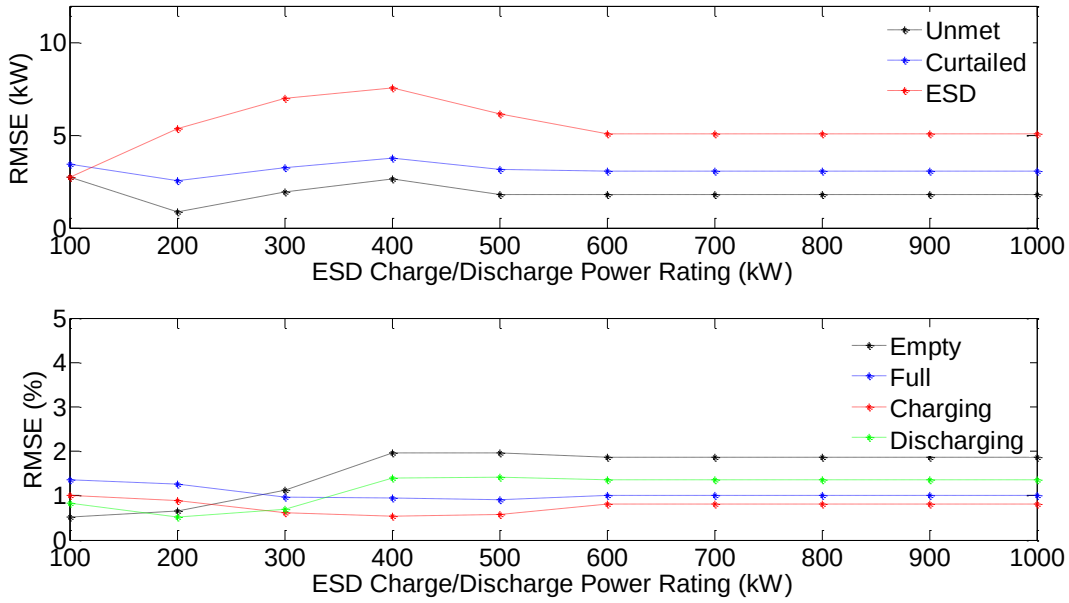


Figure 3.13 – RMSE analysis for Case C.

### 3.5.4 Case D: ESD efficiency

In the fourth case in the sensitivity analysis, the ESD round-trip efficiency is varied from 50% to 100% in 10% increments while keeping all other system components constant. The probabilistic estimates of the system performance metrics are compared to the time domain simulation results for the various store efficiencies.

Varying the ESD efficiency has little effect on the accuracy of the system metrics for $P_d$, $P_u$, and $P_{ESD}$. The average deviation for all storage capacities ranges from approximately 2 to 4 kW when varying the ESD efficiency value. Figure 3.14 shows a comparison of the probabilistic estimates and the time domain calculations of system metrics for $\eta_{rt}$ equal to 60%. The accuracy of the ESD utilization metrics, specifically $t_{dch}$ and $t_{full}$, perform relatively poorly for low efficiency values. The probabilistic estimate of the time the ESD spends in the discharge state is consistently greater than the calculation from the time domain for low efficiency values as seen in Figure 3.15. The overall deviations are shown in the RMSE analysis of Figure 3.16.

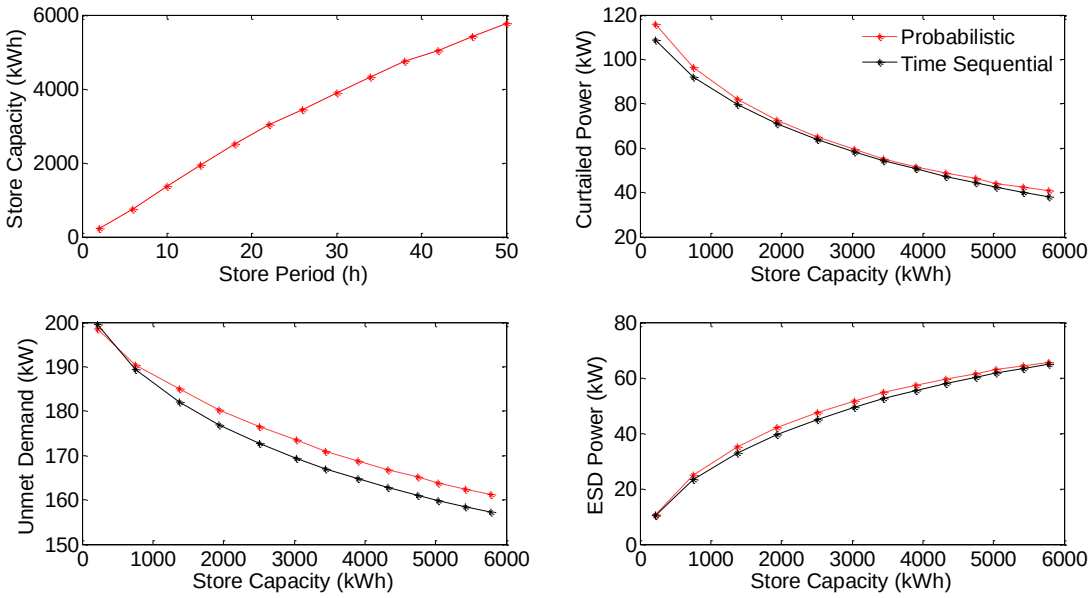


Figure 3.14 – Performance metrics for an ESD round-trip efficiency of 60%.

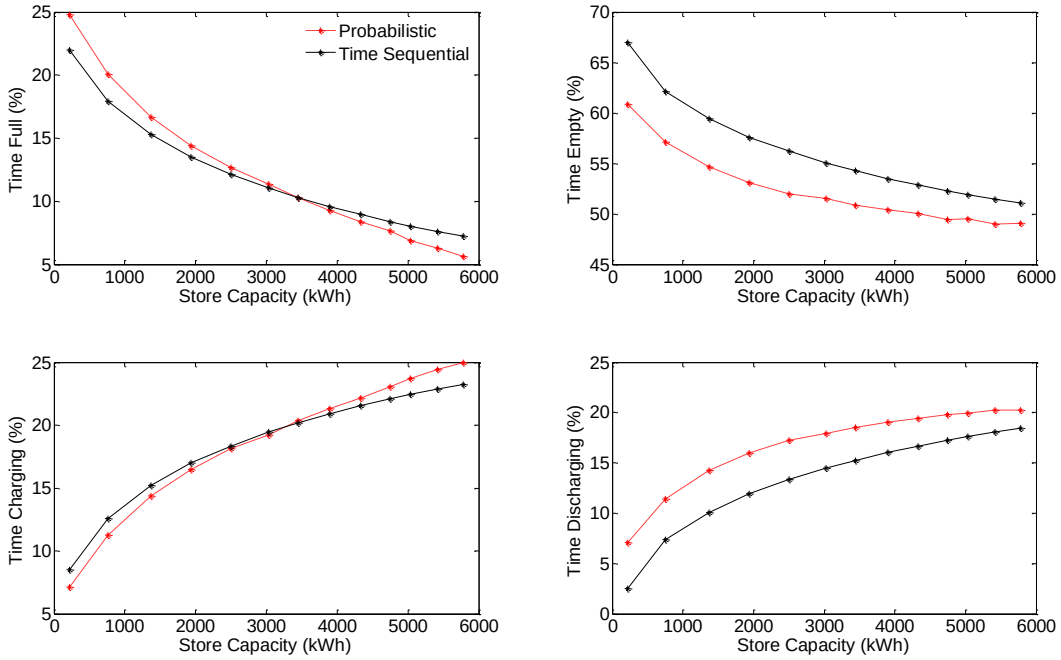


Figure 3.15 – ESD utilization metrics for round-trip efficiency of 60%.

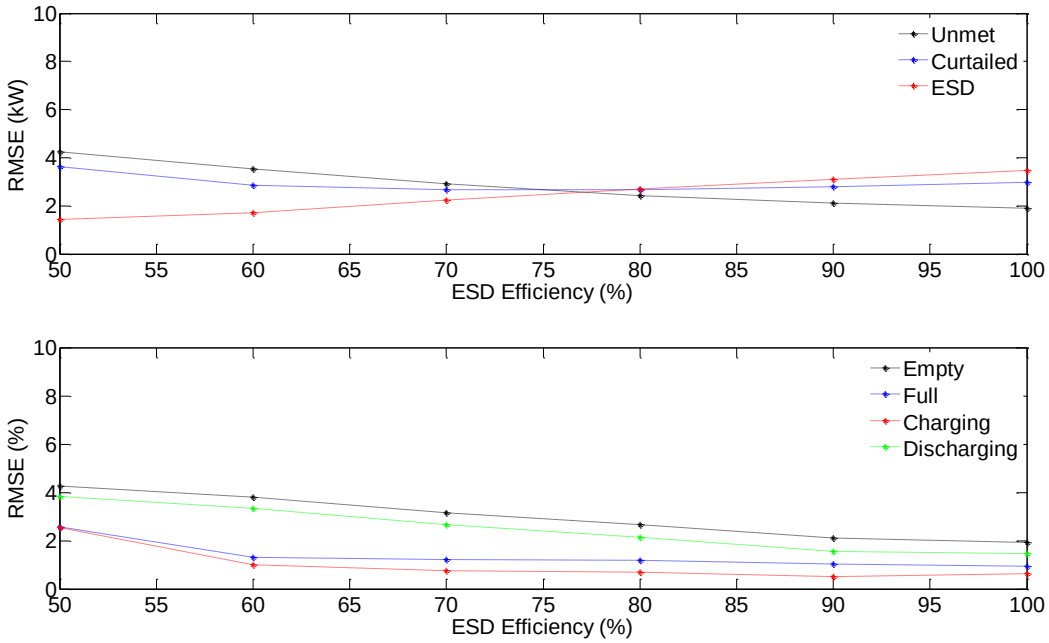


Figure 3.16 – RMSE analysis for Case D.

### 3.5.5 Case F: Backup generation

In the final case of the sensitivity analysis, the backup generation capacity is varied from 300 kW to 500 kW in 50 kW increments while all other system components are kept constant. The power system performance metrics are calculated for each backup generation capacity using the probabilistic and time sequential methodologies and the estimated values are compared.

Since the backup generator is operated during times of deficit power, the only system metrics that are affected in the analysis are the unmet demand and the amount of backup power sent to the local grid, $P_u$ and $P_b$. The probabilistic method over-estimates the backup power sent to the grid for low capacity values, resulting in increased errors in the prediction of $P_u$. An example is shown in Figure 3.17 for a backup generation capacity of 350 kW. As the backup capacity is increased to cover the firm power commitment, the unmet demand approaches 0 kW and the accuracy of the probabilistic estimates of $P_u$ and $P_b$ is increased. An example is provided for a backup capacity of 400 kW in Figure 3.18.

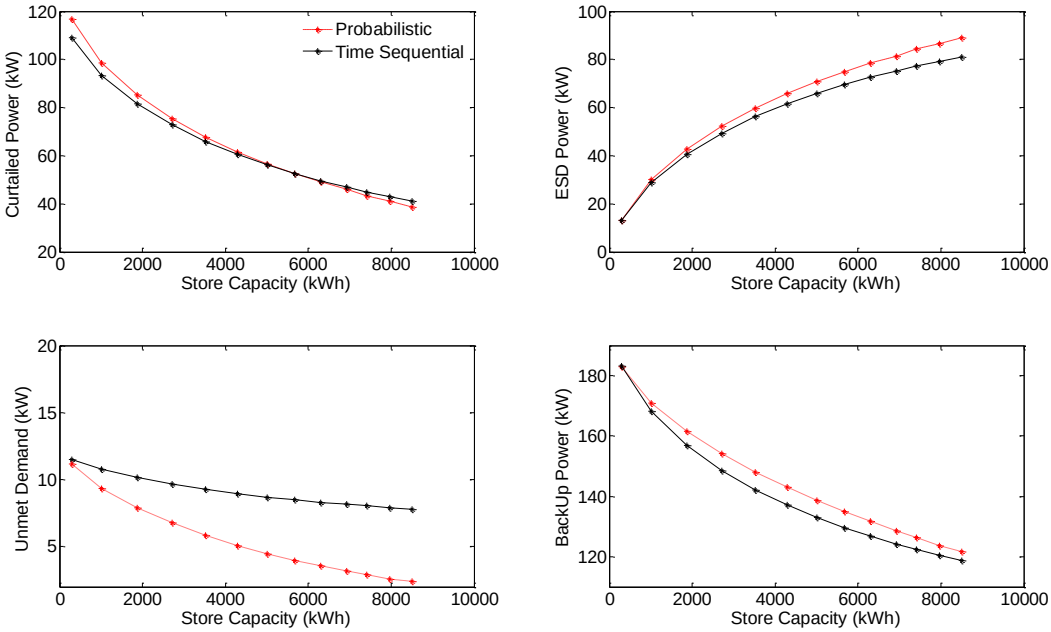


Figure 3.17 – Performance metrics for a backup generation capacity of 350 kW.

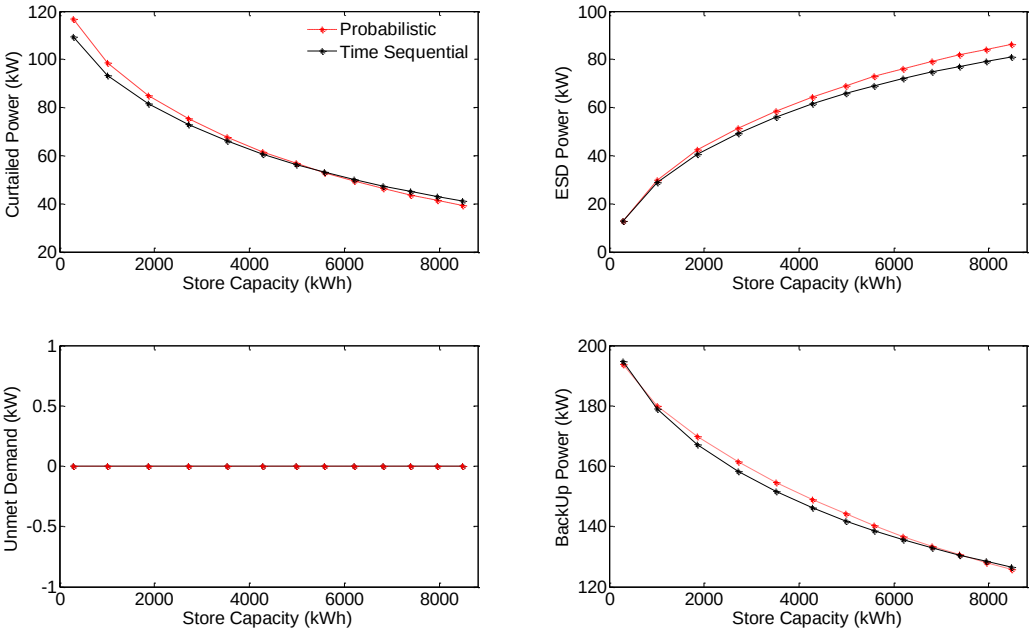


Figure 3.18 – ESD utilization metrics for a backup generation capacity of 400 kW.

The general trend of the probabilistic methods accuracy in predicting the power system performance metrics for varying backup generation capacities is reflected in the RMSE analysis in Figure 3.19.

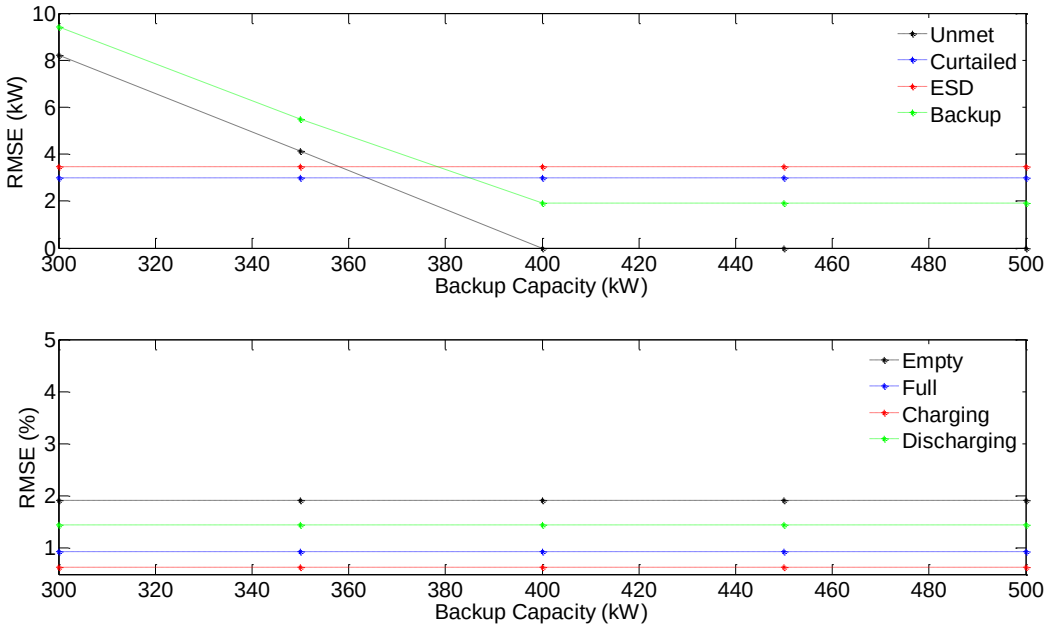


Figure 3.19 – RMSE analysis for Case E.

## 3.6 Conclusions and discussion

The validation study and sensitivity analysis presented in this chapter were conclusive of two main findings: the confidence level used to size the required storage capacity is a key parameter in the accuracy of the probabilistic estimates of system performance metrics, and the accuracy of the estimates are highly sensitive to the power system configuration. The confidence level is used as a calibration parameter, matching the probabilistic estimates to calculations from a time sequential method. The confidence level giving the most accurate estimates of the performance metrics is then used in subsequent analysis. This limits the application of the probabilistic method to analyze power system performance since a comparison to a time sequential model is necessary to compare the accuracy of the results.

Overall, the probabilistic method gives a fairly accurate representation of the behaviour of the power system once the appropriate confidence level is found. Furthermore, the computational speed is significantly improved with the probabilistic method, with program execution approximately 20 times faster than the time simulation method.

The main discrepancies between the two methods can be attributed to the probabilistic representation of the wind power and its dependence on the storage period used in the analysis. The variance values used to construct the PDFs of wind speed are calculated from the wind speed spectrum and the filters described in Appendices A and B for a specified storage period. The shape of the distribution of $p(\bar{u}_\tau)$ and $p(u(t))$ depend on the storage period, which directly affects the expected value of wind power and consequently, the expected surplus and deficit power values. For example, for the system described in Section 3.4.2 the probabilistic method predicts the expected value of wind power to be in the range of 313 kW to 322 kW for storage periods ranging from 2 to 50 hours. This is in contrast to the time sequential model that calculates a constant wind power for all storage periods of 314 kW.

When conducting future resource planning studies for remote power systems, an optimization routine is required to determine the optimal component sizing that minimizes the overall system cost. Currently, software packages solve the optimization problem by an iterative procedure in the time domain, calculating the optimal generation and storage capacities that minimize the systems net present cost while satisfying system performance constraints [11]. The probabilistic method is limited in this application since a time sequential method is required to find the correct confidence level for each power system configuration, proving to be computationally redundant.

# 4 HAIDA GWAII: A CASE STUDY

## 4.1 Introduction

In this chapter a techno-economic evaluation of integrating wind power and energy storage in a remote power system using the probabilistic method is presented. The main objective of the case study is to illustrate how the probabilistic method can be implemented to determine the potential benefit of incorporating wind power and an ESD in a remote power system to displace current fossil fuel generation. The isolated electrical network studied in the analysis is located on Haida Gwaii, British Columbia.

Haida Gwaii, also referred to as the Queen Charlotte Islands, is an archipelago of approximately 150 islands and is one of the 300 remote communities within Canada that is not connected to a major electrical grid. The islands are located approximately 400 km north of Vancouver Island and 150 km off the northwest coast of British Columbia, separated from the mainland by Hecate Strait. Over five thousand residents live on one of the two largest islands in the archipelago and are completely reliant on local generation to meet their electricity demand.

Currently, Haida Gwaii's electrical system is composed of two separate grids. The northern grid supplies electricity to the towns of Old Masset, Masset and Port Clemens, by diesel generation, referred to as the Masset DGS. The Masset DGS has a firm capacity of 8,874 kW, with an additional 2,500 kW of reserve capacity. A general schematic of the islands electrical generation resources and their location is shown in Figure 4.1. The southern grid supplies electricity to the communities of Skidegate, Queen Charlotte City and Tlell. Electricity generation in the south is dominated by hydro power produced at the Queen Charlotte Power Corporation (QCPC) facility, located at Mitchell Inlet on Moresby Island. The powerhouse at the hydro facility runs three 2 MW horizontal Francis turbines with an installed capacity of 5,700 kW, supplying almost 80% of the annual electricity delivered to the southern grid [27]. The southern grid also operates a

backup DGS located at the town of Sandspit. The Sandspit DGS is the smaller of the two diesel generating facilities with a firm capacity of 6,650 kW and an additional 2,500 kW of reserve capacity. Both the Masset and Sandspit DGS are owned and operated by BC Hydro, while the QCPC facility is owned and operated by EPCOR Power, an Independent Power Producer.

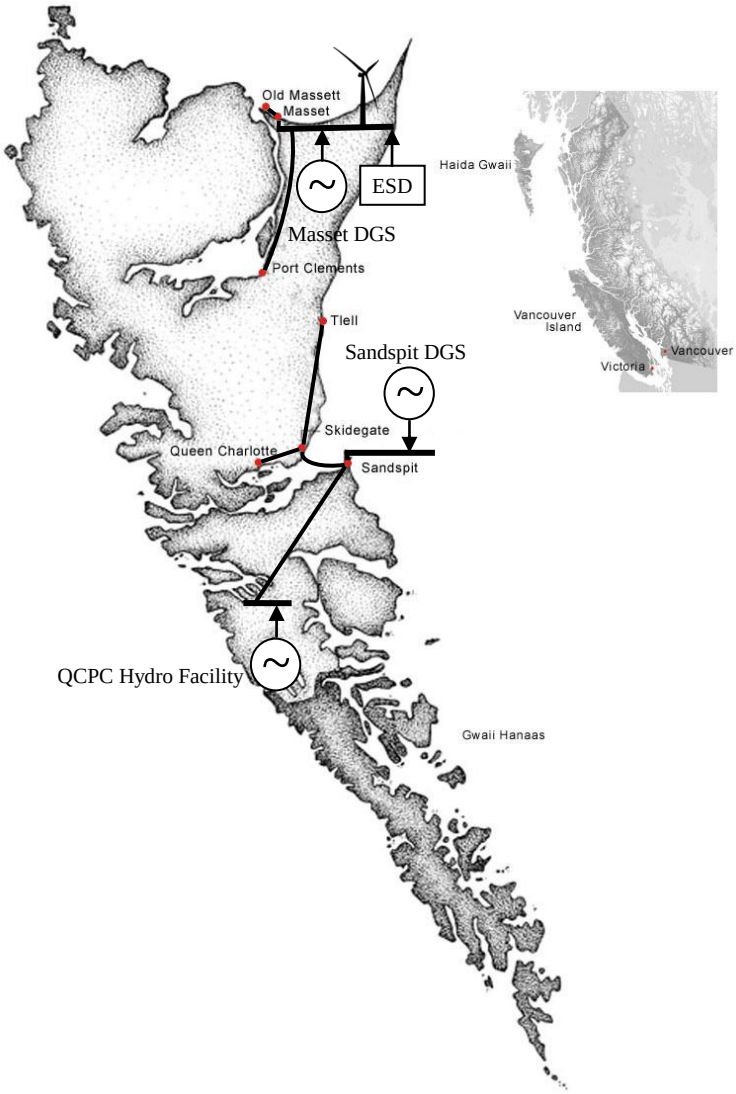


Figure 4.1 – Haida Gwaii generation asset map.

In November of 2008, BC Hydro released a draft Request for Proposals (RFP) seeking clean and cost effective alternatives for electricity generation on Haida Gwaii. Due to the high cost of energy and increased levels of GHG emissions associated with

diesel fuel, many renewable energy projects have been proposed for the region including generation from available resources such as: wave, tidal, hydro, biomass, wind and an option to link the electrical grids with an additional tie-line [28,29,30,31]. As of today, the RFP is still outstanding and the community is actively seeking alternative energy options.

Since the southern grid currently operates with contributions from renewable resources close to 80% of annual demand, the proposed case study investigates the benefits of integrating wind power and energy storage in the northern electrical grid. In the following section a techno-economic analysis of integrating wind power and energy storage in the Masset power system to displace existing diesel generation is provided. The power system is analyzed using the probabilistic method described in Chapter 2.

## 4.2 Masset DGS

In this section an overview of the current electrical generation resources, demand profile, and transmission constraints is provided for the northern grid. The current generational assets operating in the Masset DGS consists of 7 units of various ratings and manufactured models. In Table 4.1 a summary description of each unit's operational characteristics is provided.[1] The RFP states that the existing DGS units will remain as standby reserve capacity, black start, and reactive power support.

Table 4.1 – Masset DGS generation units [28].

| UNIT # | MAKE | RATING (KW) | CONDITION |
|---|---|---|---|
| MASG1 | MLW | 2108 | These units were commissioned to be replaced in 2008 due to mechanical degradation. |
| MASG2 | MLW | 2108 | |
| MASG3 | MLW | 2108 | |
| M125G1 | EMD | 2500 | Age: 21 to 30 years. |
| M172G1 | CAT | 850 | Age: < 10 years. |
| M173G1 | CAT | 850 | Age: < 10 years. |
| M174G1 | CAT | 850 | Age: < 10 years. |

[1] The different diesel generator manufacturers are: Electro Motors Division (EMD) of General Motors, Caterpillar (CAT), and Montreal Locomotive Works (MLW).

The northern grid distribution system is comprised of two overhead distribution feeder circuits, MAS 25F51 and MAS 25F52, of three-phase 25 kV and single-phase 14.4 kV distribution lines, with a transmission capacity of approximately 8,000 kVA [27]. Currently, maximum line loading levels for MAS 25F51 and 25F52 are approximately 3,300 kVA and 1,250 kVA, respectively [28]. Therefore, the proposed wind-storage system with an installed wind capacity of 1,000 kW should not cause any transmission congestion issues.

The peak load in 2008 was approximately 5.25 MW for the Masset DGS with a total generation of 27.5 GWh [27]. BC Hydro's forecasted energy load growth for the next 20 years in the northern grid is shown in Figure 4.2 and includes station service and transmission losses.

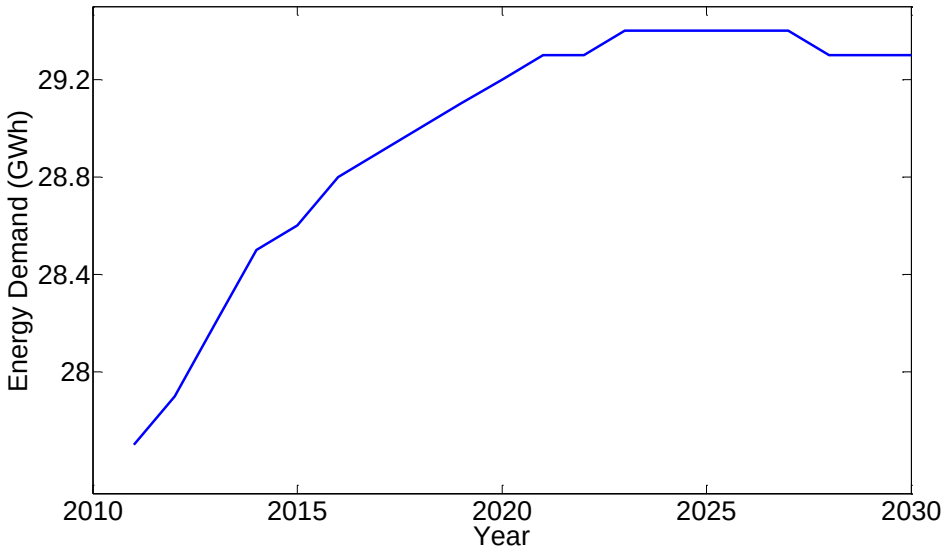


Figure 4.2 – Forecasted annual energy demand for the Masset DGS to 2030.

In the following section an economic analysis is provided for integrating 1000 kW of wind power with various energy storage technologies in the existing Masset power system.

## 4.3 LPC for Masset DGS

To estimate the potential benefits of integrating wind power and energy storage in the Masset DGS an economic analysis based on the levelized production cost (LPC) of electricity has been developed. The analysis compares the system costs and benefits for four different integration scenarios: wind power without energy storage, wind power with a NAS battery ESD, wind power with a VRB ESD, and wind power with a PH storage system.

The method provided in [2] for calculating the LPC value has been extended here to take into account the costs and benefits associated with integrating an ESD. To compare the LPC of integrating wind power and energy storage into the current power system, a simplified model of the costs associated with the current DGS is used as a reference case. The present value (PV) of a cost incurred *i* years in the future is given by:

$$PV_i = \frac{C_i}{(1 + r_d)^i}, \tag{4.1}$$

where $r_d$ is the discount rate.

If the cost is escalated at an annual rate, $r_e$, with respect to a current reference cost, $C_0$, the annual cost becomes:

$$C_i = C_0(1 + r_e)^i . \tag{4.2}$$

The net present value (NPV) for an analysis period of *Y* years is the sum of all costs discounted to present value:

$$NPV = \sum_{i}^{Y} PV_i \tag{4.3}$$

The annual costs of diesel generation can be expressed as the variable costs of fuel, $C_f$, and associated annual environmental costs, $C_{env}$, plus an operational and maintenance cost, $OM$. The variable costs associated with operation are expressed per unit of energy consumed and the fixed operational and maintenance costs are expressed per unit of

installed power capacity. The NPV for the costs associated with diesel generation can be calculated from:

$$NPV = \sum_{i}^{Y} \left[C_{f,i} + C_{env,i}\right] E_i + OM_{D,i} \,. \tag{4.4}$$

$$C_{f,i} = c_f p_f \left(\frac{1 + r_f}{1 + r_d}\right)^i \tag{4.5}$$

$$C_{env,i} = e_{CO_2} p_{CO_2} \left(\frac{1 + r_{CO_2}}{1 + r_d}\right)^i \tag{4.6}$$

$$OM_{D,i} = c_{OM,D} \cdot IC_D \left(\frac{1 + r_i}{1 + r_d}\right)^i \tag{4.7}$$

where:

$c_f =$ Consumption rate of fuel [L/kWh]
$p_f =$ Price of fuel [\$/L]
$r_f =$ Escalation rate of fuel [%/yr]
$e_{CO_2} =$ Emission rate of $CO_2$ [tonne/kWh]
$p_{CO_2} =$ Price of $CO_2$ emissions [\$/tonne]
$r_{CO_2} =$ Escalation rate of $CO_2$ price [%/yr]
$E_i =$ Annual energy production [kWh/yr]
$c_{OM,D} =$ DGS operational and maintenance cost [\$/kW]
$IC_D =$ DGS installed capacity [kW]
$r_i =$ General inflation rate [%/yr]

In Eq. (4.4) the NPV of diesel generation costs are calculated for only the operational and maintenance costs. The capital investment costs, replacement costs and salvage value of the DGS have not been included in the economic analysis. The analysis period is 20 years and the annual energy production is assumed to be the forecasted load growth given in BC Hydro's draft RFP and shown in Figure 4.2.

Both the consumption rate of diesel fuel and the associated emission rate are dependent on the loading level and the mechanical condition of the diesel unit [2,28,30]. Approximate fuel consumption rates were calculated in [28] for representative diesel

units in the Masset DGS and vary from 0.26 to 0.32 L/kWh for operational points of minimum and maximum efficiency. Similarly, a range of emission rates were calculated in [30] for various operating points using representative industry data and vary from approximately 0.85 x $10^{-3}$ to 0.7 x $10^{-3}$ tonne/kWh for minimum and maximum efficiency. The current operational point for the Masset DGS is assumed to have a $c_f$ equal to 0.285 L/kWh and $e_{CO_2}$ equal to 0.77 x $10^{-3}$ tonne/kWh. A full list of the economic assumptions used in the analysis is provided in Table 4.2.

Table 4.2 – Economic model assumptions for the DGS LPC calculation.

| PARAMETER | VALUE | UNITS |
|---|---|---|
| Y | 20 | yr |
| $r_d$ | 8 | %/yr |
| $c_f$ | 0.285 | L/kWh |
| $p_f$ | 1 | \$/L |
| $r_f$ | 2.5 | %/yr |
| $e_{CO_2}$ | 0.77 x $10^{-3}$ | tonne/kWh |
| $p_{CO_2}$ | 30 | \$/tonne |
| $r_{CO_2}$ | 1 | %/yr |
| $C_{OM}$ | 20 | \$/kW |
| $IC_D$ | 11,374 | kW |
| $r_i$ | 5 | %/yr |

The LPC can be estimated from the NPV by the following equation:

$$LPC_{DGS} = \frac{CRF(r_d, Y) \cdot NPV}{AEP}, \tag{4.8}$$

where *AEP* and *CRF* refer to the annual energy production and capital recovery factor respectively. The value of AEP is given by the average energy generated over the analysis period. The CRF is calculated by:

$$CRF(r_d, Y) = \frac{r_d(1 + r_d)^Y}{(1 + r_d)^Y - 1} \tag{4.9}$$

where $r_d$ is the discount rate and $Y$ is total number of years in the analysis period.

The LPC of electricity generation from the current DGS is calculated to be $0.385/kWh for the 20 year analysis period. This value is used as a break even metric in the subsequent cost-benefit analysis for the integration of wind power and energy storage.

## 4.4 Cost-benefit analysis

In this section a cost-benefit analysis is provided for integrating 1 MW of wind power with three different storage technology alternatives in the Masset DGS. Four scenarios are investigated in the analysis: integration of wind power only, wind power with a NAS ESD, wind power with a VRB ESD, and wind power with a PH storage system. To evaluate the benefit of the ESD, an economic model is developed that relates firm power provided by the store with increased DGS efficiency. The LPC electricity generation of each integration option are compared to the reference case of current diesel generation to evaluate the potential benefit they represent.

### 4.4.1 Integration of wind power

The NPV of costs associated with integrating wind power without energy storage can be calculated by:

$$NPV = C_{inv} + \sum_{i}^{Y} \left[C_{f,i} + C_{env,i}\right] E_i + OM_{d,i} + OM_{w,i}\,, \tag{4.10}$$

where:

$$C_{inv} = c_{P,w} IC_w\,, \tag{4.11}$$

$$E_i = E_{L,i} - E_w\,, \tag{4.12}$$

$$OM_{w,i} = c_{OM,w} \cdot IC_w \left(\frac{1 + r_i}{1 + r_d}\right)^i. \tag{4.13}$$

In Eq. (4.10) $C_{inv}$ is the capital investment, $E_i$ is the energy required by the DGS after the annual contribution of wind power has been subtracted, and $OM_w$ is the annual operational and maintenance cost associated with the wind turbine. The assumed capital investment cost, $c_{P,w}$, and fixed annual operational and maintenance costs, $c_{OM,w}$, are expressed per unit of installed wind power. The values used in the analysis were taken from [4] and are listed in Table 4.3. The total benefit of integrating wind power is calculated from the cost savings associated with the displaced diesel fuel and GHG emissions over the project lifetime compared to the reference case.

The LPC for the wind-diesel power system can be estimated from the NPV by:

$$LPC_{WD} = \frac{CRF(r_d, Y) \cdot NPV}{AEP}, \tag{4.14}$$

where $AEP$ is given by the annual average energy contribution from wind generation and the DGS.

### 4.4.2 Integration of wind power and an ESD

The method used to calculate the NPV for a project integrating wind power and an ESD includes the replacement cost for components whose lifetime is less than the analysis period, the salvage value of components whose lifetime has not expired at the end of the analysis period, and an economic model for the value of firm power in remote systems.

In a remote power system, the value of firm power provided by the wind-storage system can be related to gains in DGS efficiency, resulting in decreased fuel consumption and GHG emissions. The ESD acts to hedge against the uncertainty in wind power production, allowing the DGS to run at a more efficient operating point [32]. This is reflected in the economic model of the wind-storage system by decreasing the fuel consumption and emission rates of the DGS.

The equation for the NPV of project costs for a wind-storage system is calculated by:

$$NPV = C_{inv} + \sum_{i}^{Y}\left[C_{f,i} + C_{env,i}\right]E_i + OM_{d,i} + OM_{w,i} + OM_{ESD,i} + C_{r,i} - V_s \ , \quad (4.15)$$

The capital investment includes the cost of the wind turbine and three different terms for the ESD. The capital cost of the power conversion system, denoted by $c_{P,ESD}$, is given in units of \$/kW of installed ESD power rating, whereas the energy capital investment, $c_E$, and the balance of plant (BOP) capital cost is quoted in \$/kWh installed energy capacity. The BOP cost includes building construction, installation, interconnections, and air conditioning equipment.

$$C_{inv} = c_{P,w}IC_w + \ c_{P,ESD}P_{R,ESD} + (c_E + BOP)\zeta_\tau \ , \quad (4.16)$$

The energy required by the DGS is the difference in annual energy load, $E_{L,i}$, and energy contributed from the wind-storage system, $E_{W/ESD}$.

$$E_i = E_{L,i} - E_{W/ESD} \quad (4.17)$$

The fixed operational, maintenance and replacement costs of the ESD are given by Eq. (4.18) and (4.19), where the values of $c_{OM,ESD}$ and $c_r$ are taken from [4] and are listed in Table 4.3.

$$OM_{ESD,i} = c_{OM,ESD} \cdot P_{R,ESD}\left(\frac{1 + r_i}{1 + r_d}\right)^i \quad (4.18)$$

$$C_{r,i} = c_r\zeta_\tau\left(\frac{1}{1 + r_d}\right)^{L+1} \quad (4.19)$$

The salvage value, $V_s$, of a component in the power system that has a lifetime, $L$, longer than the analysis period is given by Eq. (4.20). In contrast, if a component needs to be replaced before the end of the analysis period it will have a salvage value given by Eq. (4.21), where $R$ is defined as the rest period, or the years after the analysis period that the reinvested component still has left in its lifetime.

$$V_s = C_{inv}\frac{CRF(r_d, L)}{CRF(r_d, L-Y)} \quad for\ L > Y\ , \tag{4.20}$$

$$V_s = C_r\frac{CRF(r_d, L)}{CRF(r_d, R)} \quad for\ L < Y\ . \tag{4.21}$$

Lastly, the fuel consumption rate used in the economic model of the wind-storage system to reflect the value of the firm power available from the ESD is assumed to be 0.27 L/kWh, a 5% reduction in consumption rate compared to the reference system. The emission rate is reduced by a similar degree to 0.72 x $10^{-3}$ tonne/kWh.

The LPC for the wind-storage power system can be estimated from the NPV by:

$$LPC_{ESD} = \frac{CRF(r_d, Y)\cdot NPV}{AEP}\ , \tag{4.22}$$

where $AEP$ is given by the average annual energy contribution from the wind-storage system and the DGS.

## 4.5 Results and discussion

In this section the results from the cost-benefit analysis are provided. The probabilistic method is used to calculate the required storage capacity and the average energy contribution from the wind-storage system. Four scenarios are investigated in the analysis: integration of wind power only, wind power with a NAS ESD, wind power with a VRB ESD, and wind power with a PH storage system. The economic model assumptions for the wind power and energy storage pricing were taken from [4] and are listed in Table 4.3. The results of the analysis compare the different integration options by the LPC method described in Section 4.4.

Table 4.3 – Economic model assumptions for wind power and ESD.

| Component | Capital Investment | | | Replacement | Lifetime | Fixed O&M |
|---|---|---|---|---|---|---|
| | $c_P$ ($/kW) | $c_E$ ($/kWh) | BOP ($/kWh) | $c_r$ ($/kWh) | L (yr) | OM ($/kW-yr) |
| Wind Power | 1,200 | --- | --- | --- | 20 | 20 |
| NaS Batteries | 150 | 250 | 0 | 230 | 15 | 20 |
| VRB | 175 | 600 | 30 | 600 | 10 | 20 |
| Pumped Hydro | 1050 | 10 | 4 | 0 | 30 | 2.5 |

The probabilistic method estimates the required storage and annual energy contribution of the wind-storage system from the techniques described in Chapter 2. The energy contribution from the wind-storage system is given by the hourly average firm power value plus the power sent directly to the load multiplied by the total number of hours in the year.

$$E_{W/ESD} = \left(P_{fp} + P_d\right) \cdot 8760\ h \tag{4.23}$$

The results from the probabilistic method are compared to calculations from the time sequential method to calibrate the confidence level $\gamma$ (see Section 3.4.3). The results for the probabilistic method and the cost-benefit analysis are provided in Table 4.4. The results from the cost benefit analysis suggest that a significant savings can be realized over the project lifetime by the integration of wind power and an ESD into the Masset DGS. The overwhelming cost associated with electrical production from diesel fuel is the primary economic driver in the current power system. Integrating wind power to displace even a modest proportion of the annual consumption of diesel fuel, in this case a maximum of 15 % total decrease over the project lifetime, is shown to be cost effective. A graphical comparison of the discounted present value of the total costs associated with each integration alternative is shown in Figure 4.3.

Table 4.4 – Cost-benefit results for wind power and ESD integration in Masset DGS.

| INTEGRATION OPTION | $\tau$ (HR) | $\eta_{rt}$ (%) | $P_{R,ch/dch}$ (kW) | $\zeta_\tau$ (kWh) | $E_{DGS}$ (MWh/yr) | $E_{W/ESD}$ (MWh/yr) | LPC ($/kWh) | TOTAL FUEL (ML) | TOTAL $CO_2$ (kt) |
|---|---|---|---|---|---|---|---|---|---|
| Masset DGS | --- | --- | --- | --- | 29000 | 0 | 0.385 | 165 | 435 |
| Wind Power | --- | --- | --- | --- | 26210 | 2790 | 0.354 | 150 | 390 |
| Wind-$ESD_{NaS}$ | 8 | 87 | 500 | 1900 | 26250 | 2750 | 0.341 | 141 | 382 |
| Wind-$ESD_{VRB}$ | 12 | 75 | 500 | 27500 | 26350 | 2650 | 0.348 | 142 | 384 |
| Wind-$ESD_{PH}$ | 24 | 78 | 500 | 5900 | 26390 | 2610 | 0.342 | 142 | 384 |

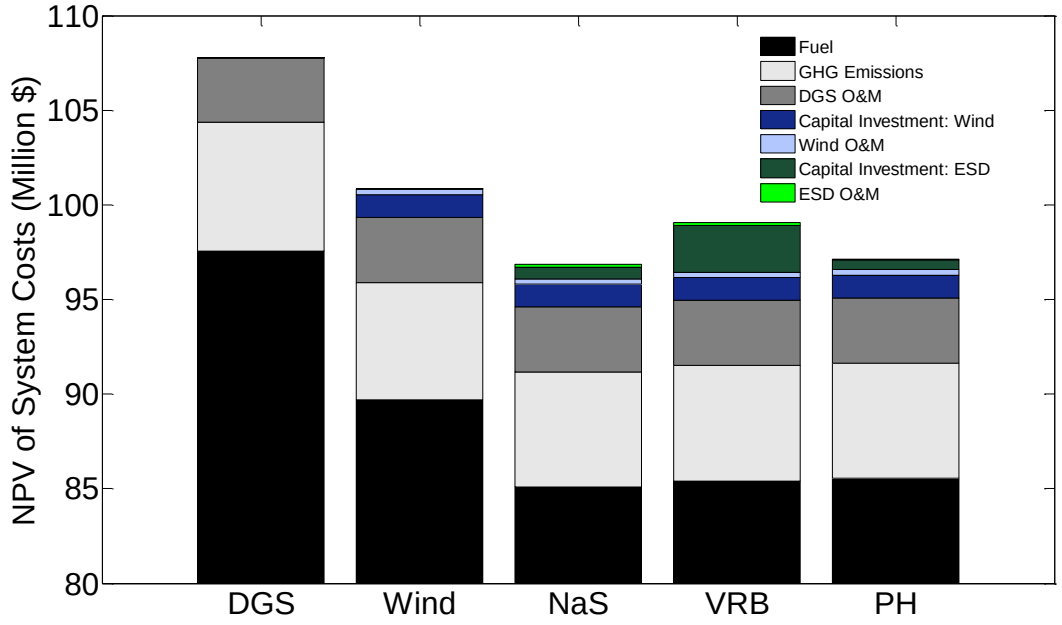


Figure 4.3 – NPV of system costs for each integration alternative in the Masset DGS.

The decrease in fuel consumption, GHG emissions, and the LPC of electricity associated with integrating an ESD is due to the assumption that including a storage device allows the DGS to operate with increased efficiency. This assumption provides a means to quantify the value provided to the local grid from integrating an ESD. However, the actual efficiency gains would be dependent on multiple factors and would need to be experimentally validated.

In this chapter an economic model has been developed to provide a cost-benefit analysis of integrating a wind-storage system in the existing Masset DGS. The results from the analysis show that integration of 1 MW of wind power capacity with a NAS battery bank rated at 500 kW and energy capacity of 1,900 kWh has a total cost savings of approximately $10 million over a 20 year project lifetime compared to the current generation mix. The case study provides an example of how the probabilistic method can be used to size power system components and evaluate the potential benefit of multiple system configurations.

# 5 CONCLUSIONS AND RECOMMENDATIONS

In this thesis a validation of the probabilistic method proposed in [17,18] for evaluating the required storage capacity and system performance of a power system with wind generation and an ESD is provided. The objective of the research was to investigate whether traditional time domain analysis can be improved by adopting the probabilistic approach. A validation study was carried out to determine the accuracy of the probabilistic method compared to a time domain simulation method. The main findings of the study show that the probabilistic method is limited in its application due to the sensitivity of system performance metrics to installed wind capacity, firm power level, and the confidence level used to size the storage capacity. A method to reduce the residuals of the probabilistic estimates compared to calculations from a time sequence simulation method is provided. A case study for a remote power system located on Haida Gwaii is included to illustrate how the method can be used in a cost-benefit analysis of wind power and energy storage integration.

There are various improvements to the method that were out of the scope of this thesis. A list is provided for recommended future work to improve the robustness of the probabilistic approach described in this work.

- Investigate the effect of different spectral estimation techniques on the accuracy of the probabilistic method. For example, a Welch estimation method could be used to estimate the wind speed spectrum.

- Include more intermittent inputs to the model; including other renewable generation sources and a variable load profile.

- Investigate the dependence structure of the confidence level on the renewable power penetration. There seems to be a relationship between the ratio of the installed wind power and firm power commitment and the confidence level. The objective of this analysis would be to improve the ability of the probabilistic method to accurately evaluate power systems with various configurations by defining a functional relationship between the wind power penetration level and the confidence level that minimizes the errors in the predicted performance metrics.

- Investigate how the method can be implemented in deregulated markets where the value of firm power is of interest.

- Expand the methodology to include multiple ESD's.

- Use the probabilistic method to model a network of linked nodes, representing an interconnected power system.

# References

[1] Kim Ah-You and Greg Leng, "Renewable Energy in Canada's Remote Communities," 1999.

[2] Ray Hunter and George Elliot, *Wind-Diesel Systems*. New York, US: Cambridge University Press, 1994.

[3] Ian Baring-Gould, "Wind/Diesel Power System Basics and Examples," in *International Wind-Diesel Workshop*, Ottawa, 2009.

[4] Susan M. Schoenung and William V. Hassenzahl, "Long vs. Short-Term Energy Storage Techologies Analysis: A Life-Cycle Cost Study," Sandia National Laboratories, Alburquerque, DOE Energy Study 2003.

[5] Electricity Storage Association. (2010, November) Electricity Storage Association. [Online]. http://www.electricitystorage.org

[6] EPRI, "EPRI-DOE Handbook of Energy Storage for Transmission and Distribution Applications," DOE, Washington, Technical 1001834, 2003.

[7] NGK. (2010, Nov) NAS Batteries: Reference Installations. [Online]. http://www.ngk.co.jp/english/products/power/nas/installation/index.html

[8] J. K. Kaldellis, M. Kaspsali, and K. A. Kavadias, "Energy balance analysis of wind-based pumped hydro storage systems in remote island electrical networks," *Applied Energy*, vol. 87, pp. 2427-2437, March 2010.

[9] J. K. Kaldellis, D. Zafirakis, K. Kavadias, and E. Kondili, "An Optimum Sizing Methodology for Combined Photovoltaic Energy Storage Electricity Generation Configurations," *Journal of Sloar Energy Engineering*, vol. 131, May 2009.

[10] B. Klockl, P. Stricker, and G. Koeppel, "On the properties of stochastic power sources in combination with local energy storage," in *Cigre Symposium on power systems with dispersed generation*, Athens, 2005.

[11] Tom Lambert, Paul Gilman, and Peter Lilienthal, "Micorpower System Modeling with HOMER," in *Integration of Alternative Sources of Energy*.: John Wiley & Sons, 2005, pp. 379-418.

[12] Bernd Klockl and George Papaefthymiou, "An effort to overcome the chronological moedling methos for energy storage devices," in *2005 International Conference on Future Power Systems* , Amsterdam, 2005, pp. 6 - 11.

[13] Roy Billinton and Bagen, "Incorporating Well-Being Considerations in Generation Systems Using Energy Storage," *IEEE Transactions on Energy Conversion*, vol. 20, no. 1, pp. 225-230, March 2005.

[14] Robert S. Weissbach, Remus E. Teodorescu, and James R. Sonnenmeier, "Comparison of Time-Based Probability Methods for Estimating Energy Storage Requirements for and Off-Grid Residence," in *IEEE Energy 2030*, Atlanta, 2008, pp. 1-4.

[15] Chad Abbey and Geza Joos, "A Stochasit Optimization Approach to Rating of Energy Storage Systems in Wind-Diesel Isolated Grids," *IEEE Transactions on Power Systems*, vol. 24, pp. 418-426, February 2009.

[16] Magnus Korpas, "Distributed Energy Sytems with Wind Power and Energy Storage," Norwegian University of Science and Technology, Trondheim, PhD Thesis 2004.

[17] John P. Barton and David G. Infield, "A probabilistic method for calculating the usefulness of a store with finite energy capacity for smoothing electricity generation from wind and solar power," *Journal of Power Sources*, vol. 162, no. 2, p. 943, Nov. 2006.

[18] John Barton, "A probabilistic method of modelling energy storage in electricity systems with intermittent renewable energy," Loughborough University, Leicestershire, PhD Thesis 2007.

[19] Det Norske Veritsa (DNV), "Environmental Conditions and Environmental Loads," Norway, Recommended practice DNV-RP-C205, 2007.

[20] Erik Peterson, Niels Mortenson, Lars Landberg, Jorgen Hojstup, and Helmut Frank, "Wind Power Meteorology," Riso National Laboratory, Rosklide, 1997.

[21] Tony Burton, David Sharpe, Nick Jenkins, and Ervin Bossanyi, *Wind Energy Handbook*. West Sussex, England: John Wiley and Sons, 2001.

[22] C.G. Justus, W.R. Hargraves, Amir Mikhail, and Denise Graber, "Methods for Estimating Wind Speed Frequency Distributions," *Journal of Applied Meteorology*, vol. 17, pp. 350-353, Nov. 1977.

[23] J.F. Manwell, J.G. McGowan, and A.L. Rogers, *Wind Energy Explained: Theory, Design and Application*. West Sussex, England: John Wiley and Sons, 2002.

[24] ENERCON, "ENERCON Wind Turbines," ENERCON Sales Department, Aurich, Product Overview 2010.

[25] Hannele Holttinen et al., "Using Standard Deviation as a Measure of Increased Operational Reserve Requirement for Wind Power," *Wind Engineering*, vol. 32, no. 4, pp. 355-378, 2008.

[26] R. Gross et al., "Renewables and the grid: understanding intermittency," *Energy*, vol. 160, pp. 31-41, February 2007.

[27] BC Hydro, "BC Hydro Haida Gwaii/Queen Charlotte Islands RFP - Draft Technical Information," Request for Proposals 2008.

[28] Hatch Energy, "Haid Gwaii/Queen Charlotte Islands Demonstration Tidal Power Plant Feasibility Study," 2008.

[29] Sheltair Group, "Haida Gwaii Community Electricity Plan," Council of Haida Nation, 2008.

[30] Susan Boronowski, "Integration of Wave and Tidal Power into the Haida Gwaii Electrical Grid," University of Victoria, Victoria, MASc Thesis 2009.

[31] Justin Burns Blanchfield, "The Extractable Power from Tidal Streams, including a Case Study for Haida Gwaii," University of Victoria, Citoria, MASc Thesis 2007.

[32] J. K. Kaldellis, D. Zafirakis, and K. Kavadias, "Techno-economic comparison of energy storage systems for island autonomous electrical networks," *Renewable and Sustainable Energy Reviews*, vol. 13, pp. 378-392, 2009.

[33] M. B. Priestley, *Spectral Anlaysis and Time Series*. New York: Academic Press Inc, 1981.

[34] Leo H Holthuijsen, *Waves in Oceanic and Coastal Waters*. Cambridge: Cambridge University Press, 2007.

[35] William Press, Saul Teukolsky, William Vetterling, and Brian Flannery, *Numerical Recipes in C*. Cambridge: Cambridge University Press, 1992.

# Appendix

## A Filter for the variance in wind speeds

Appendices A through C provide details on the filters proposed by Barton in [17,18] to estimate the statistical properties of the wind regime over the storage period. In this section, an analytical derivation of the filter used to calculate the variance in wind speeds within a storage period is presented. Most of the reference material used in the following analysis can be found in [33,34].

The model of wind speeds used in the probabilistic approach is based on the assumption that the wind speed time series can be represented by a stationary stochastic process that can be modeled by a Fourier series of the form;

$$u(t) = \sum_{i=0}^{K} A_i \cos(\omega_i t + \phi_i) , \tag{A.1}$$

$$\omega_i = 2\pi f_i , \tag{A.2}$$

where $(i = 1, \dots, K)$ are constants, $\{\omega_i\}$ are the radial frequency components given by (A.2), $\{A_i\}$ are the amplitudes corresponding to each frequency, and $\{\phi_i\}$ are independent random variables uniformly distributed on [0, $2\pi$] .

For mathematical convenience, a single harmonic of the series in (A.1) is used in the following derivation.

$$u_i(t) = A_i \cos(\omega_i t + \phi_i) \tag{A.3}$$

The first filter is designed to give the variance in wind speeds within a specified store period of length $\tau$. For a continuous time dependent function, $\varphi(t)$, the sample mean, $\bar{\varphi}_T$, and sample variance, $\sigma^2{}_{\varphi(t)}$, over a domain [$0$, $T$] are defined as:

$$\bar{\varphi}_T \equiv \frac{1}{T}\int_0^T \varphi(t)dt , \tag{A.4}$$

$$\sigma^2{}_{\varphi(t)} \equiv \frac{1}{T}\int_0^T (\varphi(t) - \bar{\varphi}_T)^2 dt\,. \tag{A.5}$$

The variance in wind speeds over the storage window is given by replacing $\varphi(t)$ with $u_i(t)$, $\bar{\varphi}_T$ with $\overline{u}_{\tau,i}$, and $T$ with $\tau$ in (A.5).

$$\sigma^2{}_{u(t)} = \frac{1}{\tau}\int_0^\tau (u_i(t) - \overline{u}_{\tau,i})^2 dt \tag{A.6}$$

The mean wind speed of the harmonic over the sample window is given by replacing $\varphi(t)$ by $u_i(t)$ and $T$ by $\tau$ in (A.4).

$$\overline{u}_{\tau,i} = \frac{1}{\tau}\int_0^\tau u_i(t)\,dt = \frac{A_i}{\omega_i \tau}(\sin(\omega_i \tau + \phi_i) - \sin\phi_i) \tag{A.7}$$

Substituting Eqs. (A.3) and (A.7) into Eq. (A.6) gives an expression for the contribution of a single harmonic to the variance of wind speeds within the store period. However, because this only represents one arbitrary sample of the entire series, the expected value of all possible storage periods is necessary to obtain a representative expression of the variance contribution from the harmonic. The expected value for a function of a random variable is given by:

$$E[g(X)] = \int_{-\infty}^{\infty} g(X)p(X)dX\,, \tag{A.8}$$

where $p(X)$ is defined as the PDF of the random variable $X$.

In the case described here, the random variable is the phase which is uniformly distributed on [0, 2π], so $p(\phi_i)$ is equal to $\frac{1}{2\pi}$ and $g(X)$ is the sample variance.

$$E\left[\sigma^2{}_{u(t)}\right] = \frac{1}{2\pi}\int_0^{2\pi} \sigma^2{}_{u(t)} d\phi_i \tag{A.9}$$

Therefore, the contribution of a harmonic to the variance in wind speeds within a storage period of length $\tau$ is given by:

$$E\left[{\sigma^2}_{u(t)}\right] = \frac{1}{2\pi}\int_0^{2\pi}\frac{1}{\tau}\int_0^{\tau}(u_i(t) - \overline{u}_{\tau,i})^2 dt\, d\phi_i \qquad \text{(A.10)}$$

Substituting the expressions for $u_i(t)$ and $\overline{u}_{\tau,i}$ given by Eqs. (A.3) and (A.7) into Eq. (A.10) and integrating over time and phase gives the first filter function for the variance of wind speeds within a store period.

$${\sigma^2}_{u(t)} = \frac{{A_i}^2}{2} - \left(\frac{A_i}{\omega_i \tau}\right)^2 (1 - \cos\omega_i \tau) \qquad \text{(A.11)}$$

## B Filter for the variance in mean wind speed

In this section an analytical derivation for the second filter, designed to calculate the variance in mean wind speeds for a specified store period of length $\tau$, is presented.

The derivation begins similarly to the first filter function with a single harmonic of the series given by (A.3). However, the definition of the sample variance is modified. In the previous filter the variability was measured relative to the sample mean wind speed to give the variance of wind speeds within the period. However, the variance of mean wind speeds is defined relative to the expected value of mean wind speeds of a storage period.

$${\sigma^2}_{\overline{u}_{\tau,i}} = \frac{1}{\tau}\int_0^{\tau}(\overline{u}_{\tau,i} - E[\overline{u}_{\tau,i}])^2 dt \qquad \text{(A.12)}$$

Equation (A.12) gives the contribution of a harmonic to the variance in mean wind speeds for a storage period of length $\tau$. The expected value of mean wind speeds is given by:

$$E\left[\overline{u}_{\tau,i}\right] = \frac{1}{2\pi}\int_0^{2\pi}\overline{u}_{\tau,i} d\phi_i = \frac{1}{2\pi}\int_0^{2\pi}\frac{A_i}{\omega_i \tau}(\sin(\omega_i \tau + \phi_i) - \sin\phi_i) d\phi_i. \qquad \text{(A.13)}$$

Integrating Eq. (A.13) gives a solution of 0. The expression for the variance reduces to:

$$\sigma^2_{\overline{u}_{\tau,i}} = \frac{1}{\tau}\int_0^{\tau} (\overline{u}_{\tau,i})^2 dt\,. \tag{A.14}$$

Similar to the previous derivation, this sample is extended to the entire series by use of the expected value operator.

$$E\left[\sigma^2_{\overline{u}_{\tau,i}}\right] = \frac{1}{2\pi}\int_0^{2\pi} \sigma^2_{\overline{u}_{\tau,i}} d\phi_i = \frac{1}{2\pi}\int_0^{2\pi}\frac{1}{\tau}\int_0^{\tau} (\overline{u}_{\tau,i})^2 dt\, d\phi_i \tag{A.15}$$

This expression gives the average contribution of the harmonic to the variance in mean wind speeds for a store period of length $\tau$. The second filter is calculated by replacing the expression attained for $\overline{u}_{\tau,i}$ in (A.7) into (A.15) and integrating over $\phi_i$.

$$\sigma^2_{\overline{u}_{\tau,i}} = \left(\frac{A_i}{\omega_i \tau}\right)^2 (1 - \cos\omega_i \tau) \tag{A.16}$$

## C Filter for the variance in the change of SOC

The third filter is designed to give the variance in the accumulated energy over a store period and is used in the method to size the required ESD capacity. The power system modeled in the derivation of the filter for the variance in $\Delta E_t$ is shown in Figure 2.1. The storage device acts to absorb surplus power and deliver deficit power according to the availability of power generated from the wind. The ESD power flows are given by $P_{net}$, which is defined in Eq. (2.1) as the difference in wind power and the firm power commitment. In this section a derivation of the filter for the variance in the change in the energy SOC of the ESD is presented.

The energy charge state of a storage device at any instant in time within the store period, $E_t$, is a function of its initial energy level, $E_0$, plus an accumulation term that tracks the power flows across the ESD boundary through time.

$$E_t = E_0 + \int_0^t P_{net}\, dt \tag{A.17}$$

The deviation in the energy state at any time can then be defined as:

$$\Delta E_t \equiv \int_0^t P_{net}\, dt\,. \tag{A.18}$$

The ESD is operated such that at the end of the specified storage period the energy state will return to its initial value.

$$E_\tau = E_0 \tag{A.19}$$

This ensures that the ESD is operating in a charge sustaining mode and will not move towards an empty or full energy state of charge. The operational requirement given by Eq. (A.19) implies that the change in energy over the store period is equal to 0.

$$\Delta E_\tau = \int_0^\tau P_{net}\, dt = 0 \tag{A.20}$$

The expression for the variance in the change in energy charge state within a storage period of length $\tau$ is given by a similar form used in the second filter derivation. The variance in the change of energy SOC of an ESD over the storage period is given by:

$$\sigma^2{}_{\Delta E_\tau} = \frac{1}{\tau}\int_0^\tau (\Delta E_t - \overline{\Delta E_\tau})^2\, dt. \tag{A.21}$$

From the operational constraint of Eq. (A.20), $\overline{\Delta E_\tau}$ is equal to 0. Therefore, the equation for the variance in the excursion of energy charge state is given by:

$$\sigma^2{}_{\Delta E_\tau} = \frac{1}{\tau}\int_0^\tau (\Delta E_t)^2\, dt. \tag{A.22}$$

To evaluate Eq. (A.22) a relationship for the instantaneous power flows of the ESD is required. The available power generated for various wind speeds is calculated from a

wind turbine power curve, $P(u)$, which relates wind speeds to convertible power values (refer to Section 2.4 for details). For the filter ${\sigma^2}_{\Delta E_\tau}$ the expected value of power sent to the ESD for a storage period is approximated by the wind power of the mean wind speed for the storage period. This is also equal to the power available to be sent to the local grid for the storage period, i.e the level of firm power.

$$E[P_w] \approx P_w(\overline{u}_\tau) = P_{fp} \tag{A.23}$$

Therefore the power flows to and from the ESD are given by:

$$P_{net} = P_w(u(t)) - P_{fp} = P_w(u(t)) - P_w(\overline{u}_\tau) \tag{A.24}$$

If the wind speed is greater than the mean wind speed of the store period there will be a power flow into the ESD. If the wind speed is less than the mean wind speed of the storage period, power flows out of the ESD and into the power system.

The ESD power flows defined in Eq. (A.24) are approximated by a first order Taylor series expansion of the wind turbine power curve, $P_w(u)$, about the mean wind speed of the storage period.

$$P_w(u(t)) \approx P_w(\overline{u}_\tau) + \frac{dP_w(u(t))}{du}(u(t) - \overline{u}_\tau) \tag{A.25}$$

Solving Eq. (A.25) for $P_{net}$ gives:

$$P_{net} = \frac{dP_w(u)}{du}(u(t) - \overline{u}_\tau) = \kappa(u(t) - \overline{u}_\tau) \tag{A.26}$$

In Eq. (A.26) the term $\kappa$ represents a conversion factor given by the gradient of the wind turbine power curve evaluated at the instantaneous wind speed (see Appendix C.1 for details on how $\kappa$ is calculated).

Using a single harmonic of the wind speed time series the equation for ${\sigma^2}_{\Delta E_\tau}$ reduces to an expression including wind speed components $u_i(t)$ and $\overline{u}_\tau$ and the power curve gradient, $\kappa$.

$$\sigma^2{}_{\Delta E_{\tau,i}} = \frac{1}{\tau}\int_0^{\tau}\left(\Delta E_{t,i}\right)^2 dt = \frac{1}{\tau}\int_0^{\tau}\left(\int_0^{t}\kappa(u_i - \overline{u}_{\tau})\,dt\right)^2 dt \qquad \text{(A.27)}$$

Substituting Eqs. (A.3) and (A.7) for the definition of instantaneous wind speeds and mean wind speed for the store period, Eq. (A.27) gives an expression for the contribution of a single harmonic to the variance in the change of SOC.

The inner integral in Eq. (A.27) represents the change in SOC up to an arbitrary point in time and the solution is given by:

$$\Delta E_{t,i} = \kappa\int_0^{t}\left(A_i\,cos(\omega_i t^* + \phi_i) - \frac{A_i}{\omega_i\tau}(sin(\omega_i\tau + \phi_i) - sin\,\phi_i)\right)dt^*, \qquad \text{(A.28)}$$

$$\Delta E_{t,i} = \frac{A_i\kappa}{\omega_i\tau}[t(sin\,\phi_i - sin(\omega_i\tau + \phi_i)) + \tau(sin(\omega_i\tau + \phi_i) - sin\,\phi_i)\,]. \qquad \text{(A.29)}$$

Finally, the expected value operator is used to calculate the average contribution of the harmonic to the variance in the change in SOC of the ESD for a store period of length $\tau$:

$$E[\sigma^2{}_{\Delta E_{t,i}}] = \frac{1}{2\pi}\int_0^{2\pi}\frac{1}{\tau}\int_0^{\tau}\left(\Delta E_{t,i}\right)^2 dt d\phi_i\,. \qquad \text{(A.30)}$$

Substituting Eq. (A.29) into the above expression and integrating over time and phase gives the final filter function for the variance in accumulated energy for a store period of length τ.

$$\sigma^2{}_{\Delta E_{t,i}} = \left(\frac{A_i\kappa}{\omega_i}\right)^2\left(\frac{5}{6} + \frac{1}{6}cos\,\omega_i\tau + \frac{2}{(\omega_i\tau)^2}(cos\,\omega_i\tau - 1)\right) \qquad \text{(A.31)}$$

## C.1 Power conversion factor calculation

In the derivation of the filter for $\sigma^2{}_{\Delta E_{t,i}}$ an explicit definition for the power conversion factor, $\kappa$, was not provided. In this section the method used to calculate the

power conversion factor used in the filter to size the required storage capacity is provided.

The power conversion factor, $\kappa$, is calculated from the ratio of the standard deviation in wind power and the variance in wind speeds. Taking the variance of Eq. (A.25) gives:

$$Var(P_w(u)) \approx Var\left(P_w(\overline{u}_\tau) + \frac{dP_w(u)}{du}(u(t) - \overline{u}_\tau)\right), \tag{A.32}$$

$$= Var\left(\frac{dP_w(u)}{du}(u(t) - \overline{u}_\tau)\right), \tag{A.33}$$

$$= \left(\frac{dP_w(u)}{du}\right)^2 Var\left(u(t) - \overline{u}_{\tau,s}\right), \tag{A.34}$$

$$= \left(\frac{dP_w(u)}{du}\right)^2 Var(u(t)). \tag{A.35}$$

Equation (A.35) can be rearranged and solved for the power conversion factor:

$$\kappa \equiv \frac{dP_w(u)}{du} = \sqrt{\frac{Var\left(P_w(u)\right)}{Var(u(t))}} = \frac{\sigma_{P_w(u)}}{\sigma_{u(t)}} \tag{A.36}$$

The value for the sampled mean wind speed used to evaluate Eq. (A.36) is the mean wind speed that gives balanced power flows into and out of the ESD. The balanced mean wind speed is used because the store experiences maximum utilization and therefore ensures the maximum capacity requirement for the ESD.

The variance of wind power can be calculated from the computational formula of variance, which in general form for a random variable X is:

$$Var(X) = E[X^2] - (E[X])^2 \tag{A.37}$$

Therefore, the variance in wind power is given by:

$$Var\left(P_w(u)\right) = E[P_w(u)^2] - (E[P_w(u)])^2. \tag{A.38}$$

In Eq. (A.38) the expected value terms are given by:

$$E[P_w(u)^2] = \int_0^\infty P_w(u)^2 p(u(t))du, \tag{A.39}$$

$$(E[P_w(u)])^2 = \left(\int_0^\infty P_w(u) p(u(t))du\right)^2. \tag{A.40}$$

The standard deviation for the distribution of wind speeds within the store period is computed from the assumption that the coefficient of variation is constant and Eq. (2.19).

$$\sigma_{u(t)_b} = \bar{u}_{\tau,b}\left(\frac{\sigma_{u(t)}}{\mu}\right)_{LT} \tag{A.41}$$

The value of $\bar{u}_{\tau,b}$ is obtained from the sampled mean wind speed which minimizes the absolute difference of $P_{ch}(\bar{u}_{\tau,s})$ and $P_{dch}(\bar{u}_{\tau,s})$.

With the methods provided in this section the value of $\kappa$ can be calculated for the specified storage period, installed wind capacity, and firm power commitment.

# D Spectral representation of wind speed

In the probabilistic method proposed by Barton in [18] spectral analysis is employed to study the statistical characteristics of the wind regime over the storage period. In this section the methods used to estimate the spectral representation of wind speeds are presented.

The variance spectrum, also commonly referred to as a power spectrum or periodogram, represents the contribution of each frequency component to the total variance of the series [34]. The energy theorem states that for a discrete data set $x_t$, the total energy of the signal can be expressed in terms of the Fourier coefficients [33].

$$E(x_t) = \sum_{t=0}^{N-1} |x_t|^2 \Delta t = \sum_{k=0}^{N-1} |A_k|^2 \Delta f \tag{A.42}$$

In Eq. (A.42) $\Delta t$ is given by the sampling time and $\Delta f = \frac{1}{N\Delta t}$. Dividing the energy of the signal by the total time, $N\Delta t$, gives the power.

$$P(x_t) = \frac{1}{N\Delta t}\sum_{t=0}^{N-1}|x_t|^2\Delta t = (N\Delta t)^{-2}\sum_{k=0}^{N-1}|A_k|^2 \tag{A.43}$$

By definition Eq. (A.43) represents the variance, denoted by the symbol $\sigma^2$, of a zero mean process:

$$\sigma^2(x_t;\ \bar{x}_t = 0) \equiv \frac{1}{N}\sum_{t=0}^{N-1}{x_t}^2 = (N\Delta t)^{-2}\sum_{k=0}^{N-1}|A_k|^2 \tag{A.44}$$

However, the variance of a process with a non-zero mean can be easily obtained by disregarding the Fourier amplitude associated with the mean of the series, $|A_0|^2$ [34]. Therefore, the total variance in the series can be calculated by summing the individual contribution from the squared amplitudes of the Fourier coefficients.

$${\sigma^2}_{x_t} = \frac{1}{N}\sum_{t=0}^{N-1}(x_t - \bar{x_t})^2 = N^{-2}\sum_{k=1}^{N-1}|A_k|^2 \tag{A.45}$$

The spectral representation of wind speeds is estimated by a using a direct Fourier transform method, calculated from the squared modulus of the discrete Fourier transform (DFT) of the original time series data. The wind spectrum is normalized according to Eq. (A.45), so that the sum of all frequency contributions is equal to the total variance of the series.

For an arbitrary time series, $x_t$, of length N the DFT is defined as:

$$A_k \equiv \sum_{t=0}^{N-1} x_t e^{-2\pi i f_k t}\,, \tag{A.46}$$

$$where \quad f_k = \frac{k}{N\Delta t}, \quad k = 0, 1, \dots, N-1\,. \tag{A.47}$$

The DFT is calculated using a fast Fourier transform (FFT) algorithm. The FFT is converted into a one-sided power spectrum by limiting the frequency range to the Nyquist frequency and multiplying the normalized squared modulus of the transform by a factor of two. For the following calculations the notation use for the variance of a single frequency component is given by $V(f_k)$.

$$V(f_0) = \frac{|A_0|^2}{N^2} = 0 \tag{A.48}$$

$$V(f_k) = \frac{2|A_k|^2}{N^2} \qquad k = 1, \dots, \frac{N}{2} - 1 \tag{A.49}$$

$$V(f_{N/2}) = \frac{|A_{N/2}|^2}{N^2} \tag{A.50}$$

When displaying spectral data of lengthy time series it is often convenient to use a logarithmic scale of frequency, allowing for better visualization of the data. A plot of the raw spectral estimates are shown in Figure A.1 on a linear and base 10 logarithmic scale of frequencies in units of cycles per hour (cph) for wind speed data from Sandspit, BC. The plotting axes have been magnified to better show the spectrum.

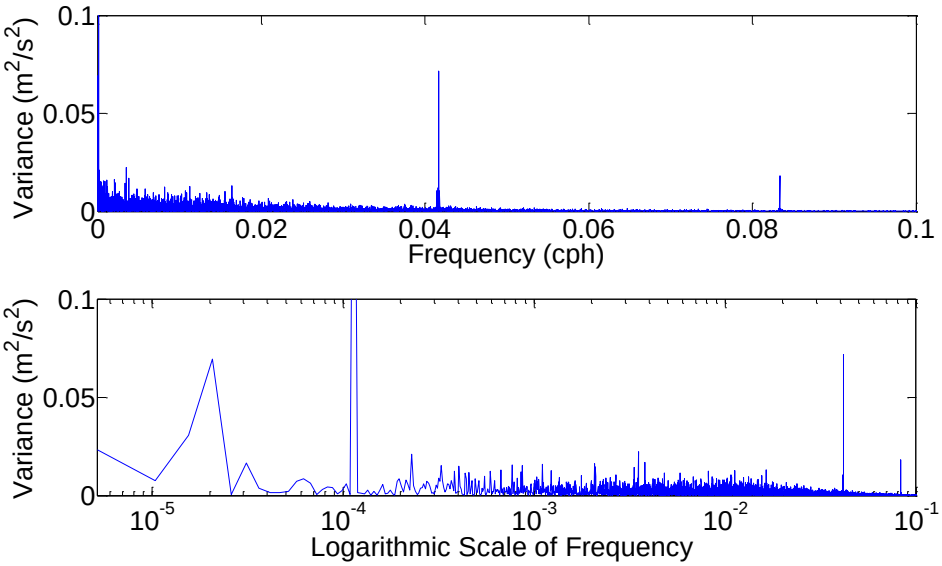


Figure A.1 – Raw variance spectrum on linear and logarithmic scale.

The direct Fourier transform method produces spectral estimates that represent frequencies within the interval of $f_k - \Delta f/2 \leq f_k \leq f_k + \Delta f/2$. The extremely high resolution of this method introduces considerable noise in the raw spectral estimates as can be seen in Figure A.1. Therefore, a method is required to smooth the spectral estimates. A simple method to reduce the variance in the spectral estimates involves summing individual components of the spectrum into discrete bins [35]. Following the method used by Barton in [17], each bin is equally spaced on a logarithmic scale and centered on a single frequency denoted by $\tilde{f}_i$, where $i = 1, \ldots, n$, and $n$ is the total number of bins. The bin width, $\mathcal{B}$, is defined to be a constant on the logarithmic scale and is given by:

$$\mathcal{B} = log10\left(\tilde{f}_{i+1}\right) - log10(\tilde{f}_i) = log10\left(\frac{\tilde{f}_{i+1}}{\tilde{f}_i}\right) \tag{A.51}$$

The value used for $\mathcal{B}$ is dependent on the data being processed and the spectral resolution required in the analysis. It should be noted that the frequency interval corresponding to the logarithmic bin width is given by $\tilde{f}_{i+1} = 10^{\mathcal{B}}\tilde{f}_i$. Therefore, lower frequency bins will have greater resolution, i.e. be narrower, than bins used to sum the

higher frequency components. The frequency bandwidth for a bin centered on $\tilde{f}_i$ is given by:

$$\Delta f_{\mathcal{B}} = \tilde{f}_{i+1} - \tilde{f}_i = \tilde{f}_i(10^{\mathcal{B}} - 1). \tag{A.52}$$

The smoothed variance spectral estimates, $\tilde{V}(\tilde{f}_i)$, are represented at the mid-frequency of the bin and are calculated by the sum of the variance components of Eqs. (A.48) to (A.50).

$$\tilde{V}(\tilde{f}_i) = \sum_{\tilde{f}_i - \Delta f_{\mathcal{B}}/2}^{\tilde{f}_i + \Delta f_{\mathcal{B}}/2} V(f_k) \tag{A.53}$$

An example is provided for hourly wind speed data for Sandspit, BC (see Section 3.4.1 for details concerning the data set). The raw wind spectrum, $V(f_k)$, is calculated according to Eqs. (A.48) to (A.50) and can be seen graphically in Figure A.1. A logarithmic bin width of 0.0525 is used, corresponding to a frequency increment of $\tilde{f}_{i+1} = 1.1284\tilde{f}_i$. The new frequencies span the range of the original $f_k$, $[f_1\ f_{\frac{N}{2}}]$, used in the raw spectral estimates, however there are only 96 frequencies which represent the original spectrum which consists of close to $10^5$ data points.

A variance spectrum for wind speeds in Sandspit, BC is shown in Figure A.2. The markers on the figure correspond to the smoothed variance values $\tilde{V}(\tilde{f}_i)$. The figure shows the relative contribution of each frequency component, $\tilde{f}_i$, to the overall variance of the time series. The frequency for the annual contribution, a total period of 8,760 hours, is equal to $10^{-3.9425}$ (cycles/hour) on a log scale. The variance contribution of the annual frequency component is significant for wind speeds in Sandspit, BC, as can be seen in the spectral plot. Seasonal contributions are shown in the frequency range of $10^{-3.3}$ to $10^{-3.1}$ (cycles/hour) for the plotted wind spectrum. Variations in wind patterns due to cyclonic storms passing every 3 to 4 days can also be seen in the variance density function for the region with frequency ranges from $10^{-2}$ to $10^{-1.85}$ (cycles/hour). This is typical for coastal sites that experience more frontal weather systems. Finally, the last

significant peak in the wind spectrum is due to a diurnal frequency of one cycle every 24 hours, or $10^{-1.38}$ (cycles/hour).

The total variance of the wind speed time series can be obtained by summing each variance contribution.

$$\sigma^2 = \sum_{i=1}^{n} \tilde{V}(\tilde{f}_i) \tag{A.54}$$

The total variance of the original time series is calculated to be 13.9628 ($m^2/s^2$) using the variance algorithm provided in MATLAB. The variance calculated by Eq. (A.54) is equal to 13.9627 ($m^2/s^2$), which is within acceptable numerical accuracy.

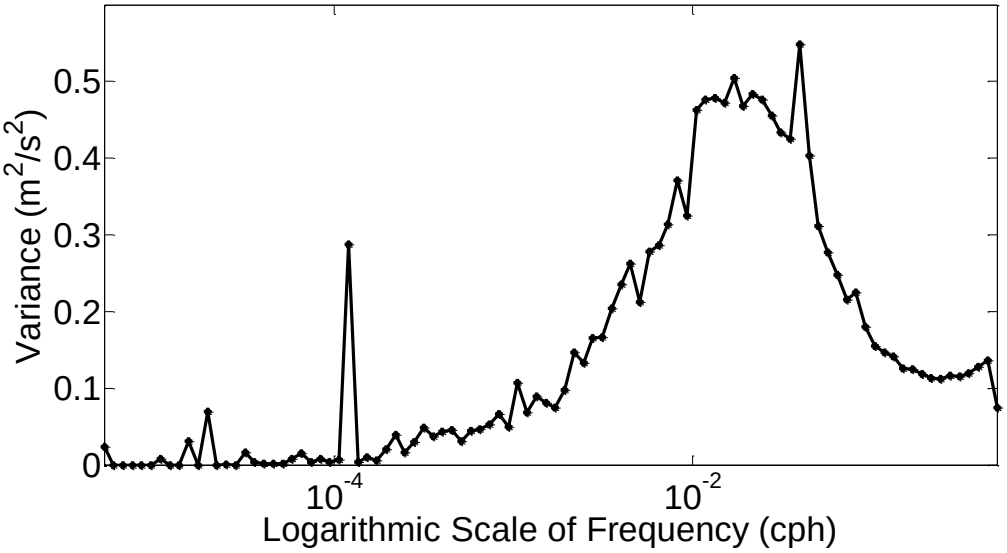


Figure A.2 – A smoothed variance spectrum of wind speeds for Sandspit, BC.

## E Variance calculation from filtered wind spectrum

The three filter functions derived in Appendix A through C are applied to the wind speed spectrum to calculate the total variance in mean wind speed for a storage period, $\sigma^2_{\overline{u}_\tau}$, the total variance in wind speeds within the storage period, $\sigma^2_{u(t)}$, and the total variance in the excursions of the state of charge, $\sigma^2_{\Delta E_t}$, for a storage period.

An example of the filters for a storage period of 24 hours is plotted on a logarithmic scale in Figure A.3. It is evident from the figure that the filter derived for the variance in mean wind speed for store period τ acts as a low pass filter and the filter designed for the variance of wind speeds within the store period acts as a high pass filter. Variance contributions from frequency components less than the store period frequency are attributable to the variance in mean wind speeds, whereas contributions from frequencies higher than the storage period are due to the variance within the store period.

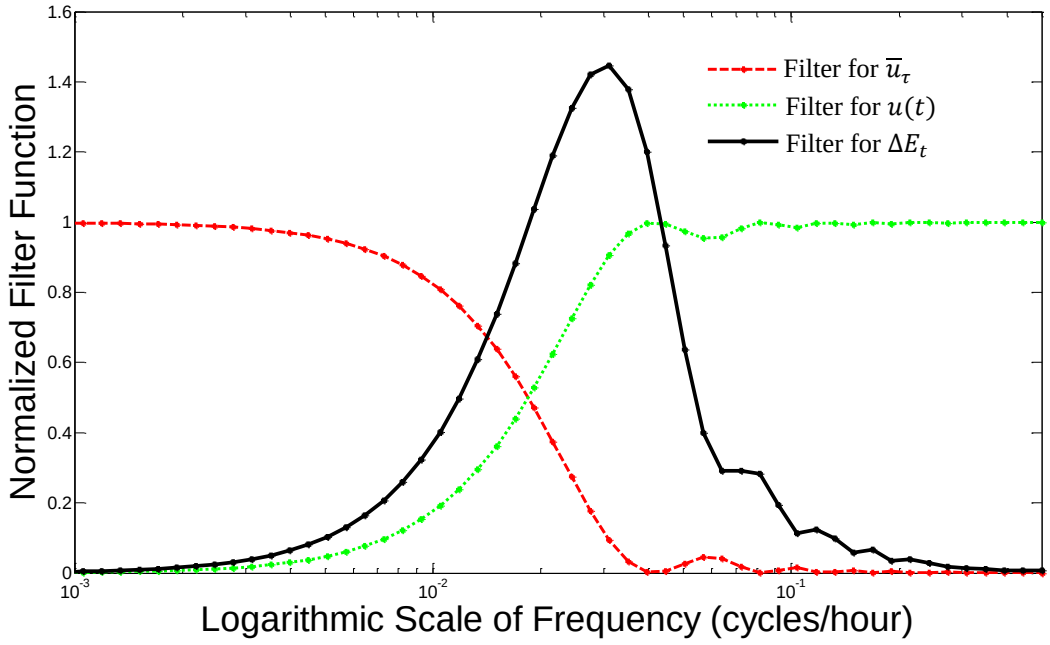


Figure A.3 – Filter functions for a 24 hour store period.

Equations (A.16), (A.11), and (A.31) are weighting functions that are applied to the squared amplitude, ${A_i}^2$, of the harmonic component corresponding to a frequency $\tilde{f}_i$. The squared amplitudes are given by the wind speed spectral estimates calculated in the previous section, denoted by $\tilde{V}(\tilde{f}_i)$ and given by Eq. (A.53). Multiplying the wind speed spectrum by the weighting functions gives three different variance spectra; the mean wind speed spectrum, $\tilde{V}_{\overline{u}_\tau}(\tilde{f}_i)$, the spectrum of fluctuations about the mean wind speed, $\tilde{V}_{u(t)}(\tilde{f}_i)$, and the spectrum of deviations in SOC, $\tilde{V}_{\Delta E_t}(\tilde{f}_i)$.

Each spectrum is shown in Figure A.4 as a function frequency on a logarithmic scale for a 24 hour storage period calculated with wind speed data from Sandspit, BC. The variance spectrum of $\Delta E_t$ is calculated for a power system comprised of 1000 kW installed wind capacity, a firm power commitment of 400 kW, and an ESD with an overall efficiency of 70% and maximum charging and discharging power limits of 300kW.

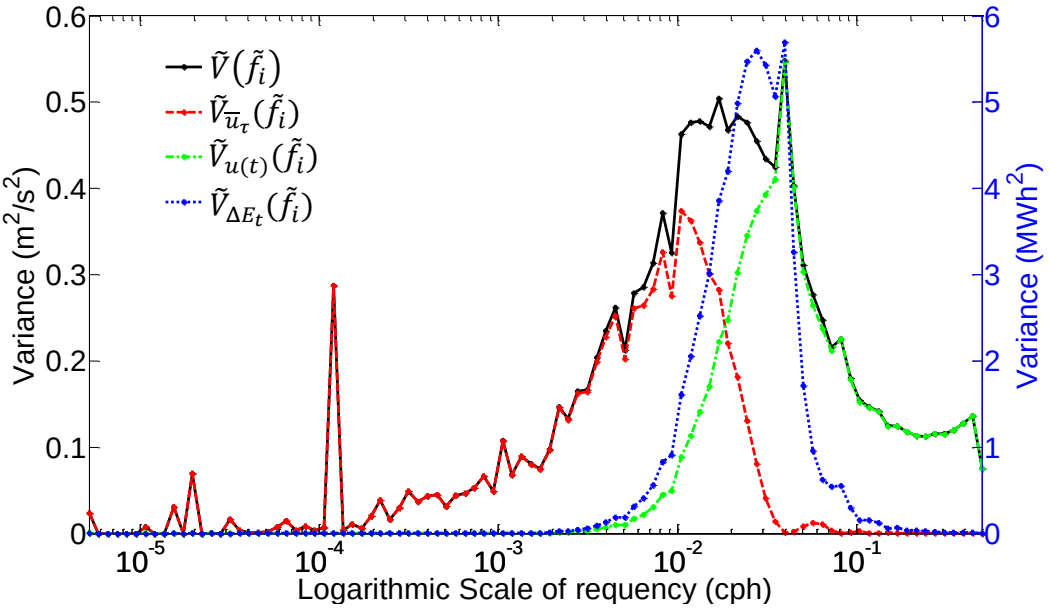


Figure A.4 – Filtered variance spectrum for a 24 hr storage period for Sandspit, BC.

The total variance associated with $\overline{u}_\tau$, $u(t)$, and $\Delta E_t$ is calculated by summing the individual variance contributions from each frequency component of the filtered spectra.

$$\sigma^2{}_{\overline{u}_\tau} = \sum_{i=1}^{n} \tilde{V}_{\overline{u}_\tau}(\tilde{f}_i) \tag{A.55}$$

$$\sigma^2{}_{u(t)} = \sum_{i=1}^{n} \tilde{V}_{u(t)}(\tilde{f}_i) \tag{A.56}$$

$$\sigma^2{}_{\Delta E_t} = \sum_{i=1}^{n} \tilde{V}_{\Delta E_t}(\tilde{f}_i) \tag{A.57}$$

The variance calculations of Eqs. (A.55), (A.56), and (A.57) are used in the probabilistic representation of wind speed and the calculation of the required storage capacity.

# F ESD utilization metrics

The calculations of the ESD utilization metrics are referenced from methods presented in [18]. In the following section a summary of the calculations of the ESD utilization performance metrics is provided.

The ESD is assumed to be operating in one of four operational states: charging, discharging, full, or empty. The fraction of time that the ESD will be operating in each state is calculated from the PDF of net system power and an assumed time-domain representation of the power flow to and from the store. When the expected value of net system power is positive, more power is generated than required by the load, the ESD is assumed to operate in only three of the four possible states: full, charging, and discharging. If the expected value of net system power is negative, load exceeds the available wind generation, the ESD is assumed to operate in an empty, discharging, or charging mode only.

## F.1 Surplus net system power

For a net system power PDF with expected surplus generation the ESD is assumed to operate in full, charging, and discharging modes only. For negative values of net system power the ESD is assumed to be in a discharging state only. Therefore, the fraction of time the store spends in a discharging state, $t_{dch}$, can be calculated from the probability distribution of net system power. An example of a net system power PDF with surplus generation is shown in Figure A.5. The example shown is a simplified net power PDF and is included to illustrate the basic concepts of the utilization metrics. The shaded region of the PDF represents the probability that there is a net deficit power, which corresponds to the fraction of time the ESD is in a discharging state:

$$t_{dch} = Pr(P_{net} < 0) = \int_{-\infty}^{u^*} p(u)du\,, \tag{A.58}$$

where $u^*$ is the wind speed where the wind power is equal to the firm power commitment $P_w(u^*) = P_{fp}$.

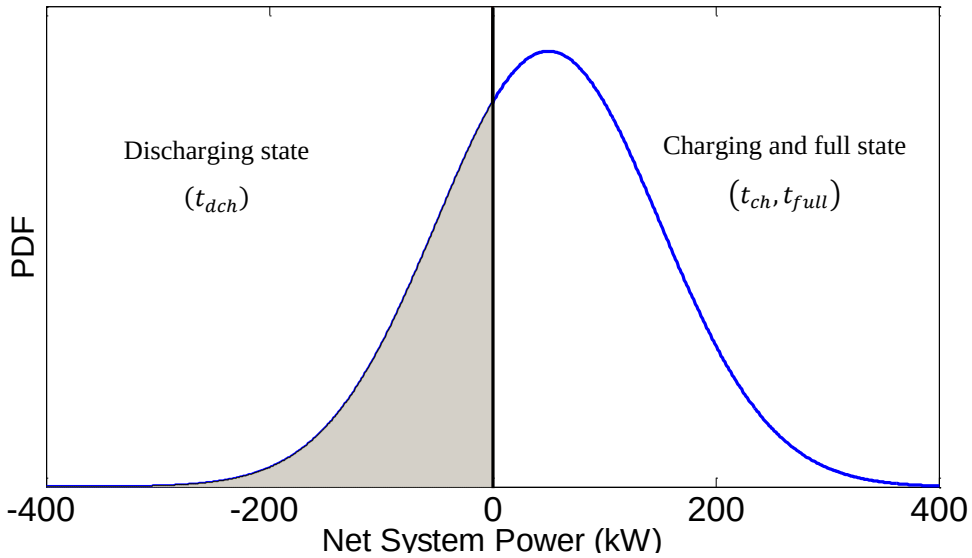


Figure A.5 – PDF of net system power with an expected surplus generation.

The positive portion of the net power PDF represents the probability the ESD is in a charging or full operational state. To calculate the fraction of time the store spends charging, $t_{ch}$, and the fraction of time the store spend full, $t_{full}$, requires a method to distinguish the two operating states. In [18] a time domain model is used to evaluate the fraction of time the store spends charging. A triangular wave function is assumed to represent power flows to and from the ESD and is shown in Figure A.6 for surplus net system power.

The ESD operates in a steady state over the storage period; therefore the energy released due to discharging the ESD is equal to the energy gained during charging, including efficiency loss.

The discharging and charging energy can be computed from the area of the shaded triangles in Figure A.6.

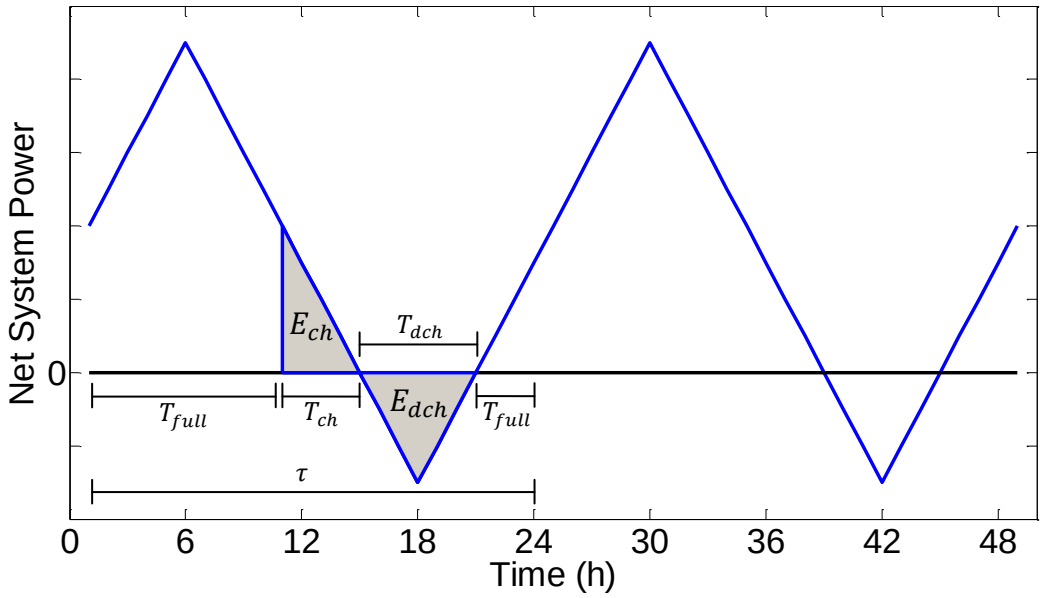


Figure A.6 – Time domain model of ESD power flows to calculate utilization metrics for surplus net system power.

The efficiency of the ESD is defined as:

$$\eta = \frac{E_{out}}{E_{in}} = \frac{E_{dch}}{E_{ch}} \ . \tag{A.59}$$

Solving for the area of the triangles, including the efficiency loss, an expression of the time the ESD spends charging is given by:

$$T_{ch} = T_{dch}\sqrt{\frac{1}{2\eta}} \tag{A.60}$$

Dividing Eq. (A.60) by the total storage period $\tau$ gives an expression for the fraction of time the ESD spends in a charging state.

$$t_{ch} = t_{dch}\sqrt{\frac{1}{2\eta}} \tag{A.61}$$

The fraction of time the store spends full is given by:

$$t_{full} = 1 - t_{dch} - t_{ch} \tag{A.62}$$

$$t_{empty} = 0 \tag{A.63}$$

## F.2 Deficit net system power

For a net system power PDF where the load exceeds generation, the ESD is assumed to operate in empty, discharging, and charging modes only. For positive values of net system power the ESD is assumed to be in a charging state only. Therefore, the fraction of time the store spends in a charging state, $t_{ch}$, can be calculated from the probability distribution of net system power. An example of a net system power PDF with an expected net deficit system power is shown in Figure A.7.

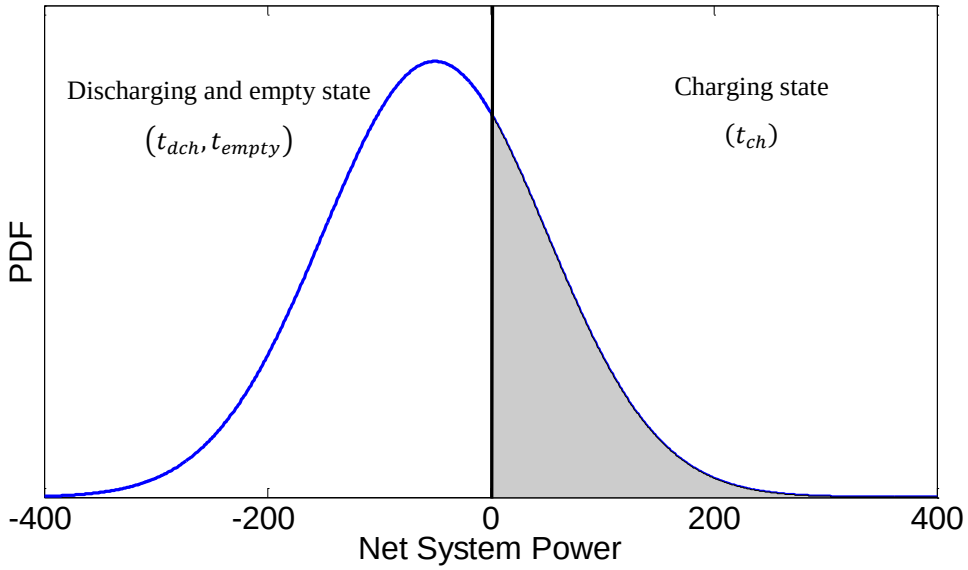


Figure A.7 – PDF of net system power with an expected deficit generation.

The shaded region of the PDF represents the probability that there is a net surplus power, which corresponds to the fraction of time the ESD is in a charging state:

$$t_{ch} = Pr(P_{net} > 0) = 1 - \int_{-\infty}^{u^*} p(u)du\,, \tag{A.64}$$

where $u^*$ is the wind speed where the wind power is equal to the firm power commitment $P_w(u^*) = P_{fp}$.

The fraction of time the ESD spends discharging and empty is calculated from the time domain representation of power flows. A graphical example is shown in Figure A.8.

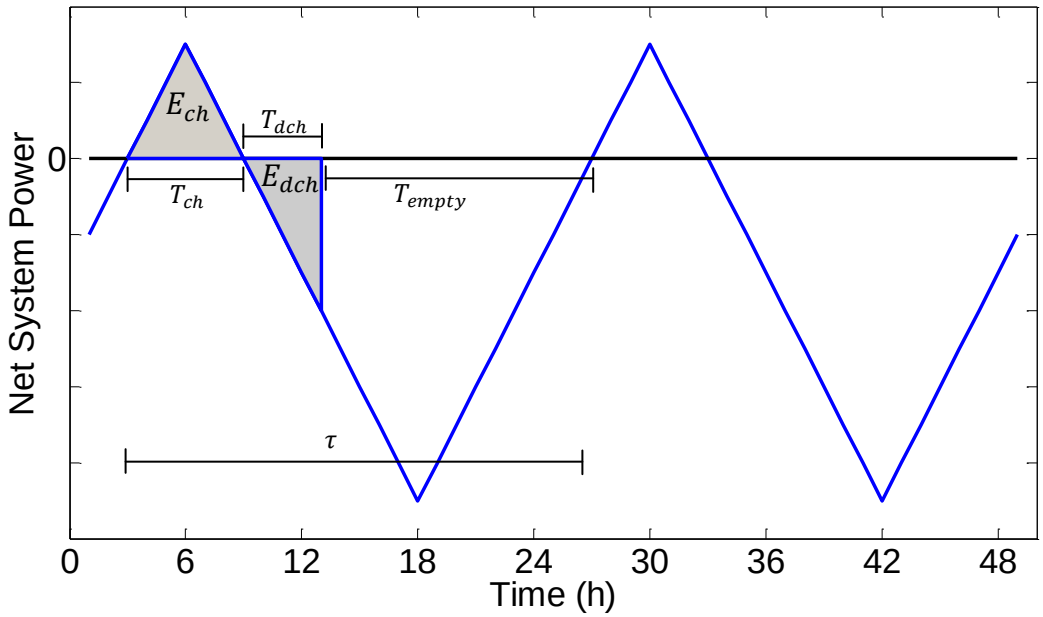


Figure A.8 – Time domain model of ESD power flows to calculate utilization metrics for deficit net system power.

The fraction of time the ESD spends discharging and empty are calculated from Eq. (A.59). Solving for the area of the shaded triangles in Figure A.8 gives an expression for the time that the ESD spend discharging.

$$T_{dch} = T_{ch}\sqrt{\frac{\eta}{2}} \tag{A.65}$$

Dividing Eq. (A.65) by the total storage period gives the fraction of the time the ESD spends discharging.

$$t_{dch} = t_{ch}\sqrt{\frac{\eta}{2}} \tag{A.66}$$

The fraction of time the ESD spends in an empty operational state is given by:

$$t_{empty} = 1 - t_{ch} - t_{dch} \tag{A.67}$$

$$t_{full} = 0 \tag{A.68}$$

## G Estimating Weibull shape factor by method of moments

The mean and variance of a random variable $X$ described by a Weibull probability distribution are given by:

$$E[X] = c \cdot \Gamma\left(1 + \frac{1}{k}\right), \tag{A.69}$$

$$Var(X) = c^2\left[\Gamma\left(1 + \frac{2}{k}\right) - \Gamma^2\left(1 + \frac{2}{k}\right)\right], \tag{A.70}$$

where $c$ and $k$ are defined as the scale and shape parameters of the distribution and $\Gamma$ is the gamma function [22].

The coefficient of variation, defined as the ratio of the standard deviation to the mean, can be used to estimate the Weibull parameters $c$ and $k$.

$$CV = \frac{\sigma}{\bar{x}} = \frac{\sqrt{Var(X)}}{\bar{x}} = \sqrt{\frac{\Gamma\left(1 + \frac{2}{k}\right)}{\Gamma^2\left(1 + \frac{1}{k}\right)} - 1} \tag{A.71}$$

Therefore, given the value of $\bar{x}$ and $\sigma$, Eq. (A.71) can be solved for the Weibull shape parameter $k$. Figure A.9 shows a functional form of Eq. (A.71) recommended in [22] for various shape parameter values. The inverse function is used in the probabilistic methodology to calculate the Weibull shape parameter $k$.

$$CV \approx k^{-.9208}, \tag{A.72}$$

$$k = CV^{-1.086} = \left(\frac{\sigma}{\bar{x}}\right)^{-1.086}, \tag{A.73}$$

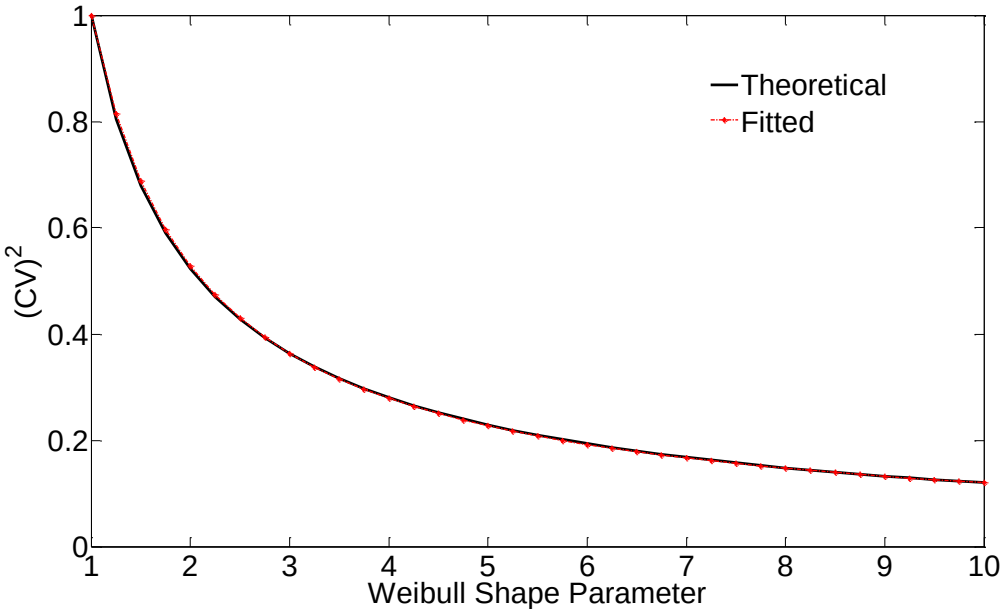


Figure A.9 – Weibull shape parameter estimation from CV value.

## H Time sequential simulation ESD control algorithm

This section provides details on the control algorithms used in the time domain model. There are four different scenarios dependent on the value of the surplus or deficit power at time *t* and if it is above or below the maximum rated charging or discharging constraints. In the rest of this section $P_{R,dch}$ is assumed to be positive, $P_{req}$ is defined as the required power from the backup generator, $P_{R,b}$ represents the maximum backup rating, and the following notation is used for the net surplus and deficit power:

$$P_{surp}(t) = \begin{cases} P_{net}(t) & if\ P_{net}(t) > 0 \\ 0 & if\ P_{net}(t) < 0 \end{cases} \quad \text{(A.74)}$$

$$P_{def}(t) = \begin{cases} |P_{net}(t)| & if\ P_{net}(t) < 0 \\ 0 & if\ P_{net}(t) > 0 \end{cases} \quad \text{(A.75)}$$

For the scenario where the surplus power exceeds the maximum charging rate the operation control algorithm is given by expression (A.76). If the surplus power is less

than the maximum charging rate the control algorithm is given by expression (A.76) but the charging power is defined as $P_{ch}(t) = \eta_{ch} P_{surp}(t)$.

$$
\begin{aligned}
&if\ P_{surp}(t) \geq P_{R,ch} \\
&\quad P_{ch}(t) = \eta_{ch} P_{R,ch}(t) \\
&\quad if\ E(t) = \zeta_{ESD} \\
&\qquad P_{ch}(t) = 0 \\
&\qquad P_d(t) = P_{surp}(t) \\
&\qquad E(t+1) = \zeta_{ESD} \\
&\qquad t_{full} = t_{full} + 1 \\
&else\ if\ E(t) + P_{ch}(t)\Delta t > \zeta_{ESD} \\
&\qquad P_{ch}(t) = (\zeta_{ESD} - E(t))/\Delta t \\
&\qquad P_d(t) = P_{surp}(t) - {\eta_{ch}}^{-1} P_{ch}(t) \\
&\qquad E(t+1) = \zeta_{ESD} \\
&\qquad t_{ch} = t_{ch} + 1 \\
&else\ P_d(t) = P_{surp}(t) - P_{R,ch} \\
&\qquad E(t+1) = E(t) + P_{ch}\Delta t \\
&\qquad t_{ch} = t_{ch} + 1
\end{aligned}
\tag{A.76}
$$

If the deficit power is greater than or equal to the maximum discharging rate of the ESD the operation control algorithm is given by expression (A.77). If the deficit power is less than the maximum discharging rate the control algorithm is given by expression (A.77) with the discharge power being defined as $P_{dch}(t) = {\eta_{dch}}^{-1} P_{def}(t)$.

$$
\begin{aligned}
&if\ P_{def}(t) \geq P_{R,dch} \\
&P_{dch}(t) = {\eta_{dch}}^{-1} P_{R,dch}(t) \\
&\quad if\ E(t) = 0 \\
&\quad\quad P_{dch}(t) = 0 \\
&\quad\quad E(t+1) = 0 \\
&\quad\quad t_{empty} = t_{empty} + 1 \\
&\quad\quad P_{req}(t) = P_{def}(t) \\
&\quad\quad if\ P_{req}(t) > P_{R,b} \\
&\quad\quad\quad P_b(t) = P_{R,b} \\
&\quad\quad\quad P_u(t) = P_{req}(t) - P_b(t) \\
&\quad\quad else \\
&\quad\quad\quad P_b(t) = P_{req}(t) \\
&\quad\quad\quad P_u(t) = 0 \\
&\quad else\ if\ E(t) - P_{dch}(t)\Delta t < 0 \\
&\quad\quad P_{dch}(t) = E(t)/\Delta t \\
&\quad\quad E(t+1) = 0 \\
&\quad\quad t_{dch} = t_{dch} + 1 \\
&\quad\quad P_{req}(t) = P_{def}(t) - \eta_{dch} P_{dch}(t) \\
&\quad\quad if\ P_{req}(t) > P_{R,b} \\
&\quad\quad\quad P_b(t) = P_{R,b} \\
&\quad\quad\quad P_u(t) = P_{req}(t) - P_b(t) \\
&\quad\quad else \\
&\quad\quad\quad P_b(t) = P_{req}(t) \\
&\quad\quad\quad P_u(t) = 0 \\
&\quad else\ E(t+1) = E(t) - P_{dch}(t)\Delta t \\
&\quad\quad t_{dch} = t_{dch} + 1 \\
&\quad\quad P_{req}(t) = P_{def}(t) - \eta_{dch} P_{dch}(t) \\
&\quad\quad if\ P_{req}(t) > P_{R,b} \\
&\quad\quad\quad P_b(t) = P_{R,b} \\
&\quad\quad\quad P_u(t) = P_{req}(t) - P_b(t) \\
&\quad\quad else \\
&\quad\quad\quad P_b(t) = P_{req}(t) \\
&\quad\quad\quad P_u(t) = 0
\end{aligned}
\tag{A.77}
$$